H-Glu-Val-Asn-Sta-Val-Ala-Glu-Phe-4Gl-3Gl-4Gl-3Gl-4Gl-Asp(ODhc)-NH_2 (**6a**)

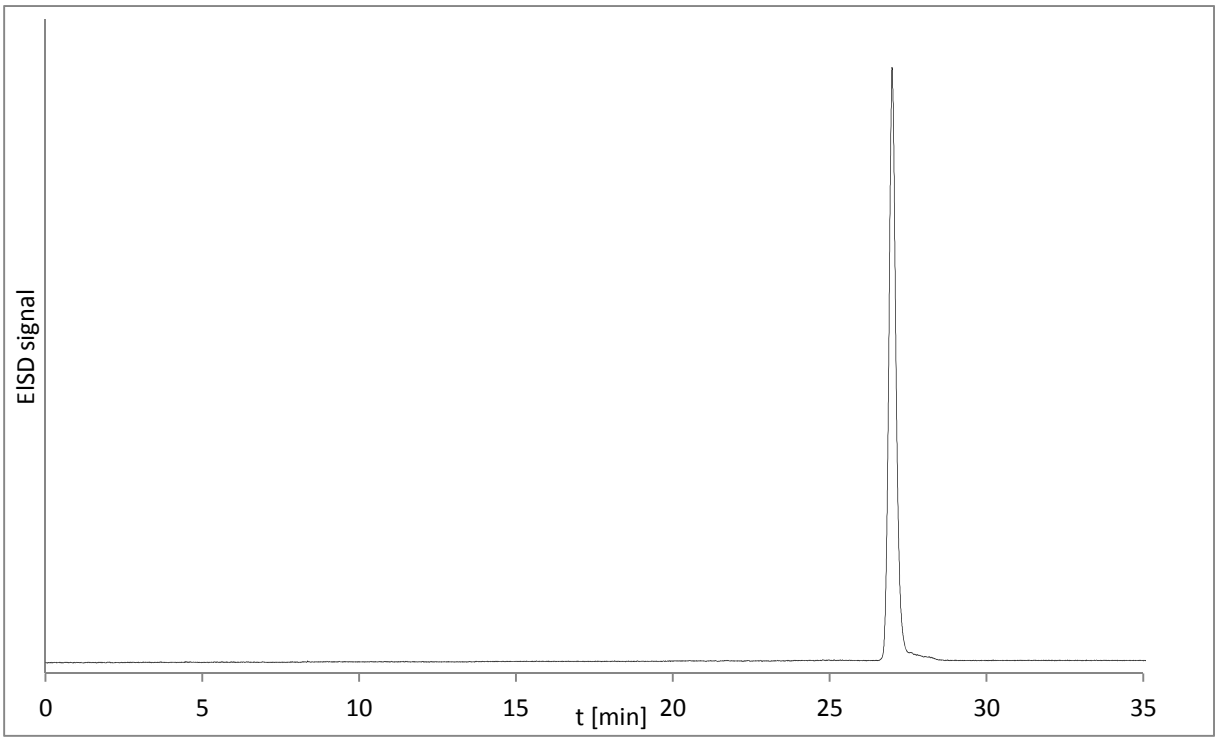

ESI-MS (positive mode), low resolution:

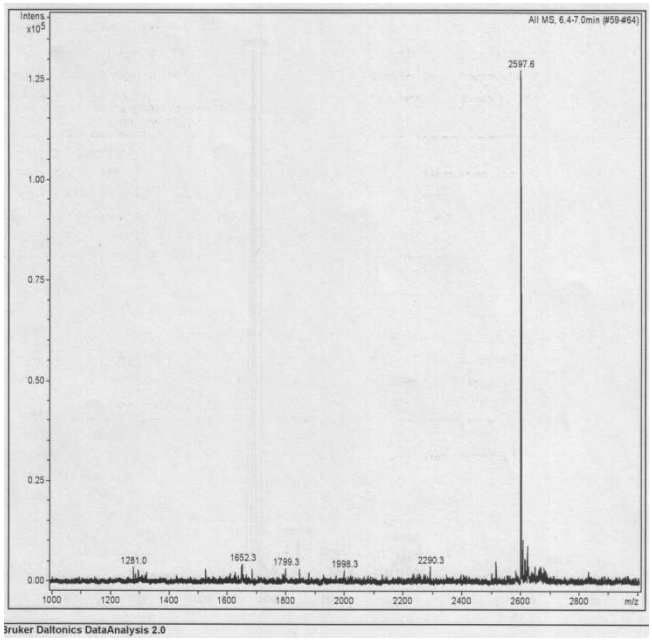

Mass reconstruction from ESI-MS (positive mode), high resolution:

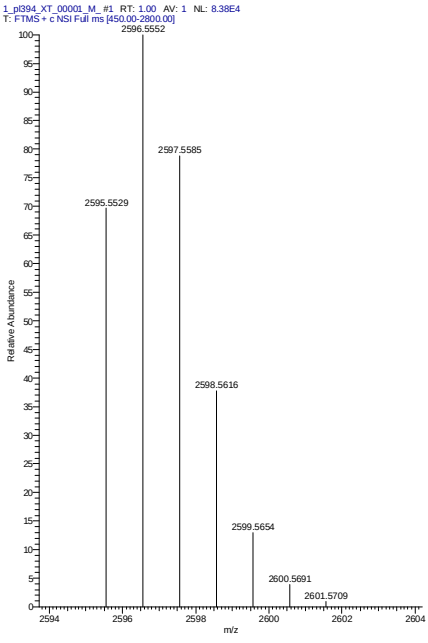

H-Glu-Val-Asn-Sta-Val-Ala-Glu-Phe-4Gl-3Gl-4Gl-3Gl-4Gl- Asp(OChol)-NH_2 (**6b**)

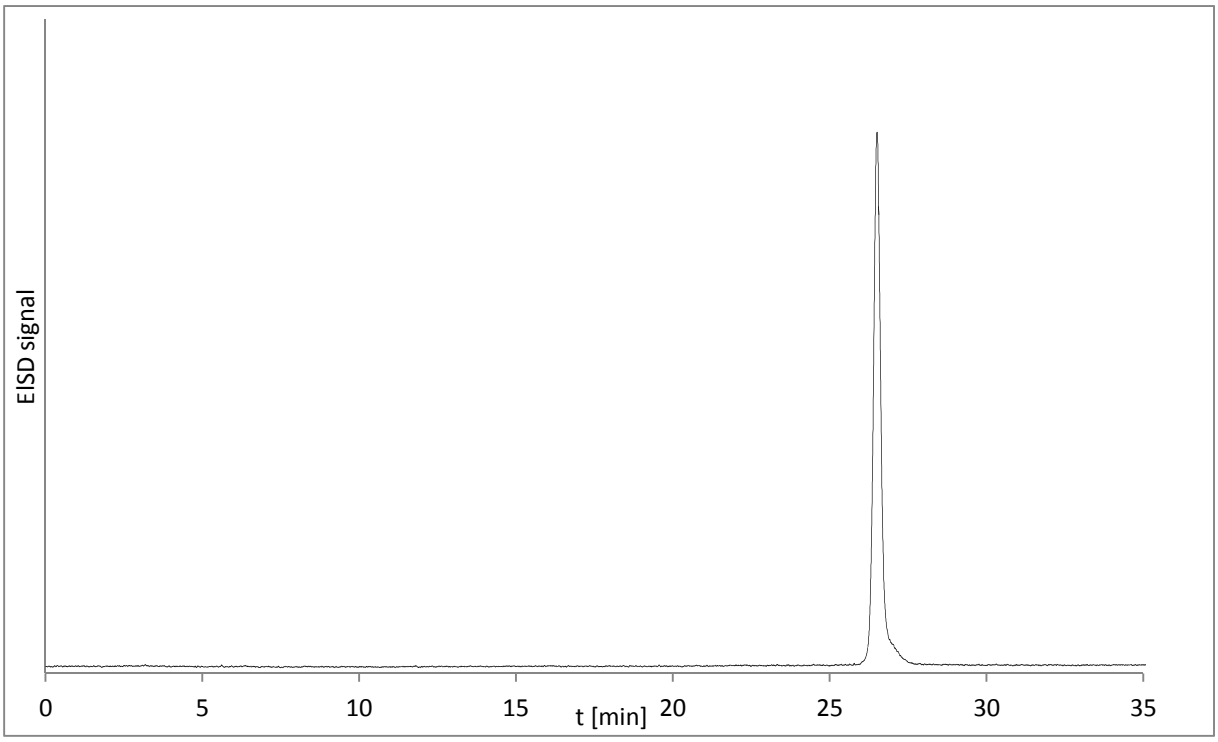

ESI-MS (positive mode), high resolution:

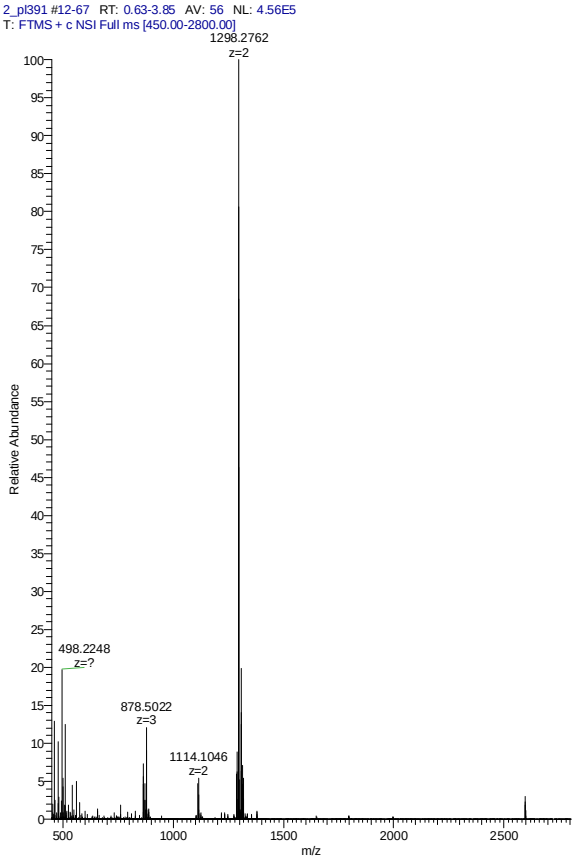

Mass reconstruction from ESI-MS (positive mode), high resolution:

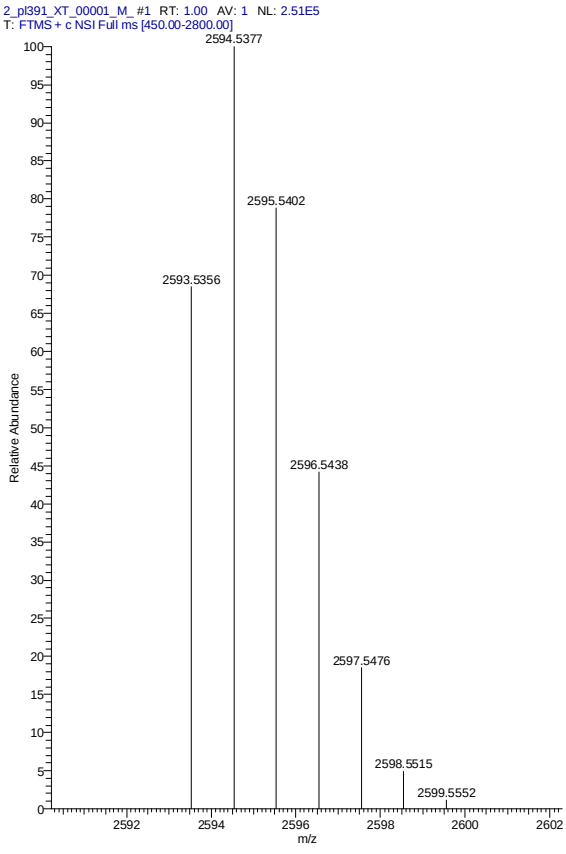

H-Glu-Val-Asn-Sta-Val-Ala-Glu-Phe-4Gl-3Gl-4Gl-3Gl-4Gl- Asp(O-*n*$C_{14}H_{29}$)-NH_2 (**6c**)

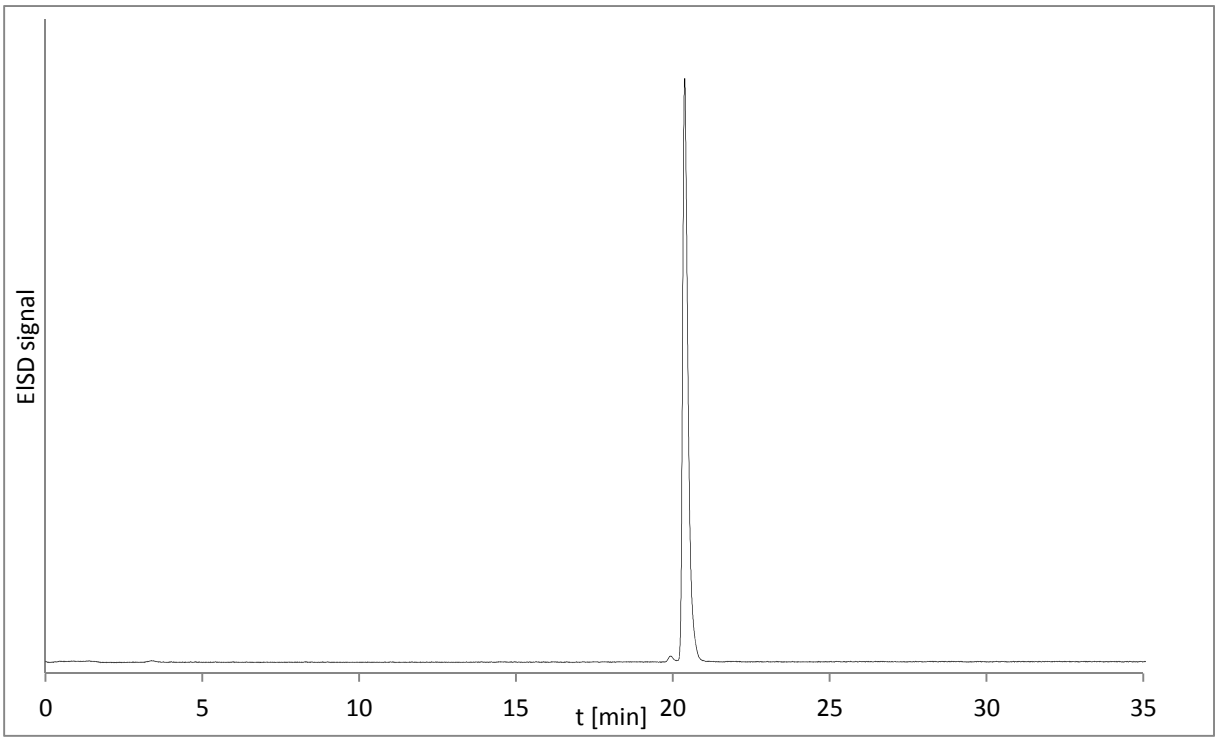

ESI-MS (positive mode), high resolution:

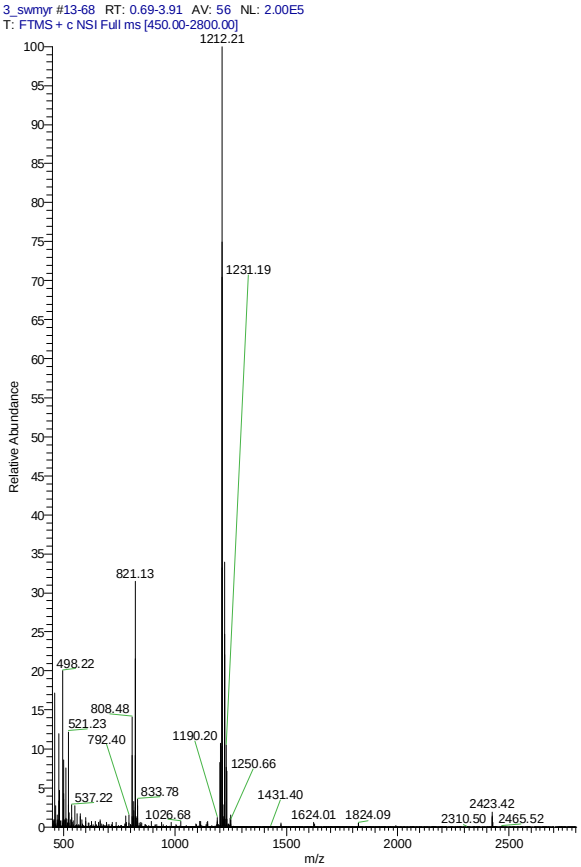

Mass reconstruction from ESI-MS (positive mode), high resolution:

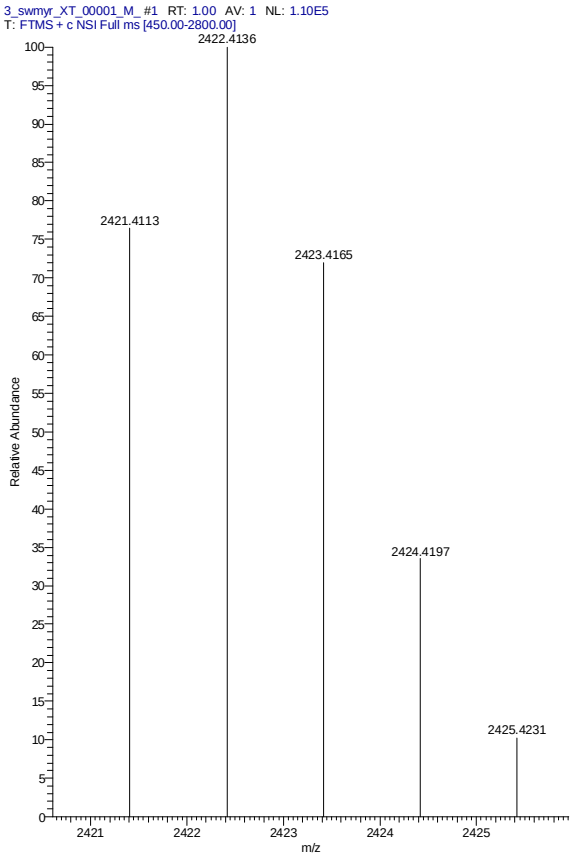

H-Glu-Val-Asn-Sta-Val-Ala-Glu-Phe-4Gl-3Gl-4Gl-3Gl-4Gl- Asp(O-nC$_{16}$H$_{33}$)-NH$_2$ (**6d**)

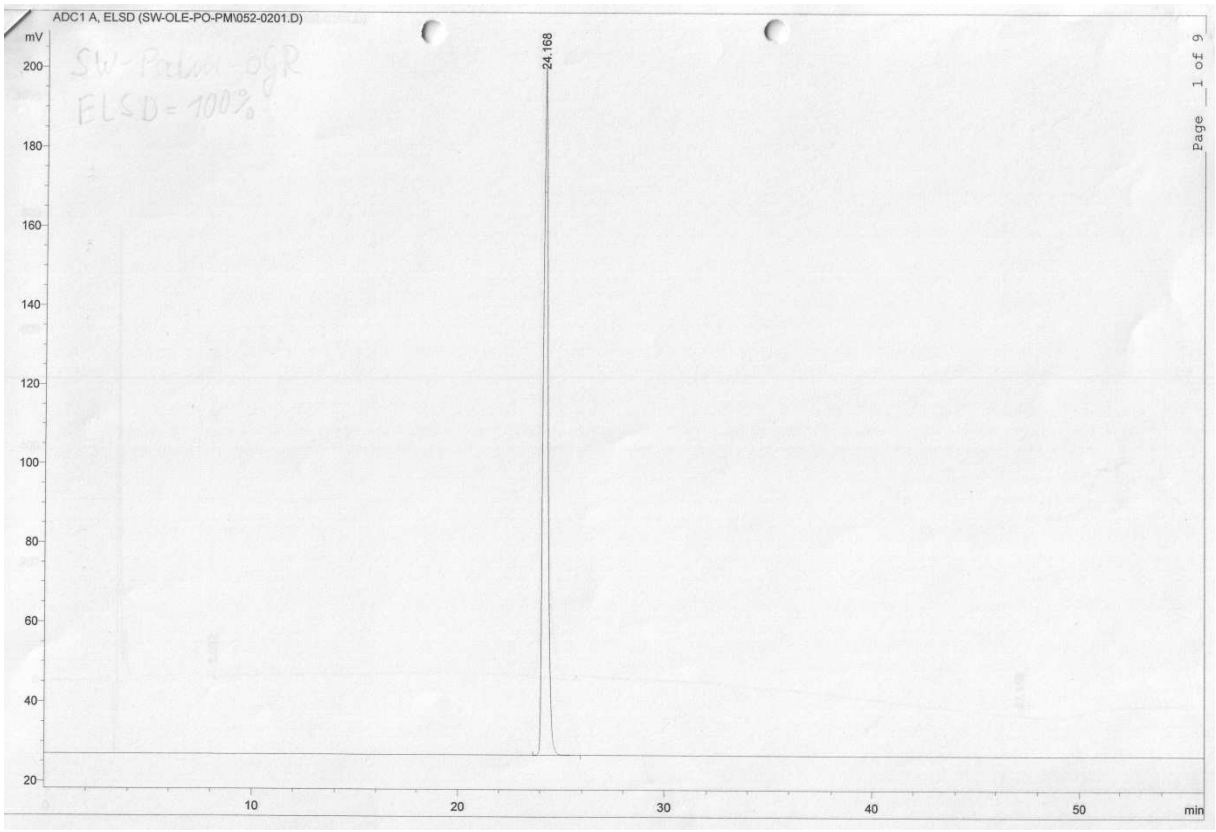

Differently from the description in the experimental section: eluent A: H_2O/MeCN (85:15) + 0.1% CF_3COOH and eluent B: MeCN + 0.1% CF_3COOH. Gradient from 10% to 100% B in 45 min.

ESI-MS (positive mode), high resolution:

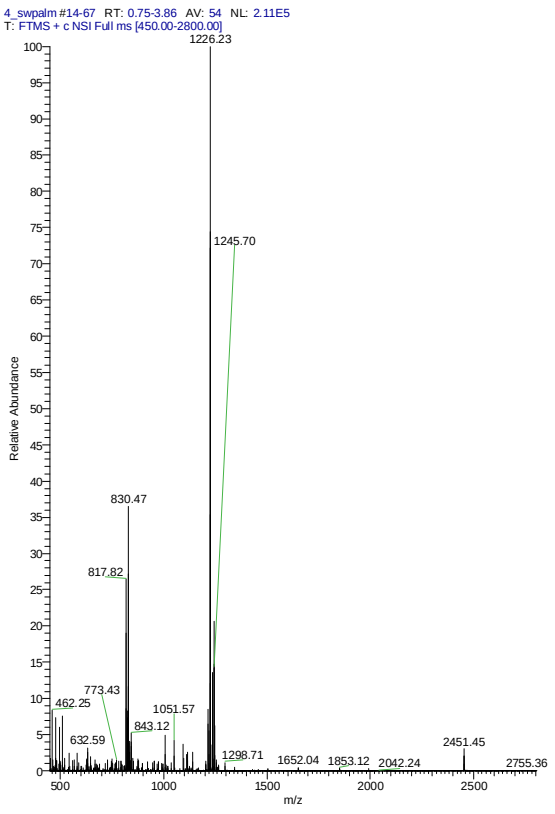

Mass reconstruction from ESI-MS (positive mode), high resolution:

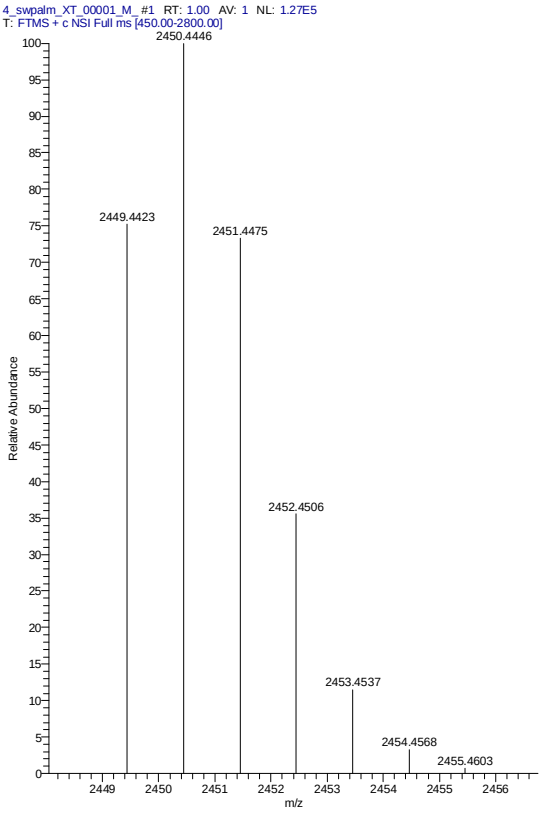

H-Glu-Val-Asn-Sta-Val-Ala-Glu-Phe-4Gl-3Gl-4Gl-3Gl-4Gl-Asp(O-*n*$C_{18}H_{37}$)-NH_2 (**6e**)

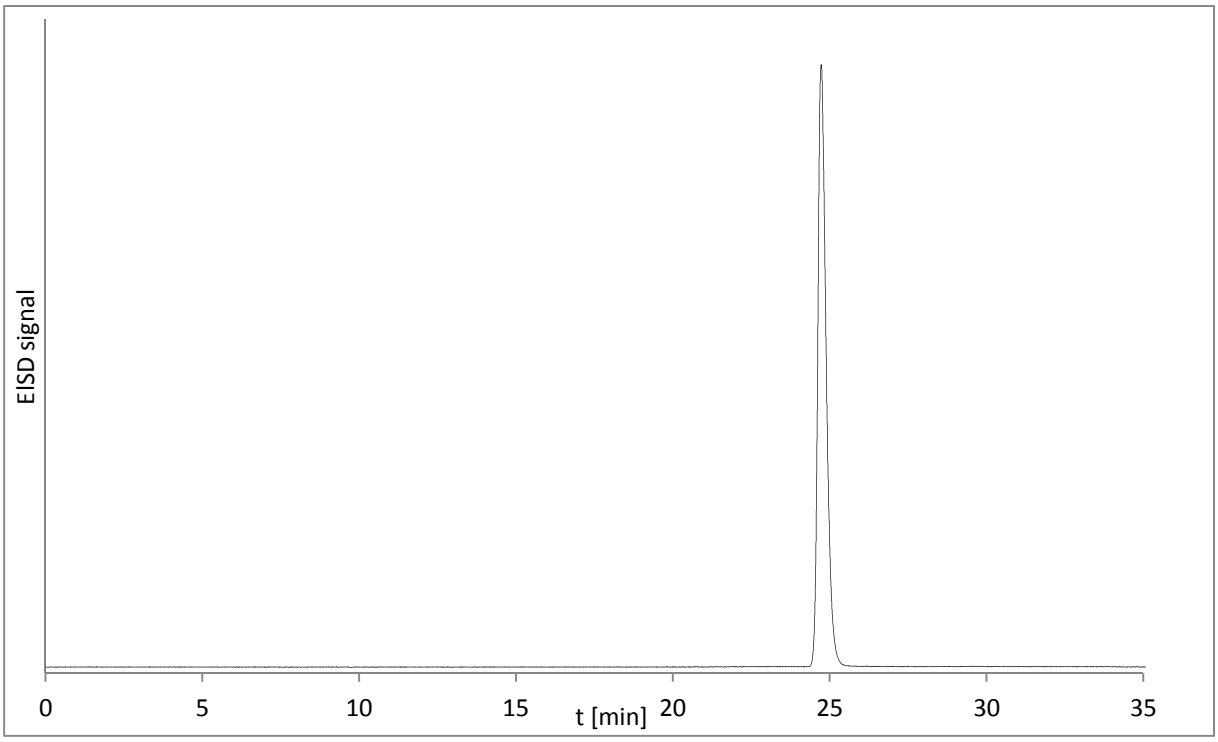

ESI-MS (positive mode), low resolution:

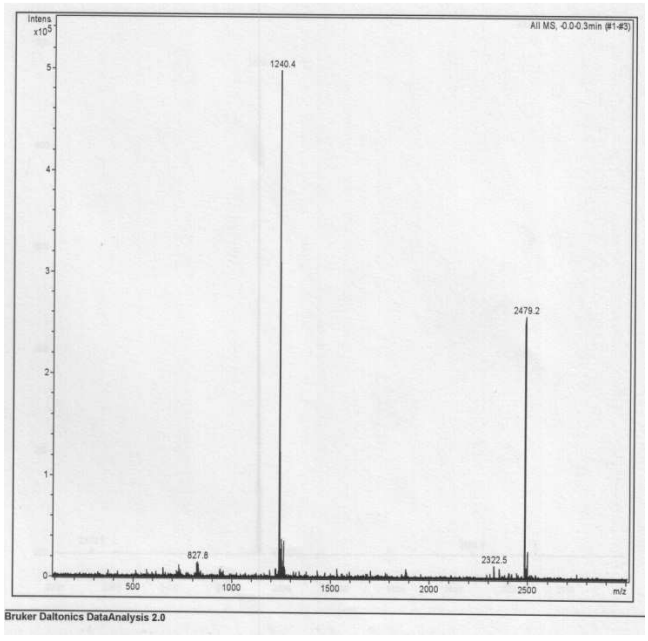

Mass reconstruction from ESI-MS (positive mode), high resolution:

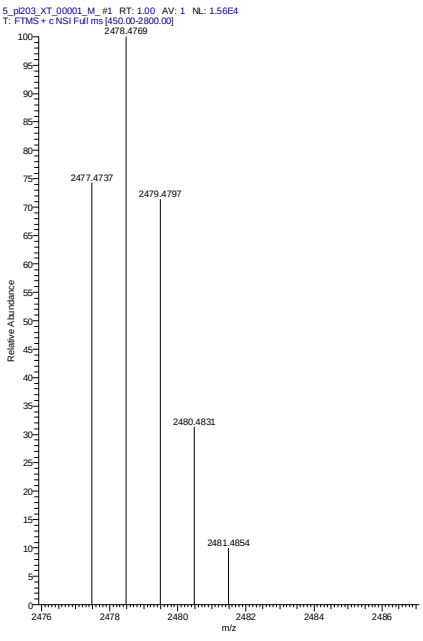

H-Glu-Val-Asn-Sta-Val-Ala-Glu-Phe-4Gl-3Gl-4Gl-3Gl-4Gl-Asp(O-*n*$C_{18}H_{37}$)-NH_2 (**6e**)

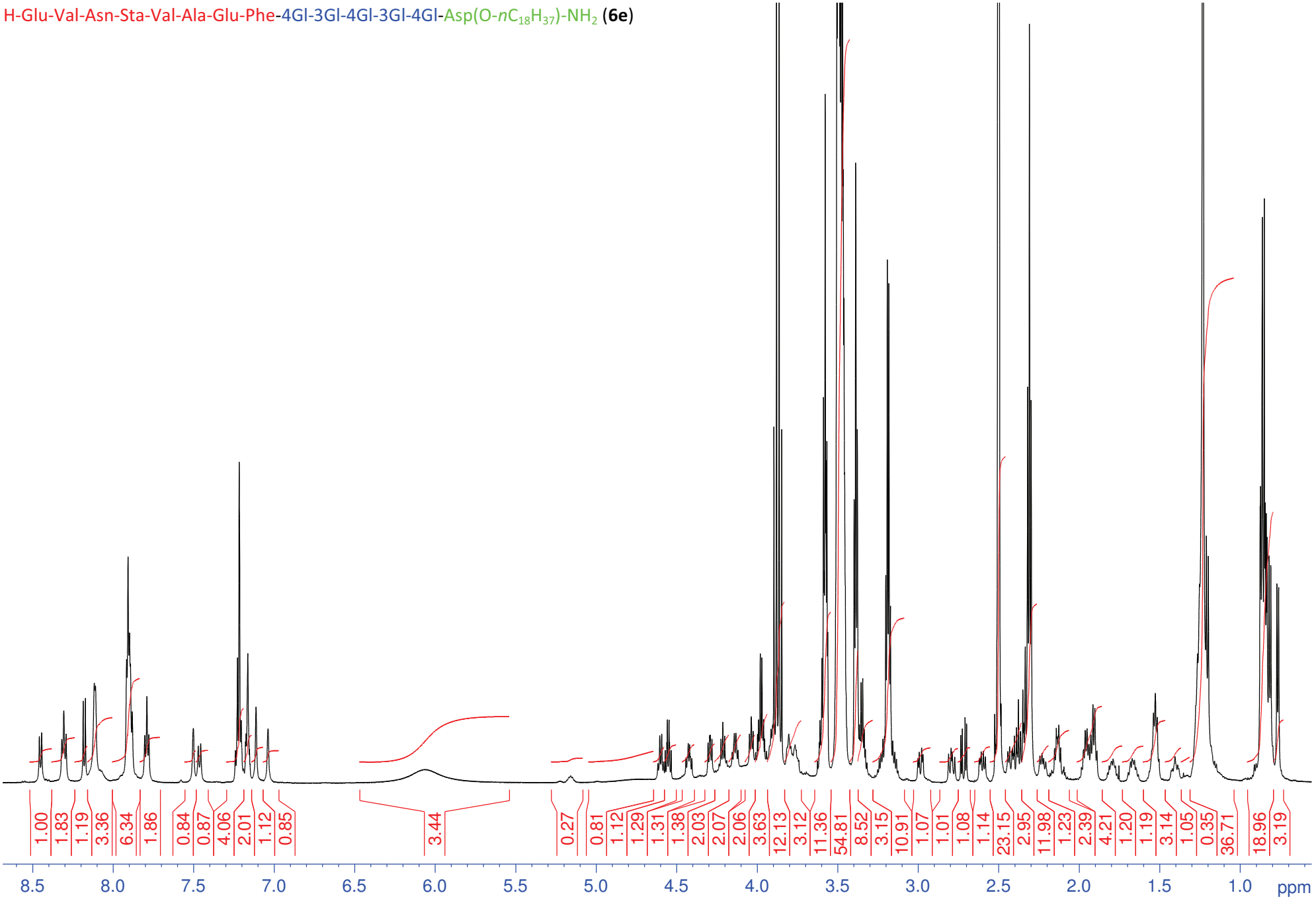

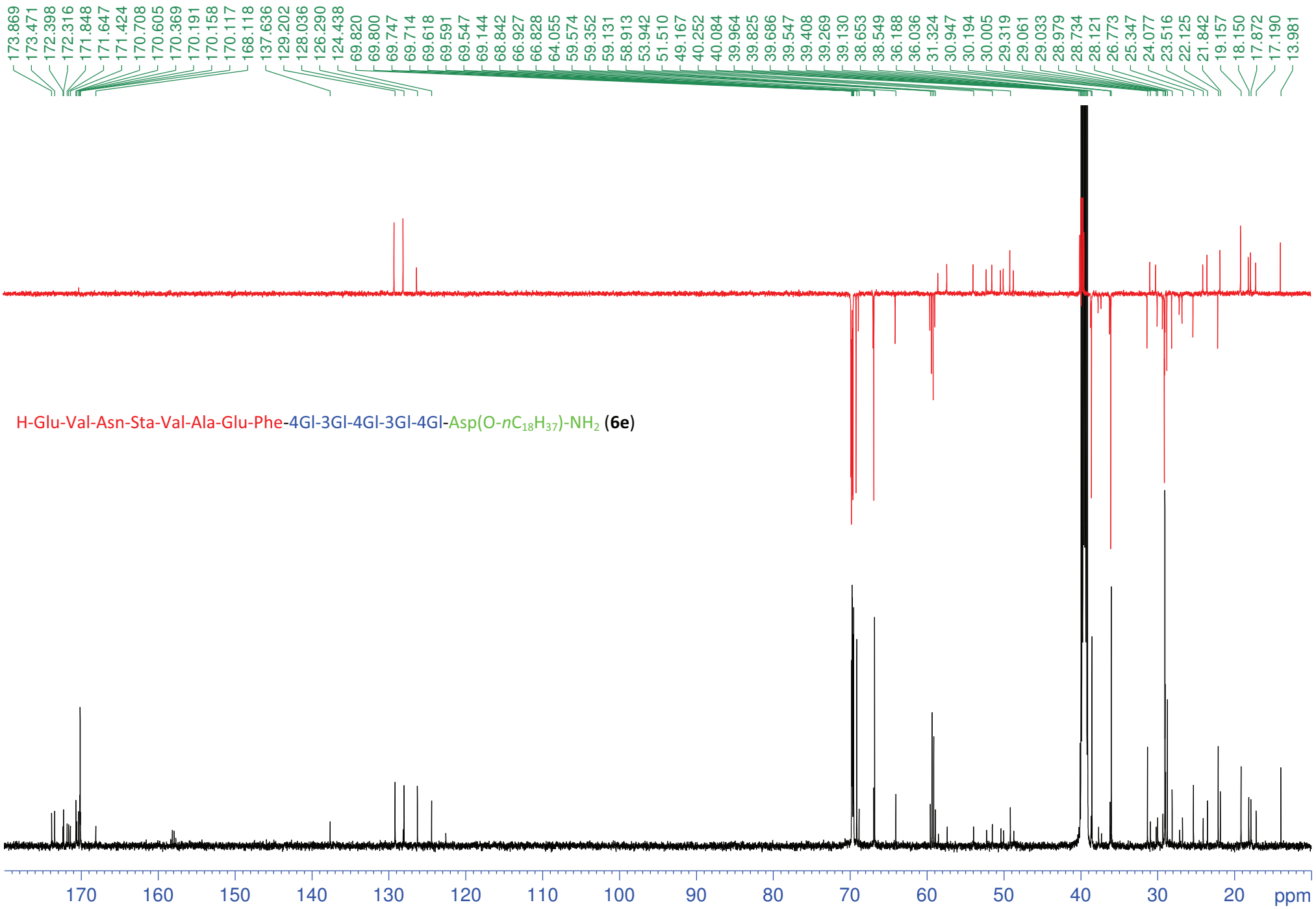

H-Glu-Val-Asn-Sta-Val-Ala-Glu-Phe-4Gl-3Gl-4Gl-3Gl-4Gl-Asp(O-*n*$C_{20}H_{41}$)-NH_2 (**6f**)

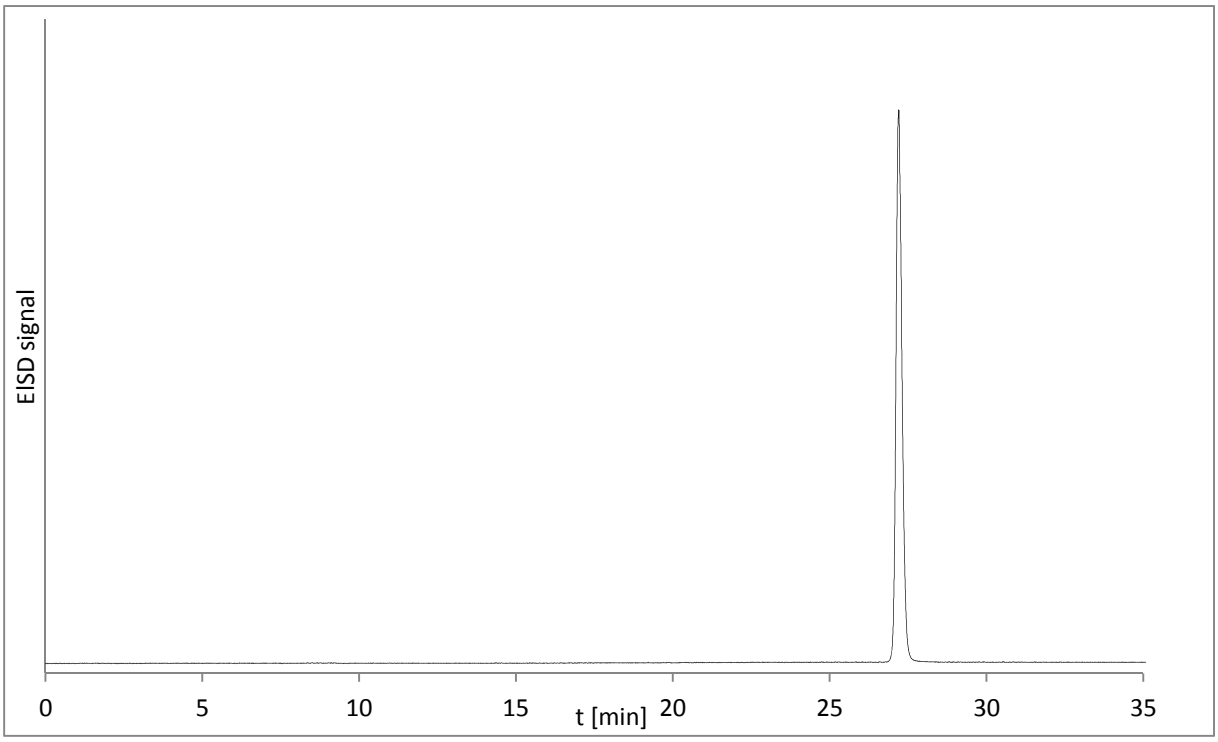

ESI-MS (positive mode), high resolution:

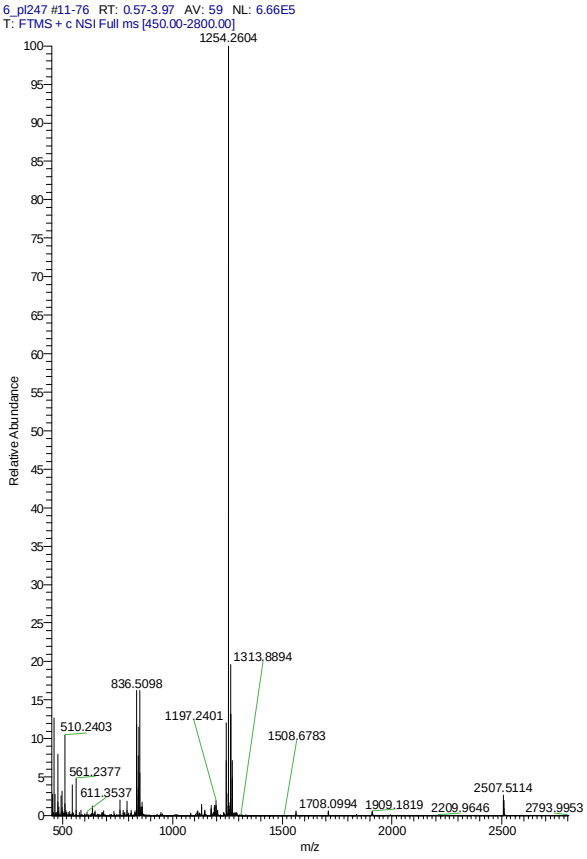

Mass reconstruction from ESI-MS (positive mode), high resolution:

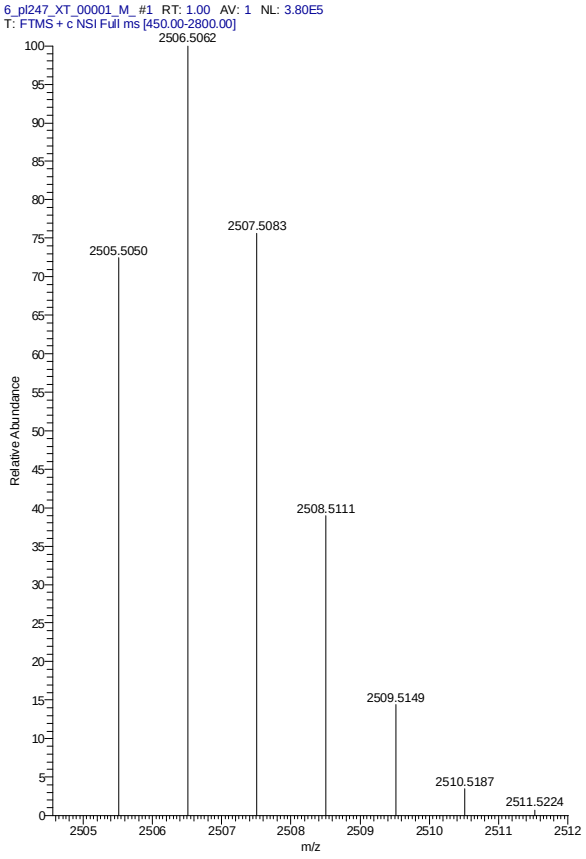

H-Glu-Val-Asn-Sta-Val-Ala-Glu-Phe-4Gl-3Gl-4Gl-3Gl-4Gl-Asp(O-*n*$C_{22}H_{45}$)-NH_2 (**6g**)

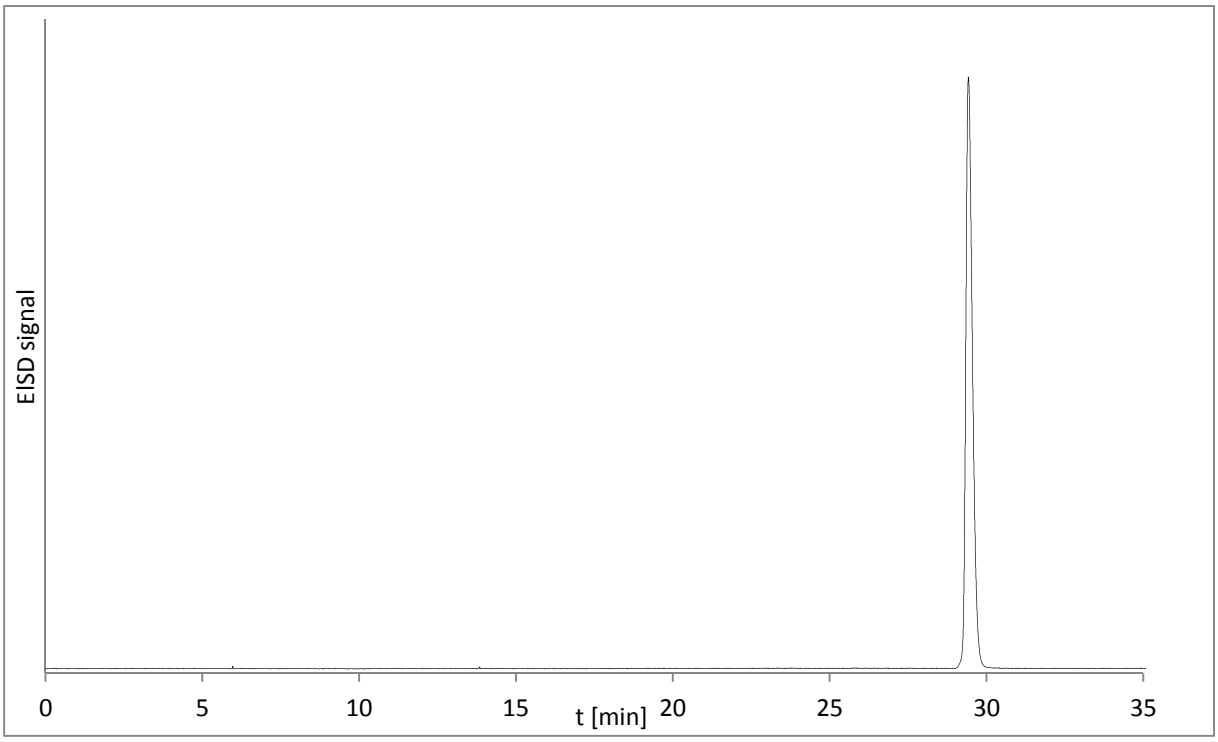

ESI-MS (positive mode), high resolution:

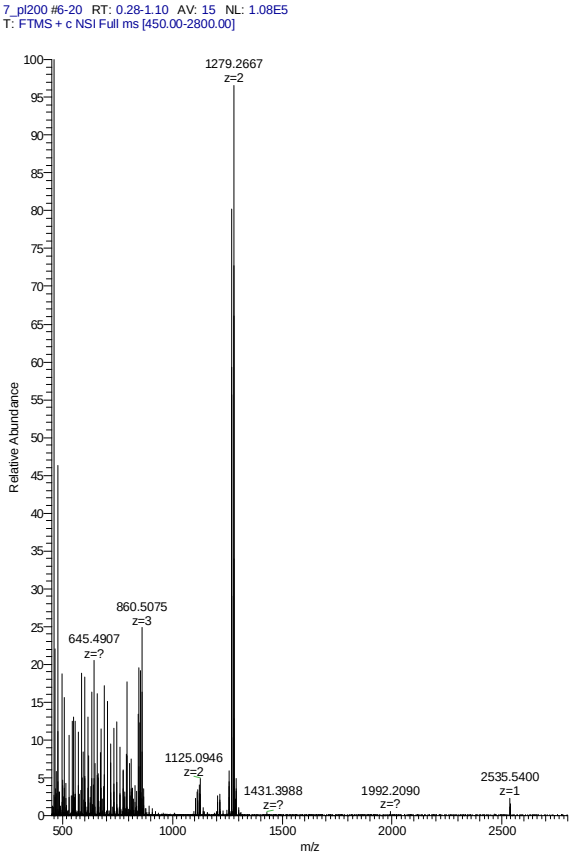

Mass reconstruction from ESI-MS (positive mode), high resolution:

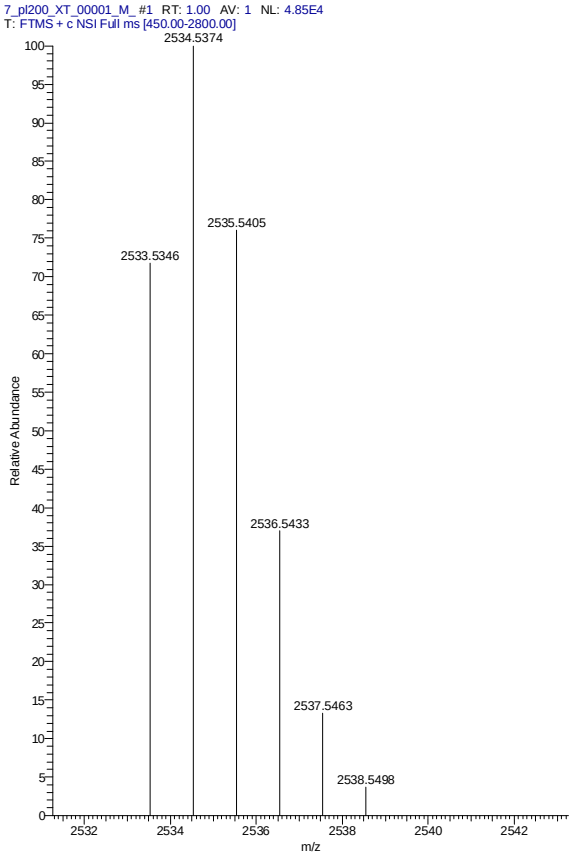

H-Glu-Val-Asn-Sta-Val-Ala-Glu-Phe-4Gl-3Gl-4Gl-3Gl-4Gl-Asp(O-*n*$C_{22}H_{45}$)-NH_2 (**6g**)

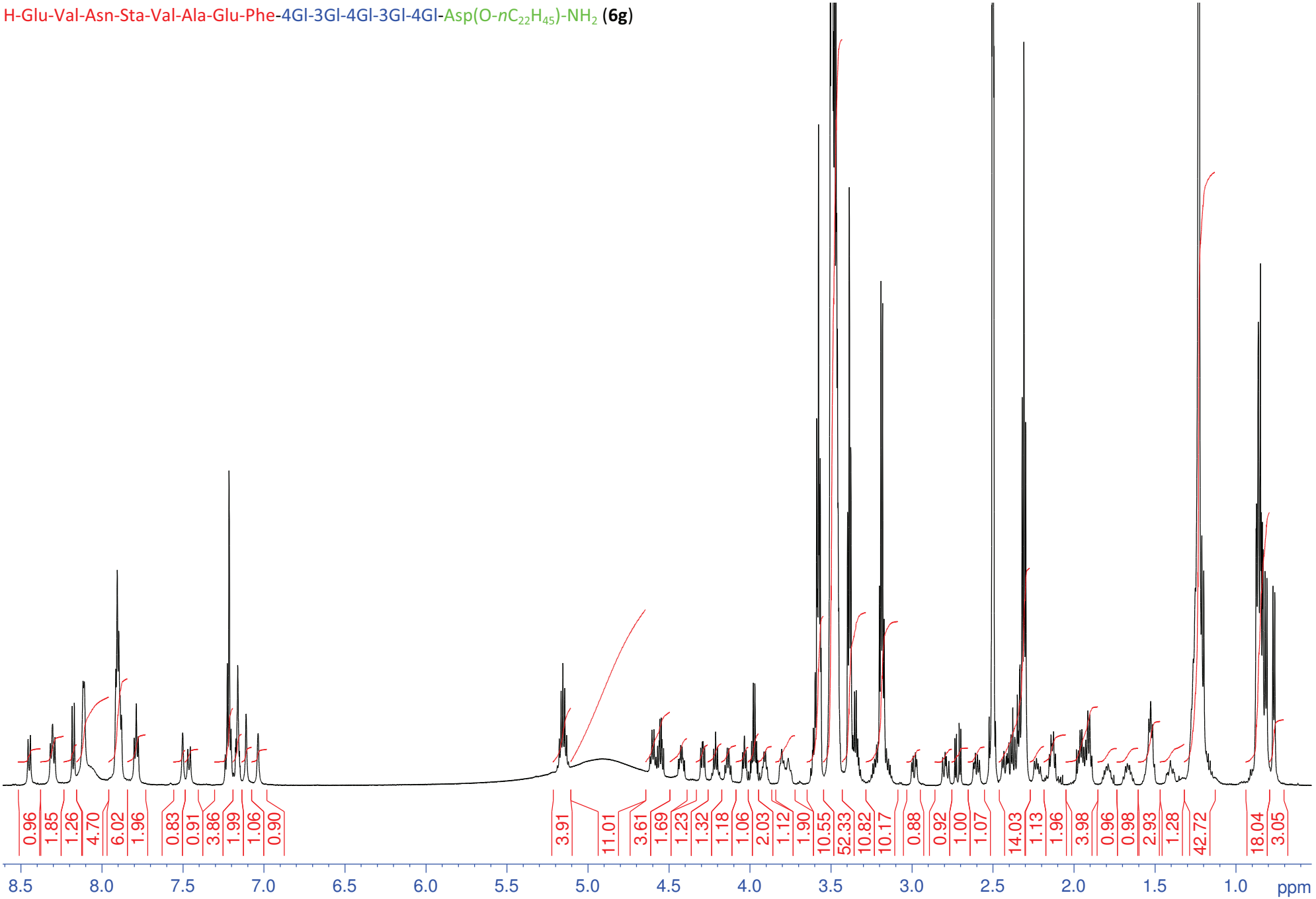

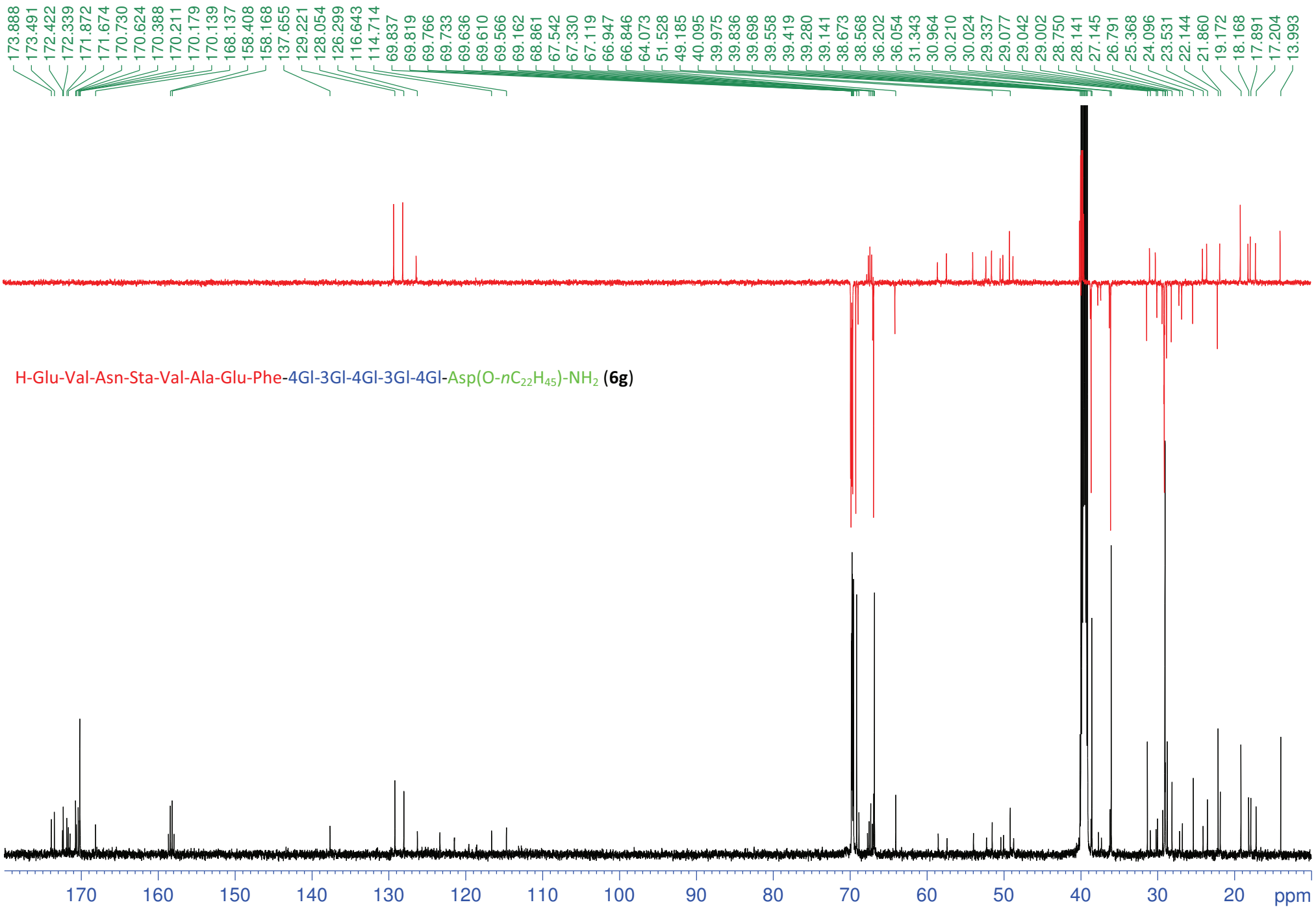

H-Glu-Val-Asn-Sta-Val-Ala-Glu-Phe-4Gl-3Gl-4Gl-3Gl-4Gl-Asp(O-*n*$C_{24}H_{49}$)-NH_2 (**6h**)

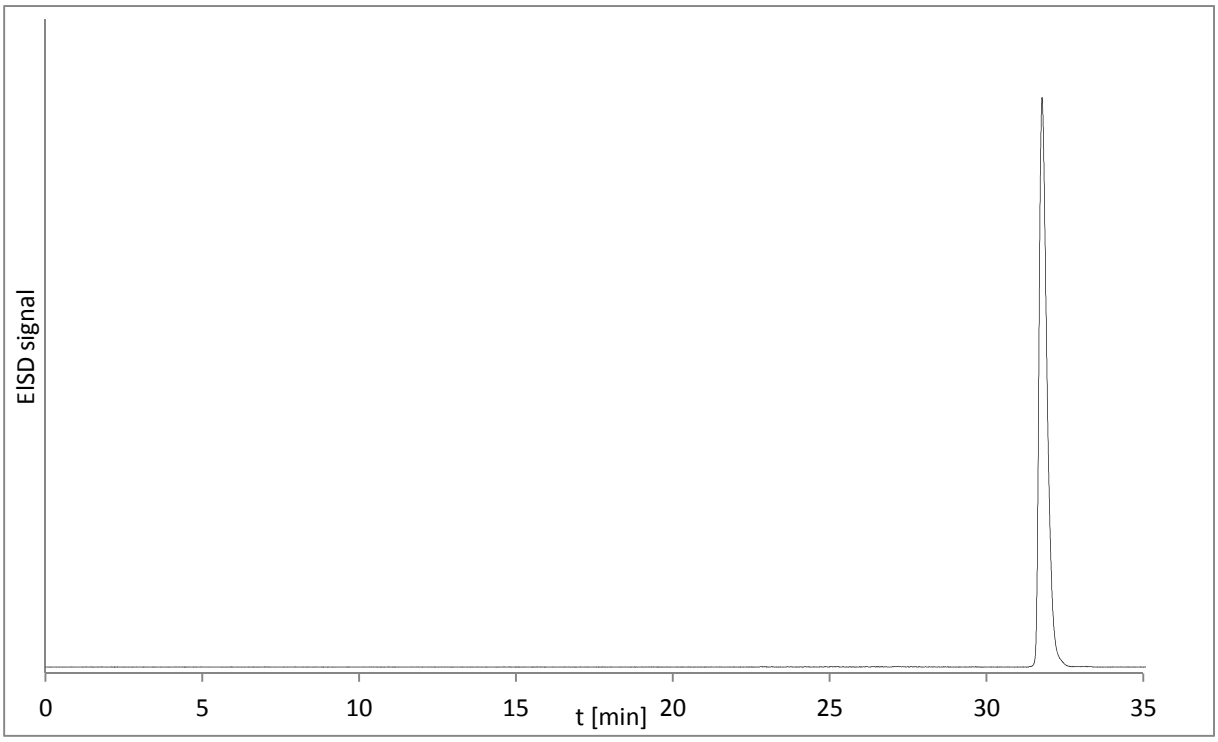

ESI-MS (positive mode), high resolution:

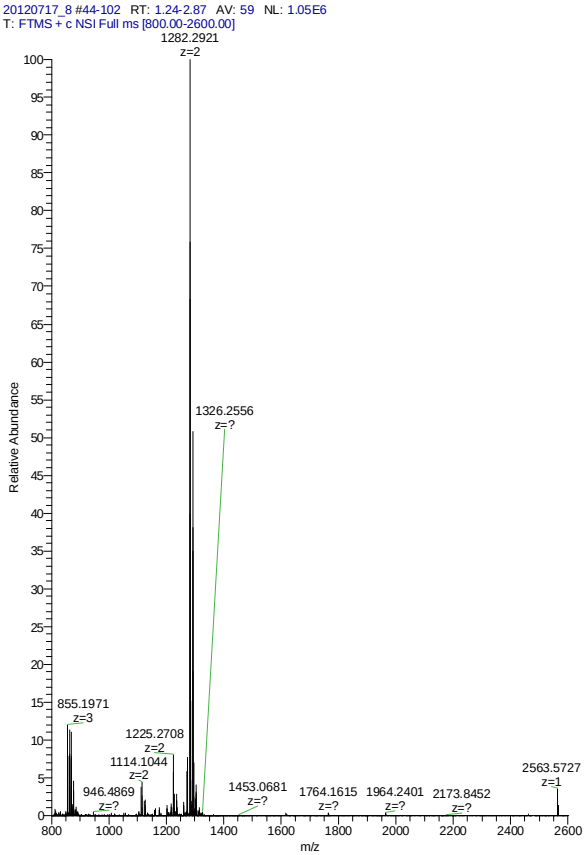

Mass reconstruction from ESI-MS (positive mode), high resolution:

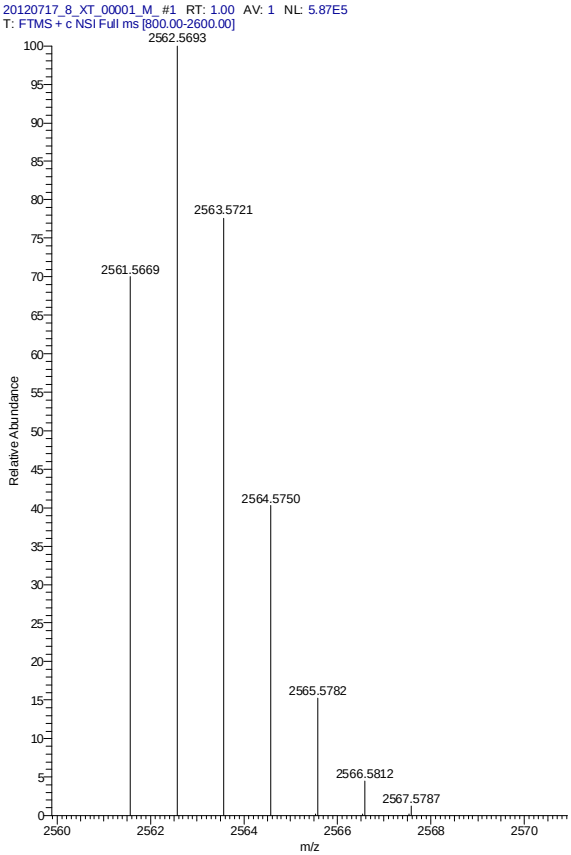

H-Glu-Val-Asn-Sta-Val-Ala-Glu-Phe-4Gl-3Gl-4Gl-3Gl-4Gl-Asp(O-*n*$C_{24}H_{49}$)-NH_2 (**6h**)

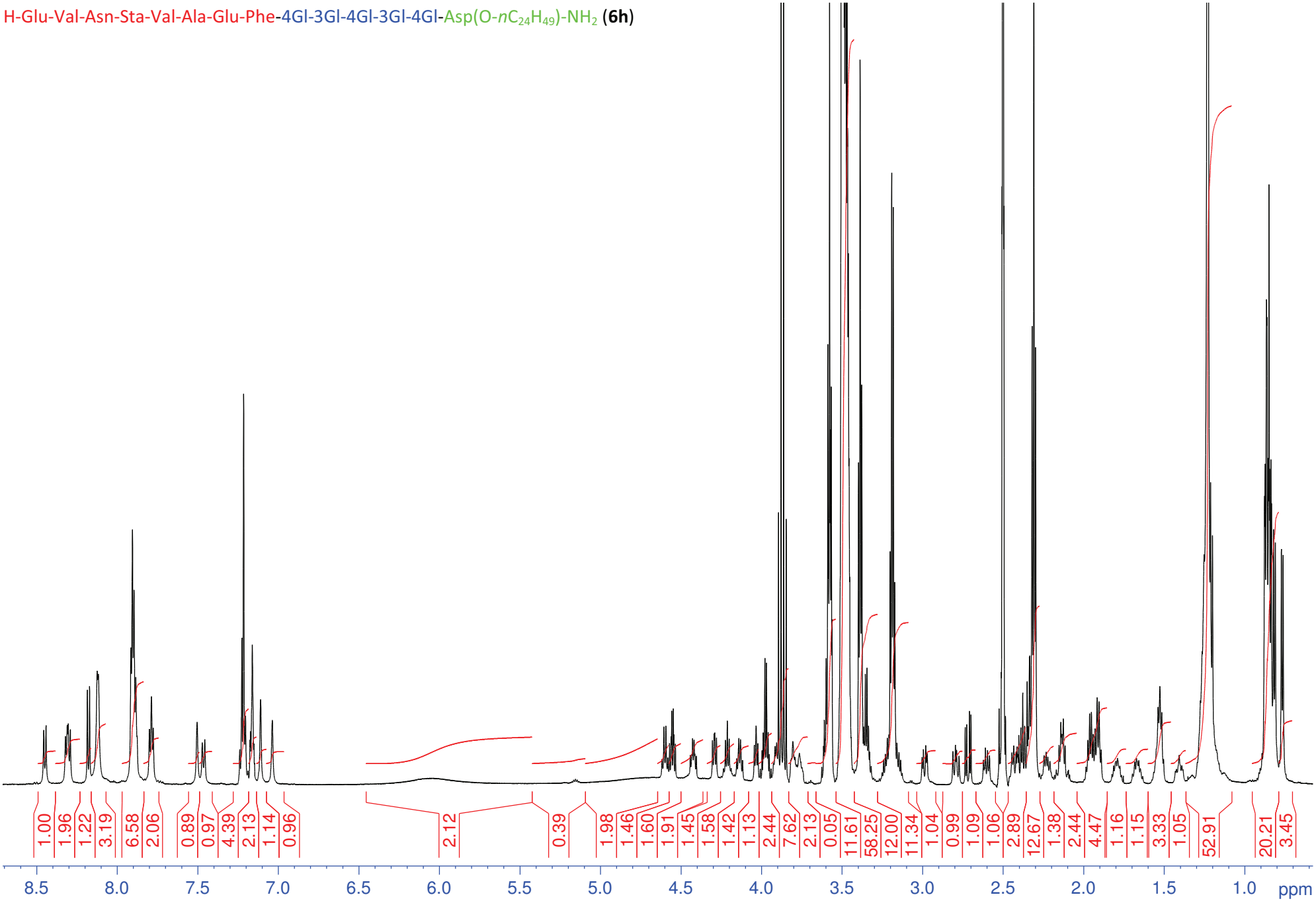

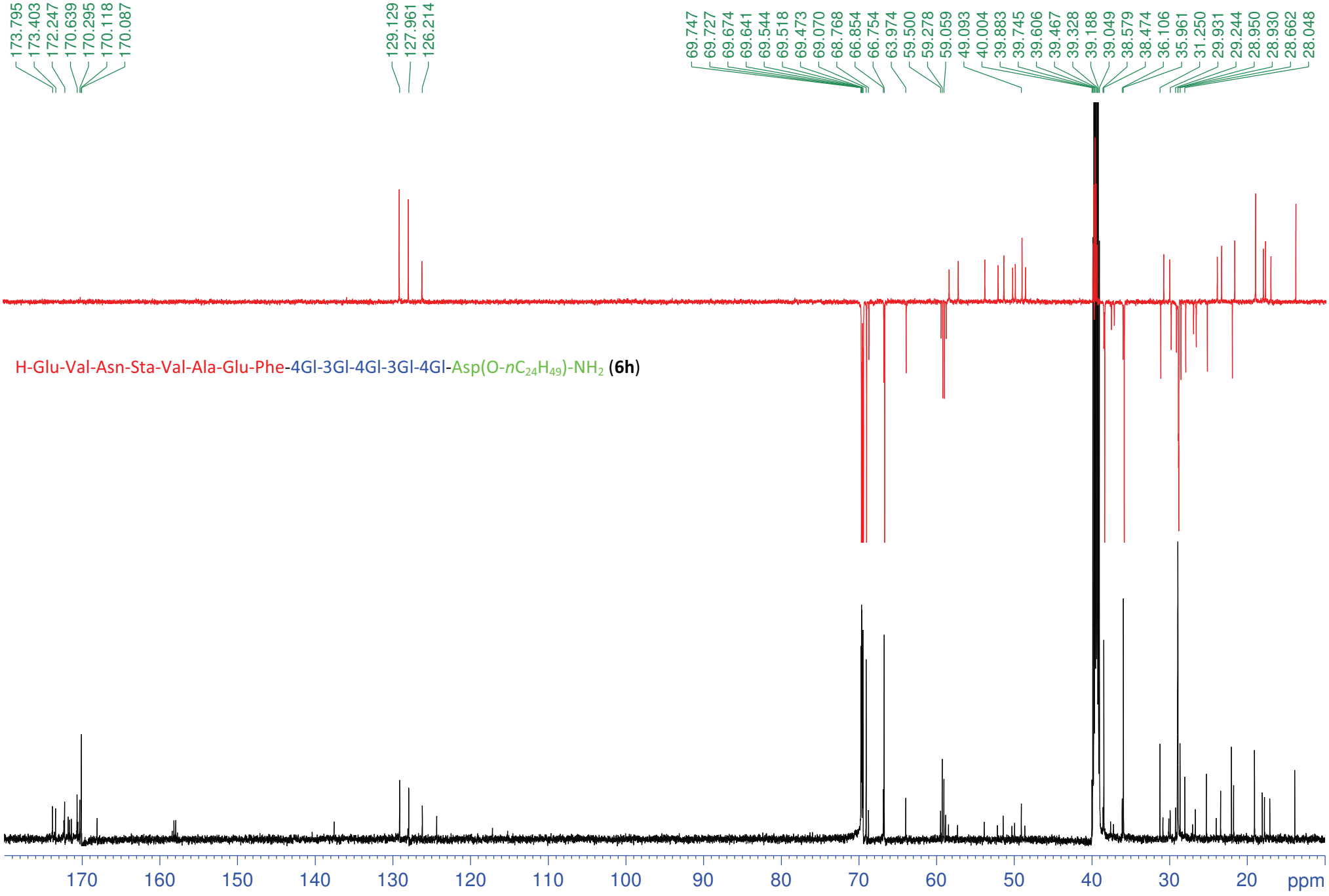

H-Glu-Val-Asn-Sta-Val-Ala-Glu-Phe-4Gl-3Gl-4Gl-3Gl-4Gl-Asp(O-*n*$C_{26}H_{53}$)-NH_2 (**6i**)

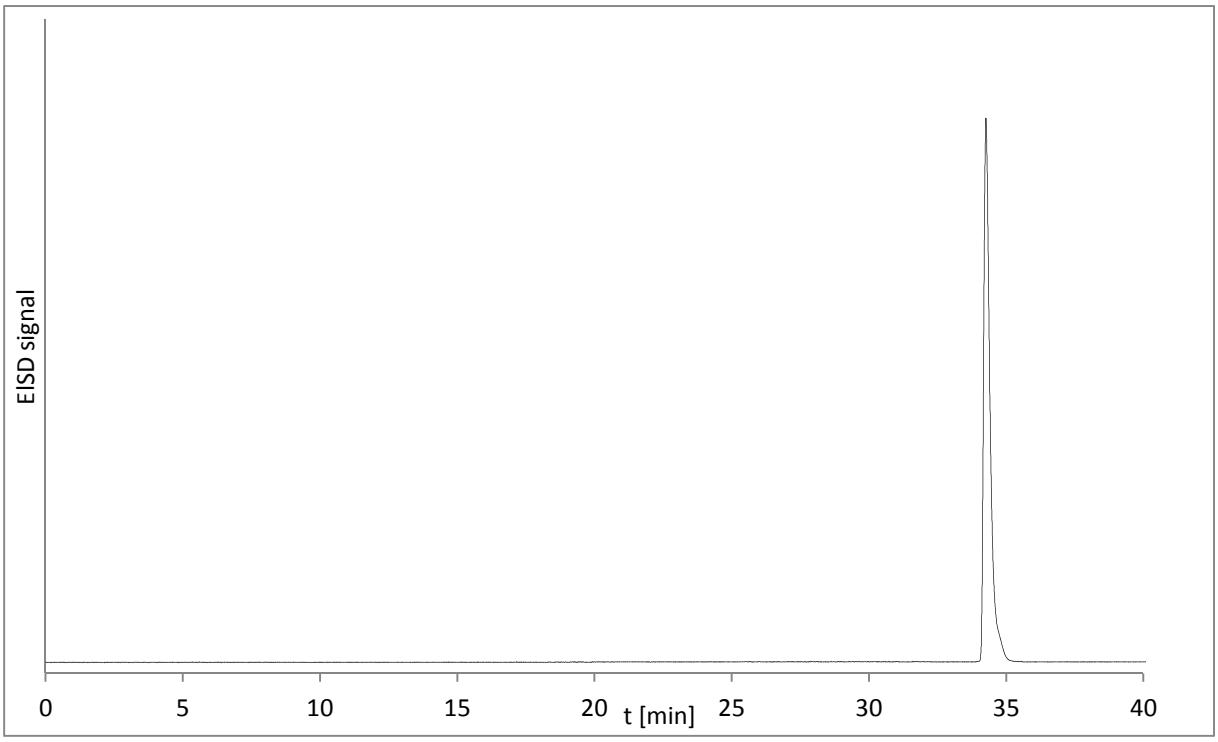

ESI-MS (positive mode), high resolution:

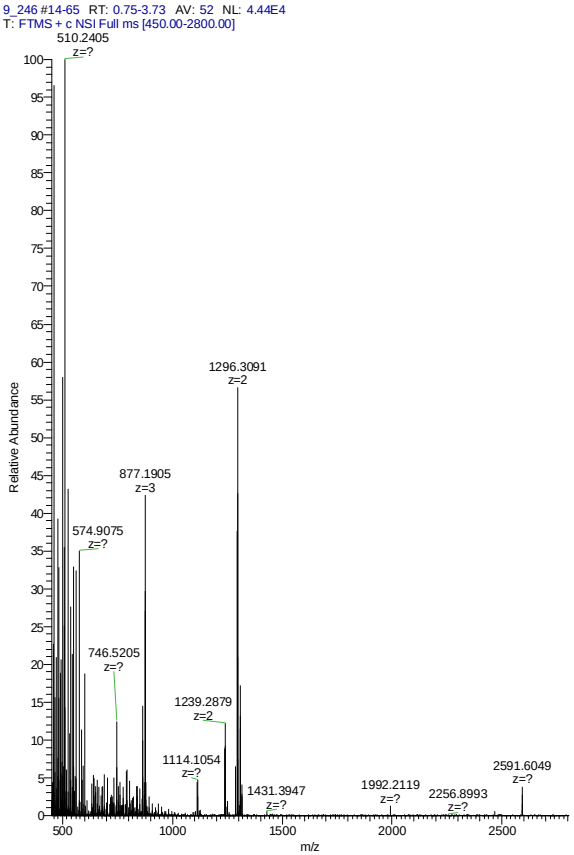

Mass reconstruction from ESI-MS (positive mode), high resolution:

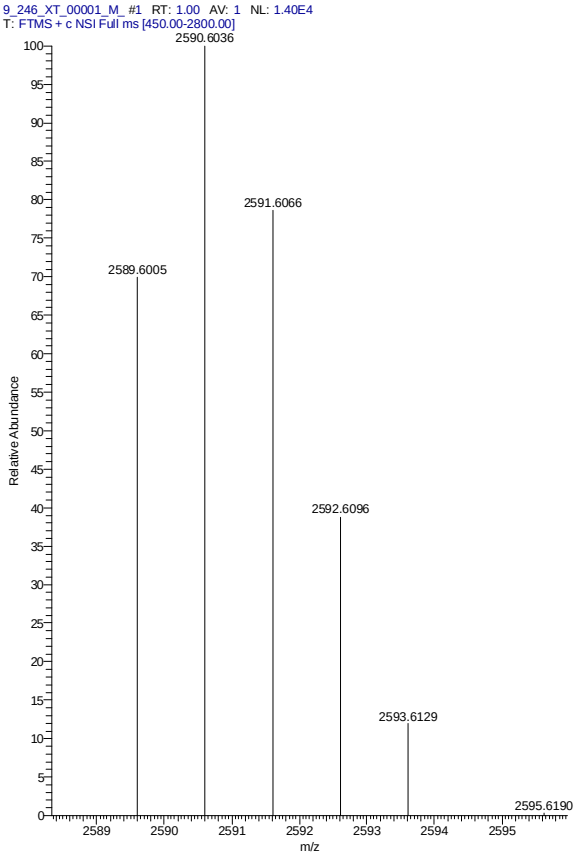

H-Glu-Val-Asn-Sta-Val-Ala-Glu-Phe-4Gl-3Gl-4Gl-3Gl-4Gl-Asp(O-*n*$C_{26}H_{53}$)-NH_2 (**6i**)

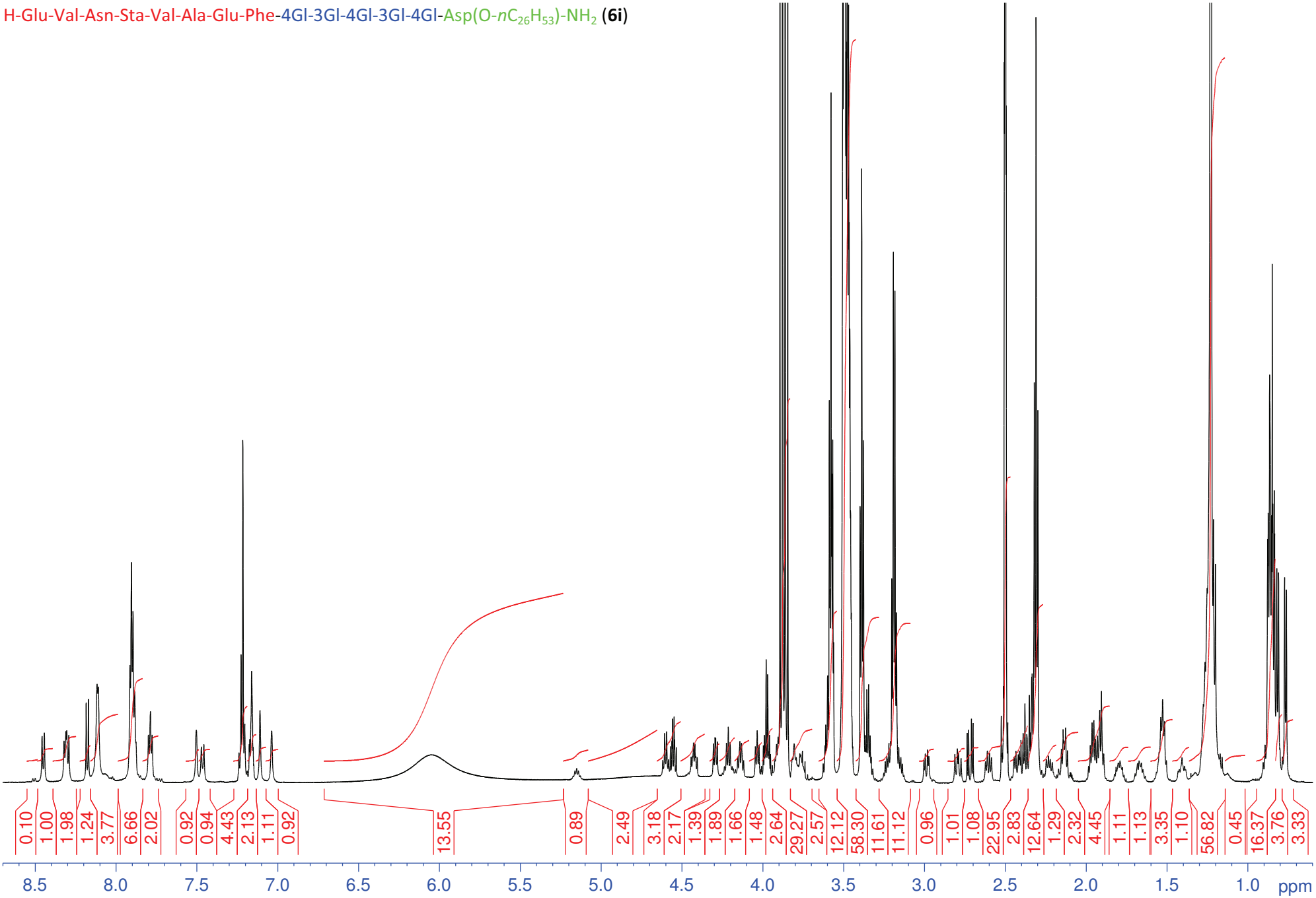

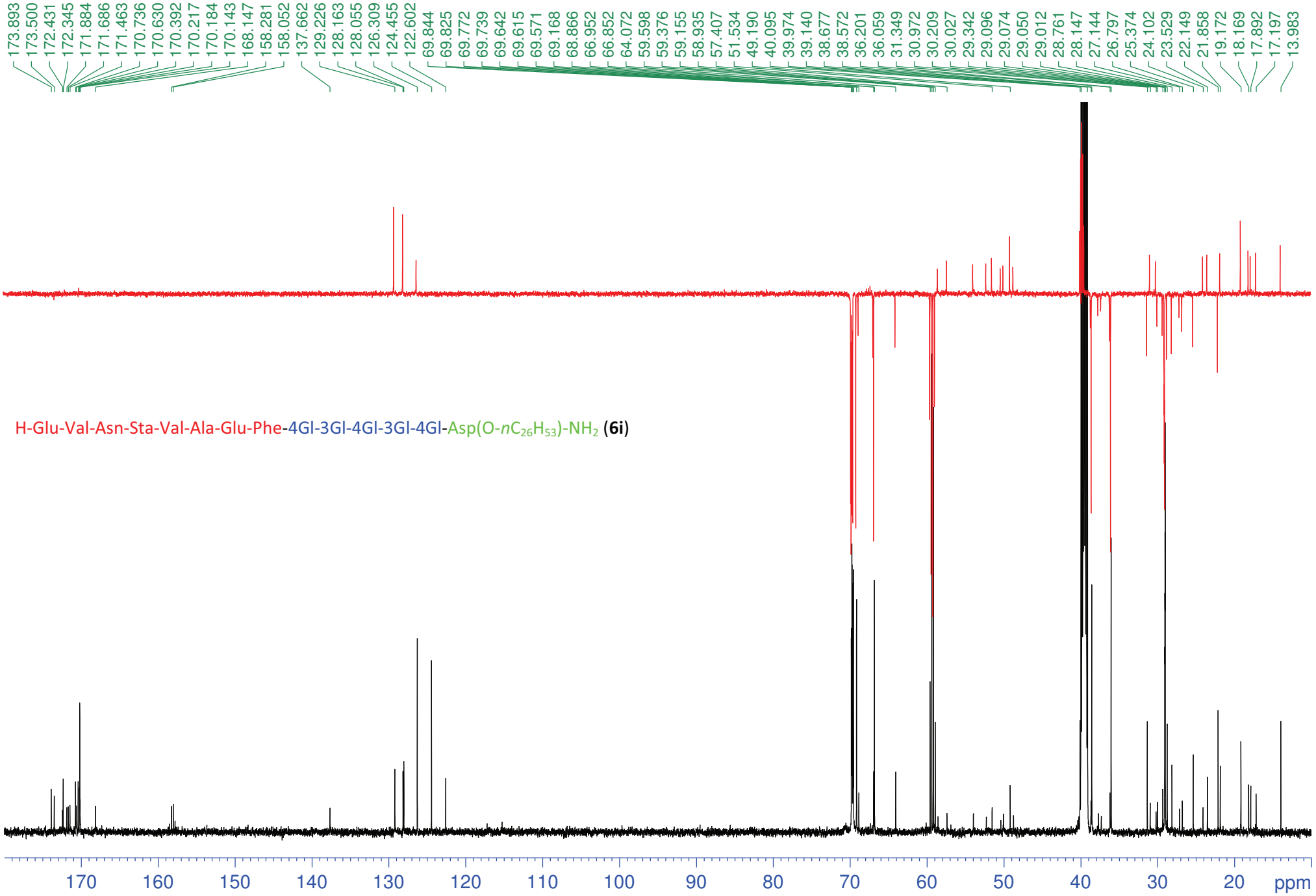

H-Glu-Val-Asn-Sta-Val-Ala-Glu-Phe-4Gl-3Gl-4Gl-3Gl-4Gl- Asp(O-oleyl)-NH_2 (**6j**)

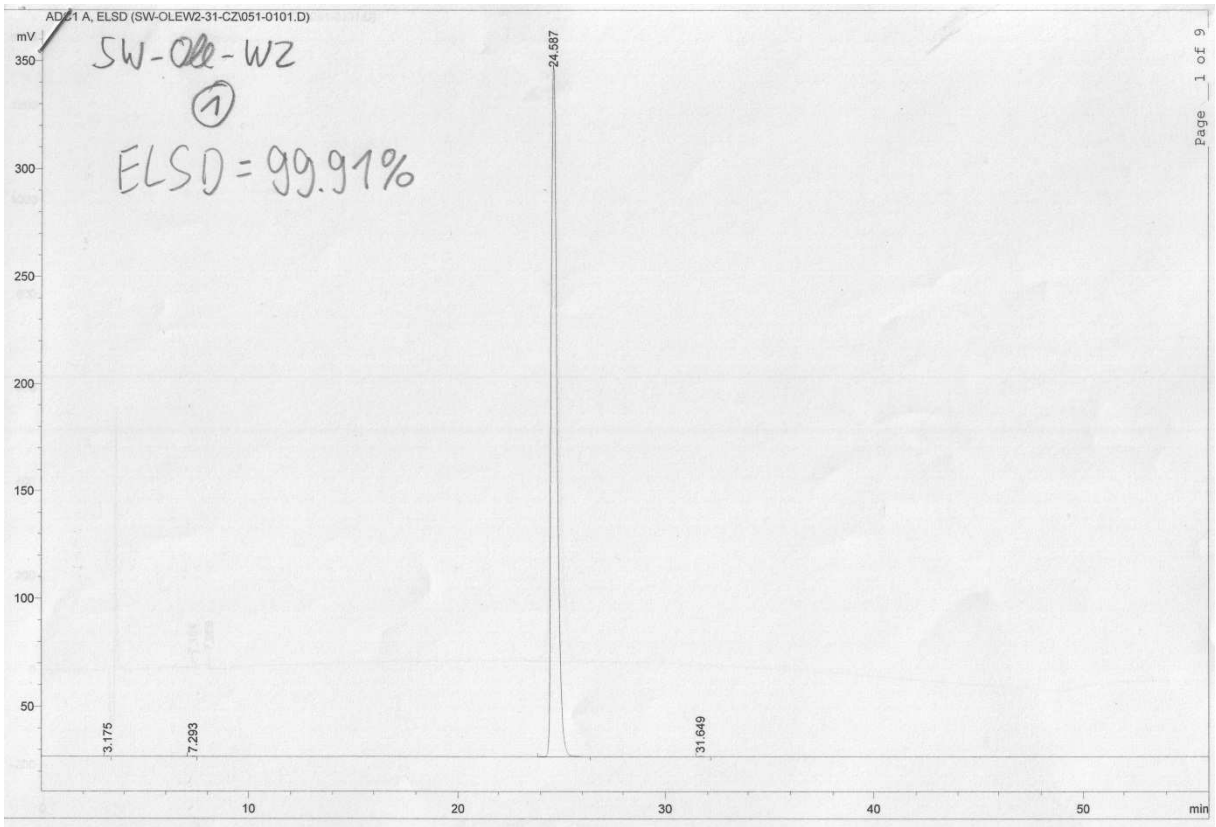

Differently from the description in the experimental section: eluent A: H_2O/MeCN (85:15) + 0.1% CF_3COOH and eluent B: MeCN + 0.1% CF_3COOH. Gradient from 10% to 100% B in 45 min.

ESI-MS (positive mode), low resolution:

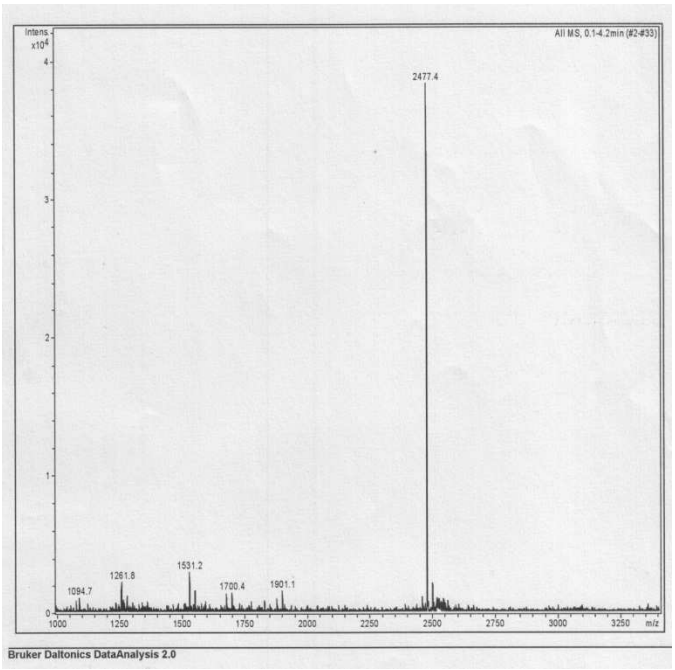

Observed mass distribution from ESI-MS (positive mode) for $[M + H]^+$, high res.:

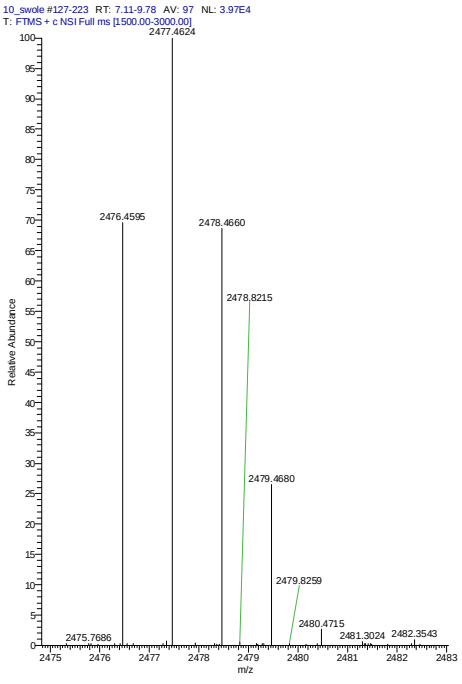

H-Glu-Val-Asn-Sta-Val-Ala-Glu-Phe-6Gl- Asp(ODhc)-NH_2 (**7a**)

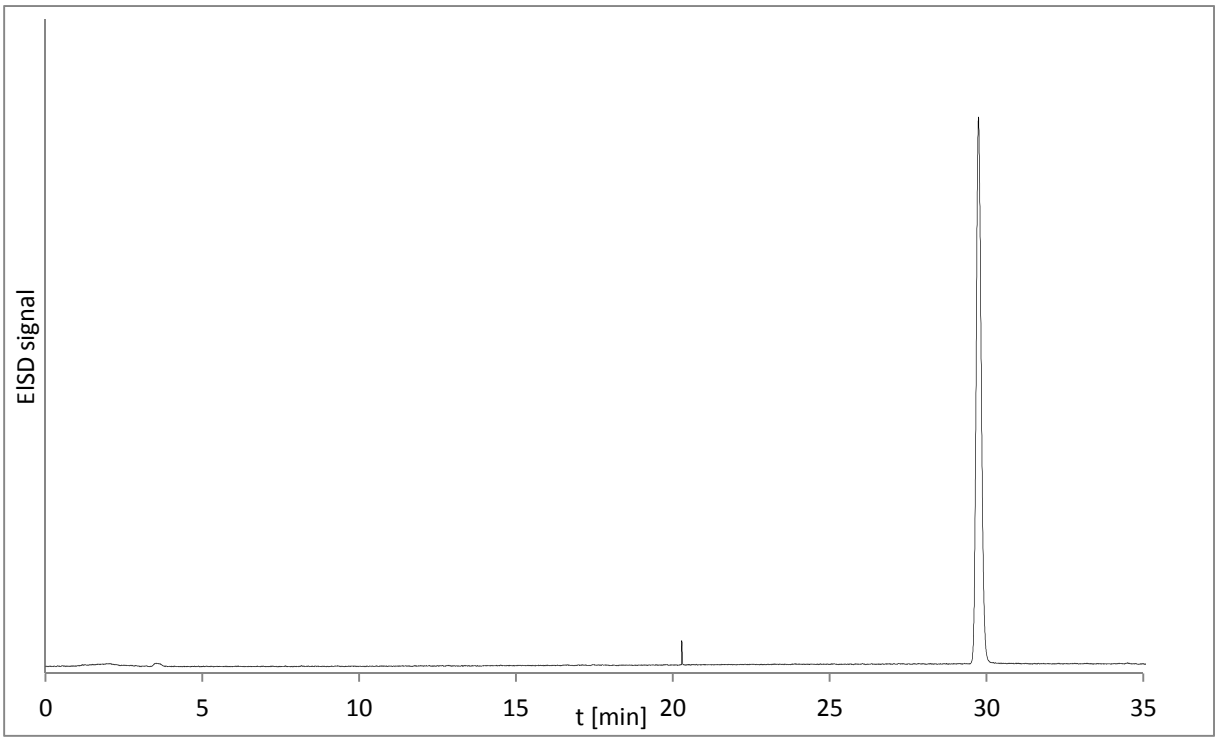

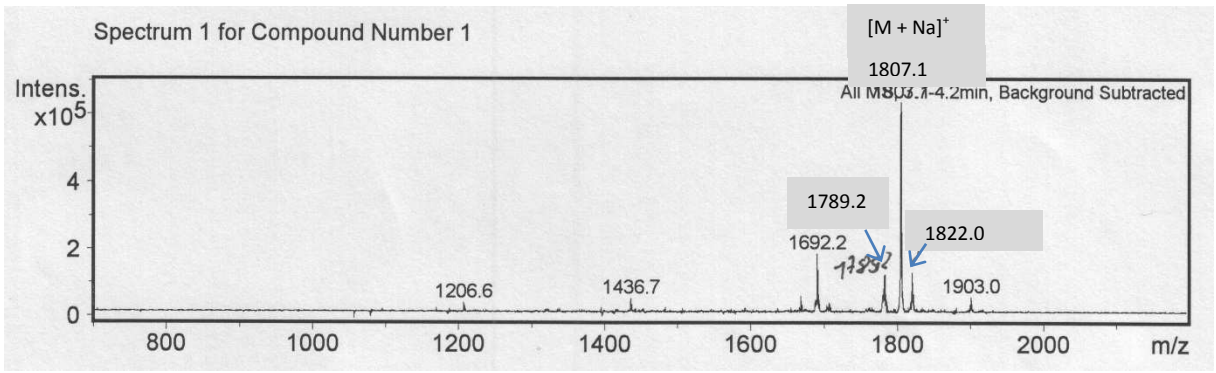

Observed mass distribution from ESI-MS (positive mode) for $[M + H]^+$, high resolution :

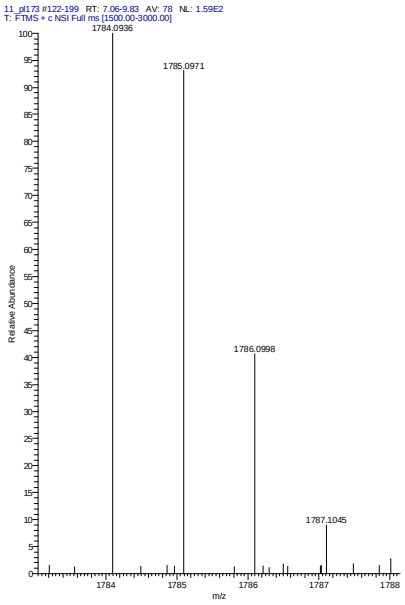

H-Glu-Val-Asn-Sta-Val-Ala-Glu-Phe-6Gl- Asp(ODhc)-NH_2 (**7a**)

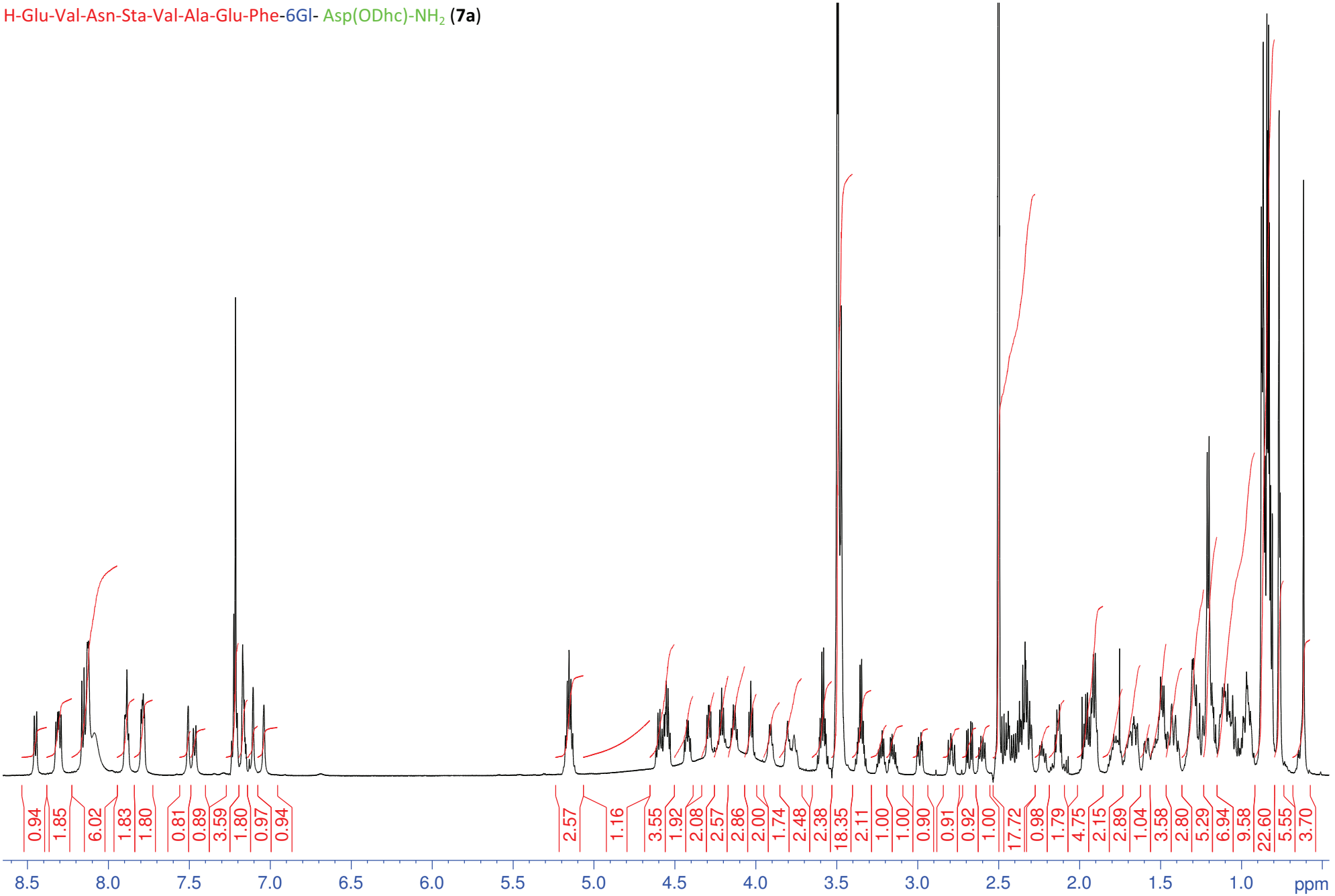

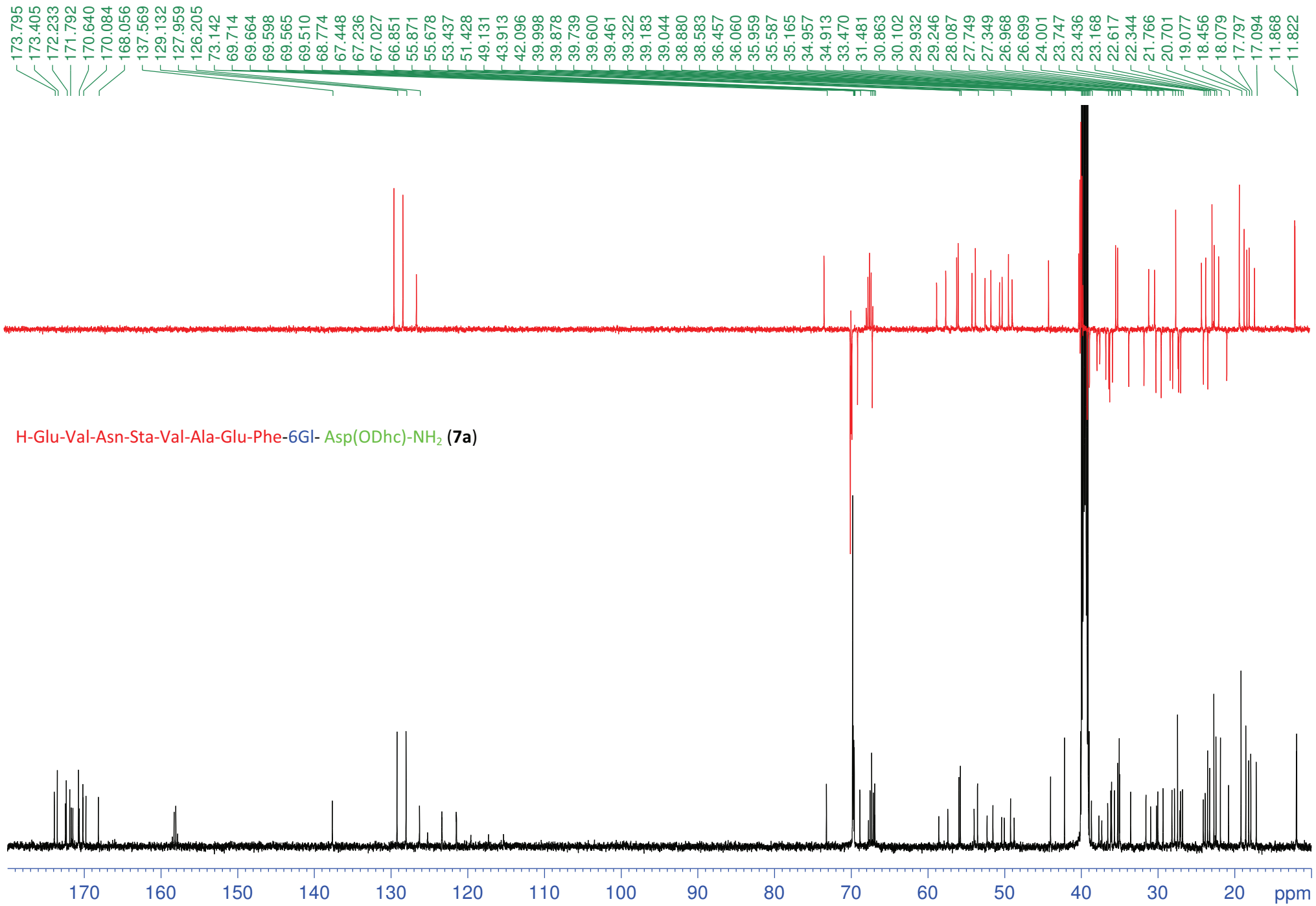

H-Glu-Val-Asn-Sta-Val-Ala-Glu-Phe-3Gl-3Gl-Asp(ODhc)-NH_2 (**7b**)

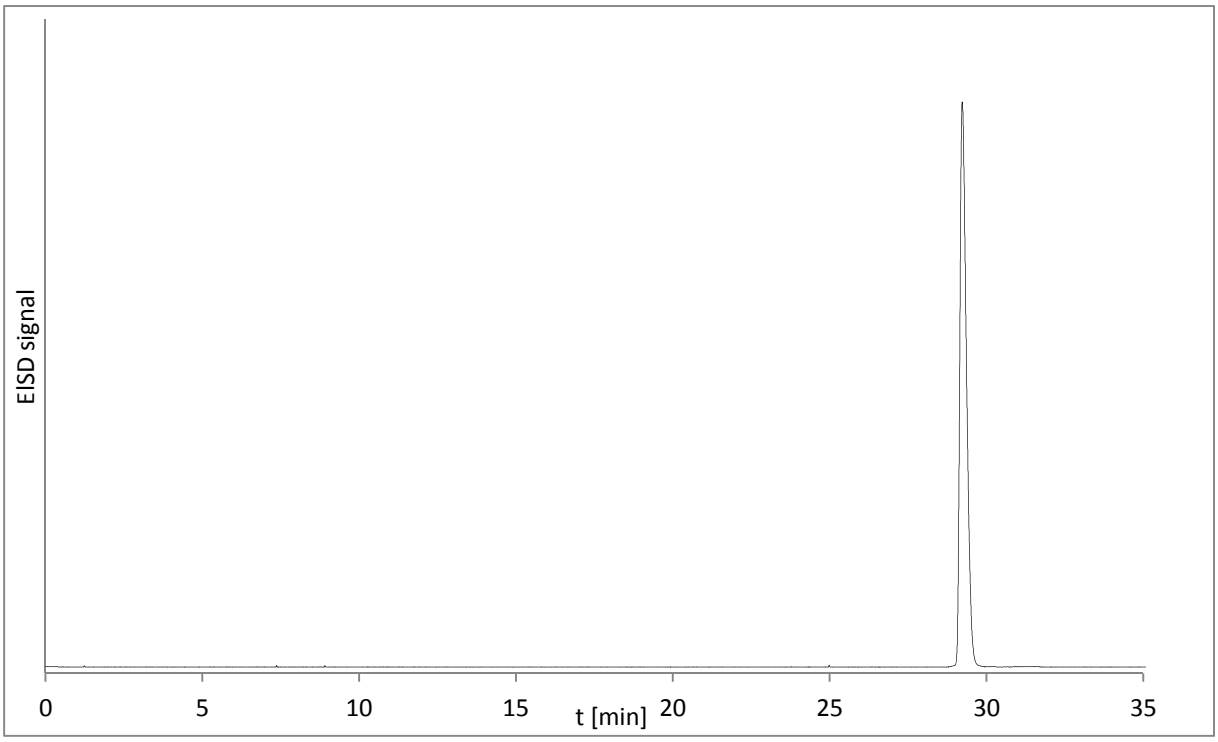

ESI-MS (positive mode), high resolution:

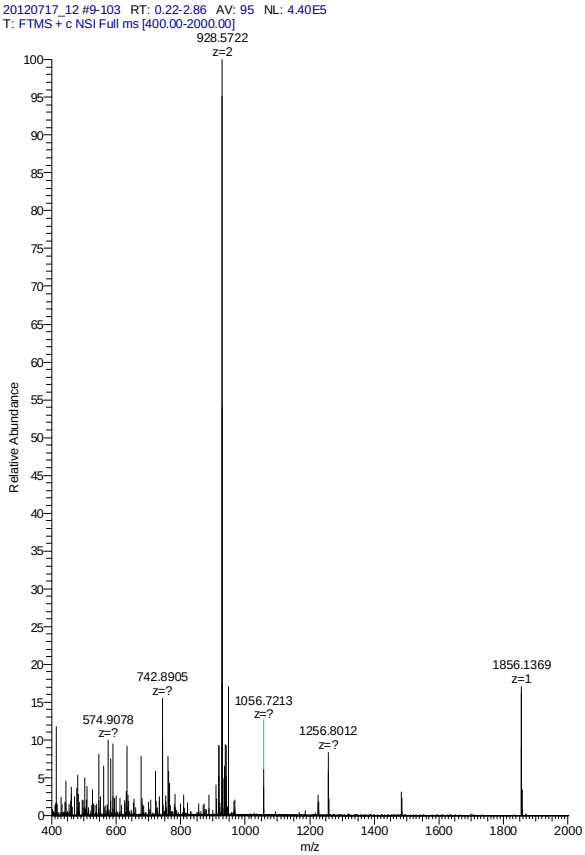

Mass reconstruction from ESI-MS (positive mode), high resolution:

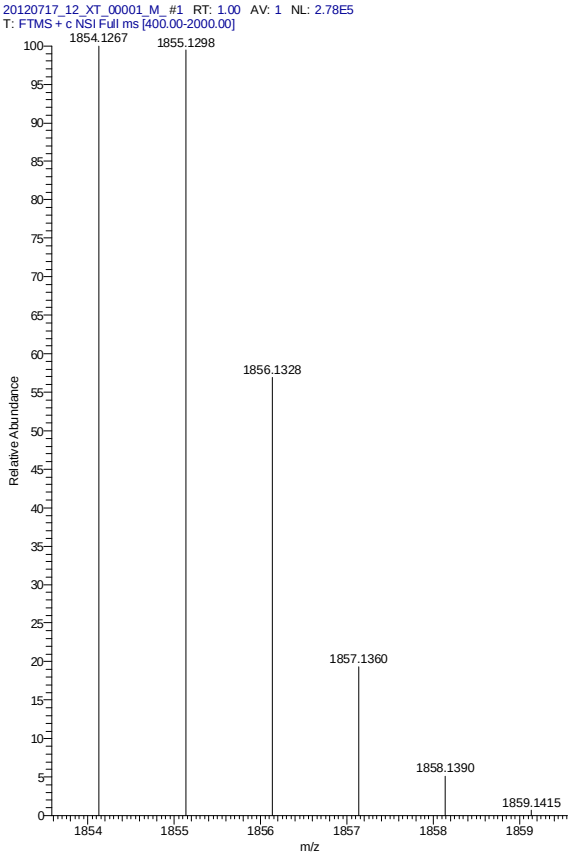

H-Glu-Val-Asn-Sta-Val-Ala-Glu-Phe-8Gl-Asp(ODhc)-NH_2 (**7c**)

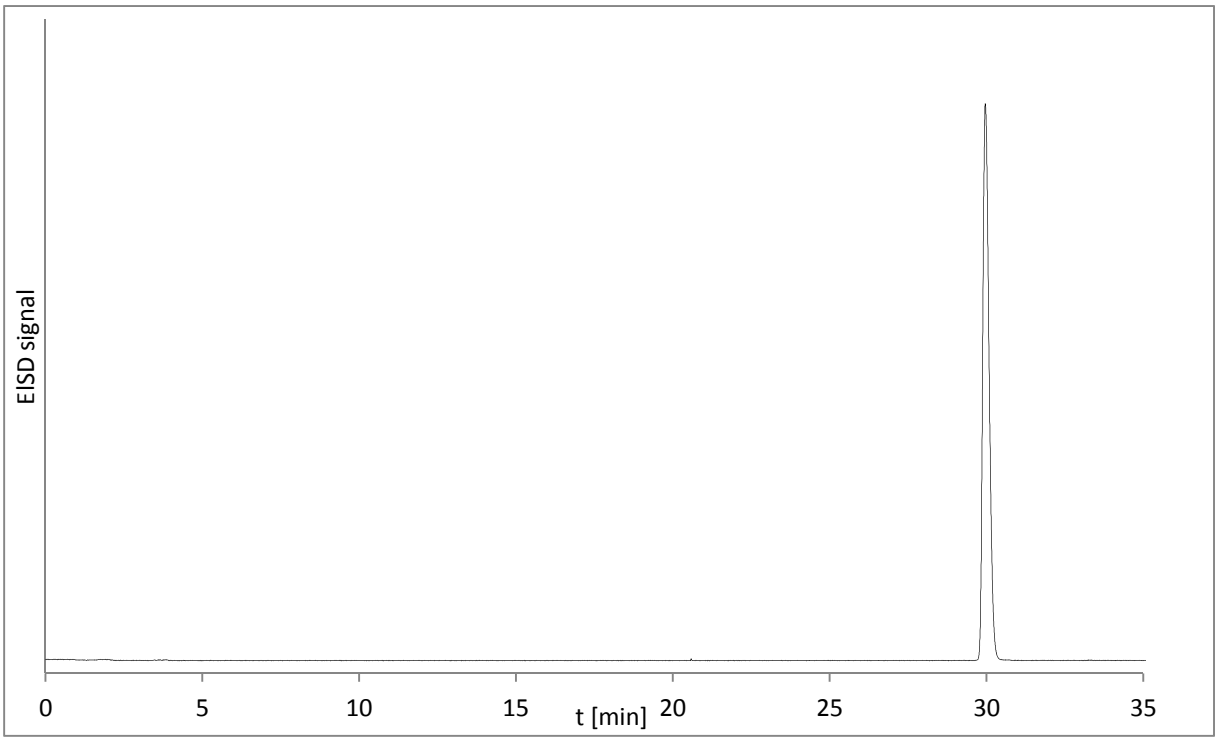

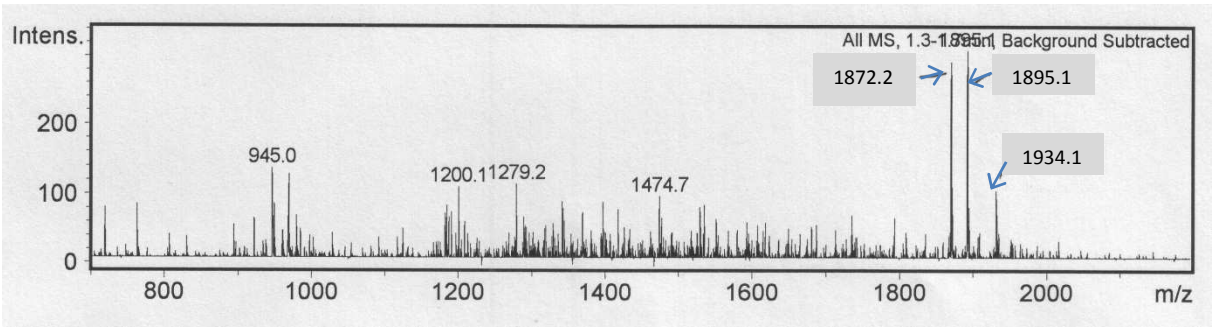

Mass reconstruction from ESI-MS (positive mode), high resolution:

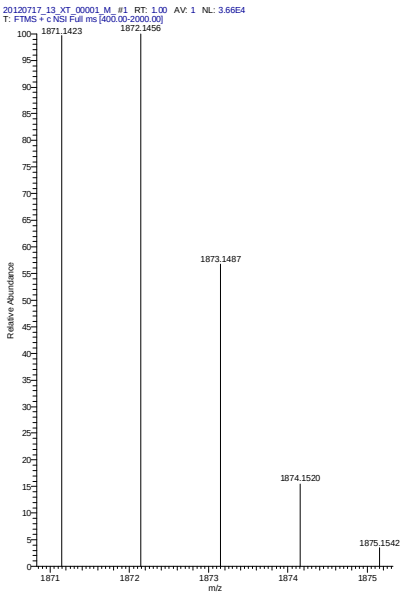

H-Glu-Val-Asn-Sta-Val-Ala-Glu-Phe-3Gl-4Gl-Asp(ODhc)-NH_2 (**7d**)

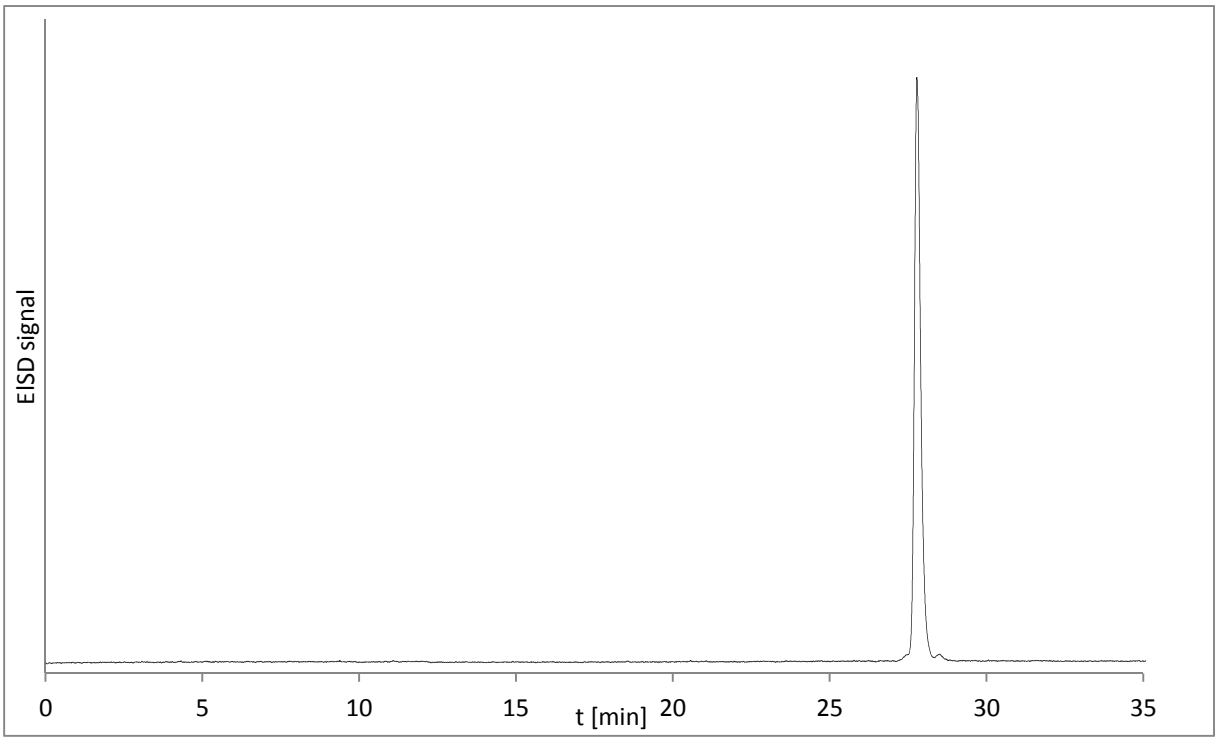

ESI-MS (positive mode), high resolution:

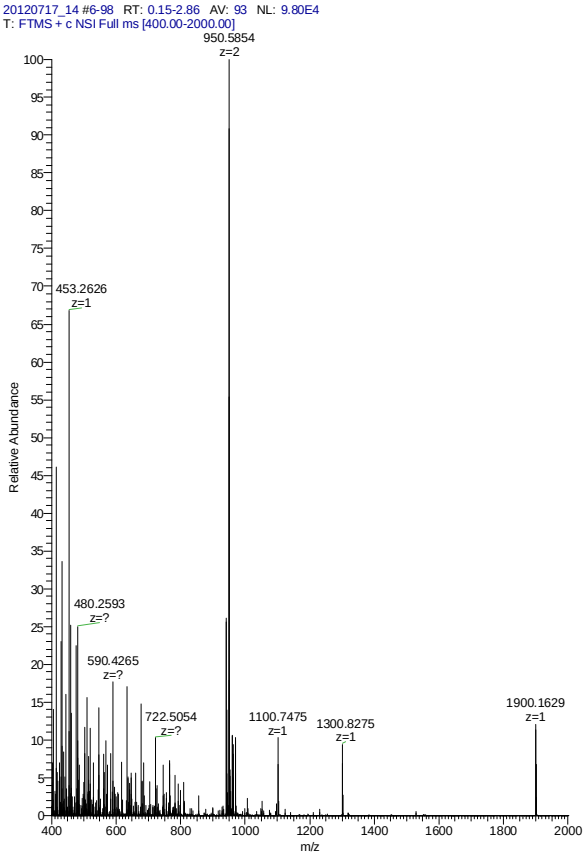

Mass reconstruction from ESI-MS (positive mode), high resolution:

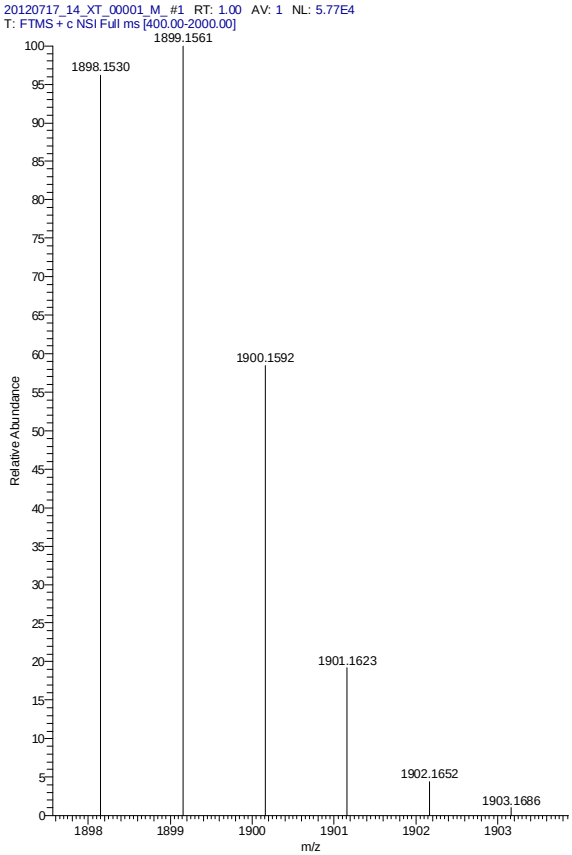

H-Glu-Val-Asn-Sta-Val-Ala-Glu-Phe-3Gl-3Gl-3Gl-Asp(ODhc)-NH_2 (**7e**)

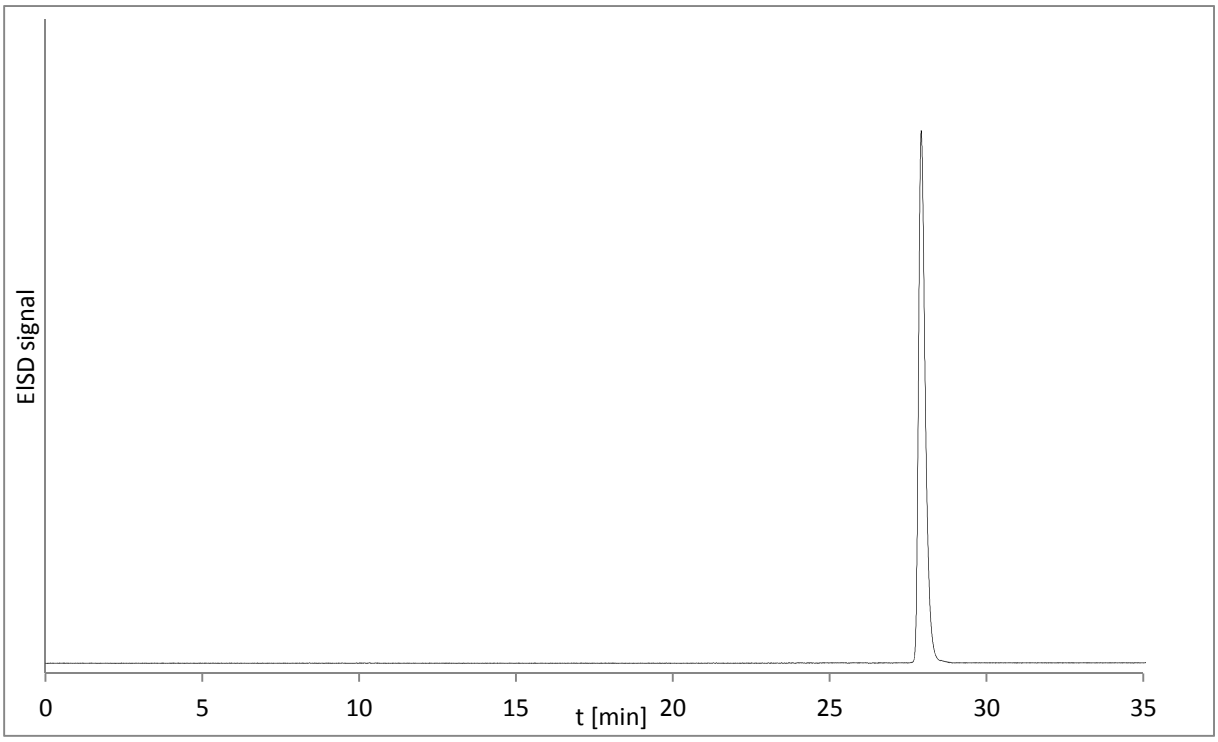

ESI-MS (positive mode), high resolution:

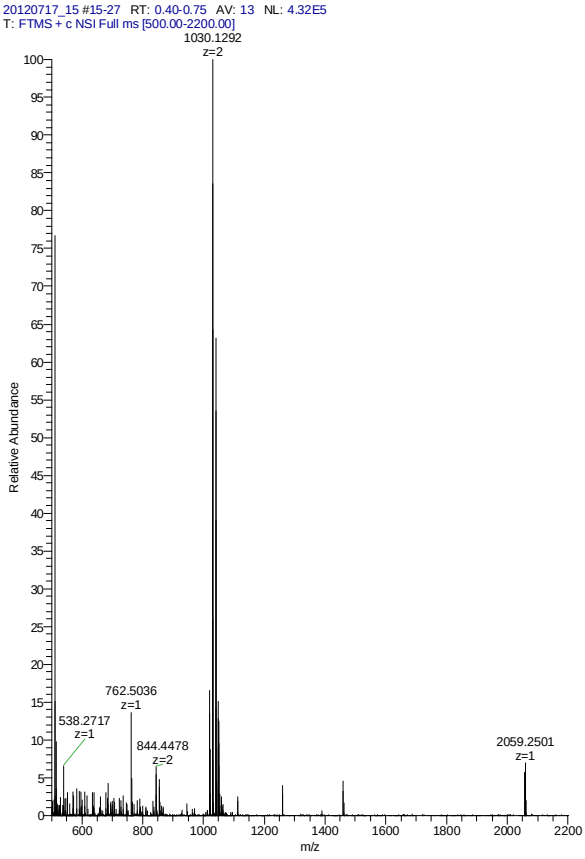

Mass reconstruction from ESI-MS (positive mode), high resolution:

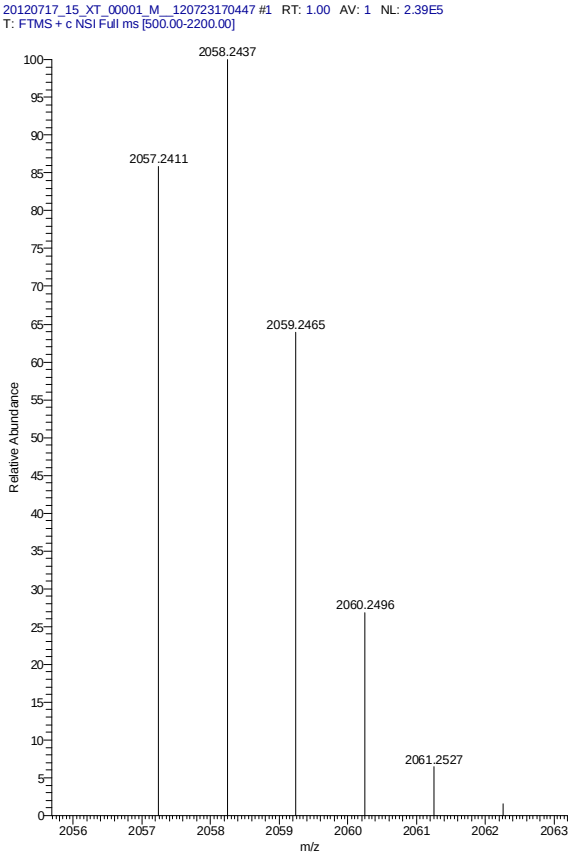

H-Glu-Val-Asn-Sta-Val-Ala-Glu-Phe-12Gl-Asp(ODhc)-NH_2 (**7f**)

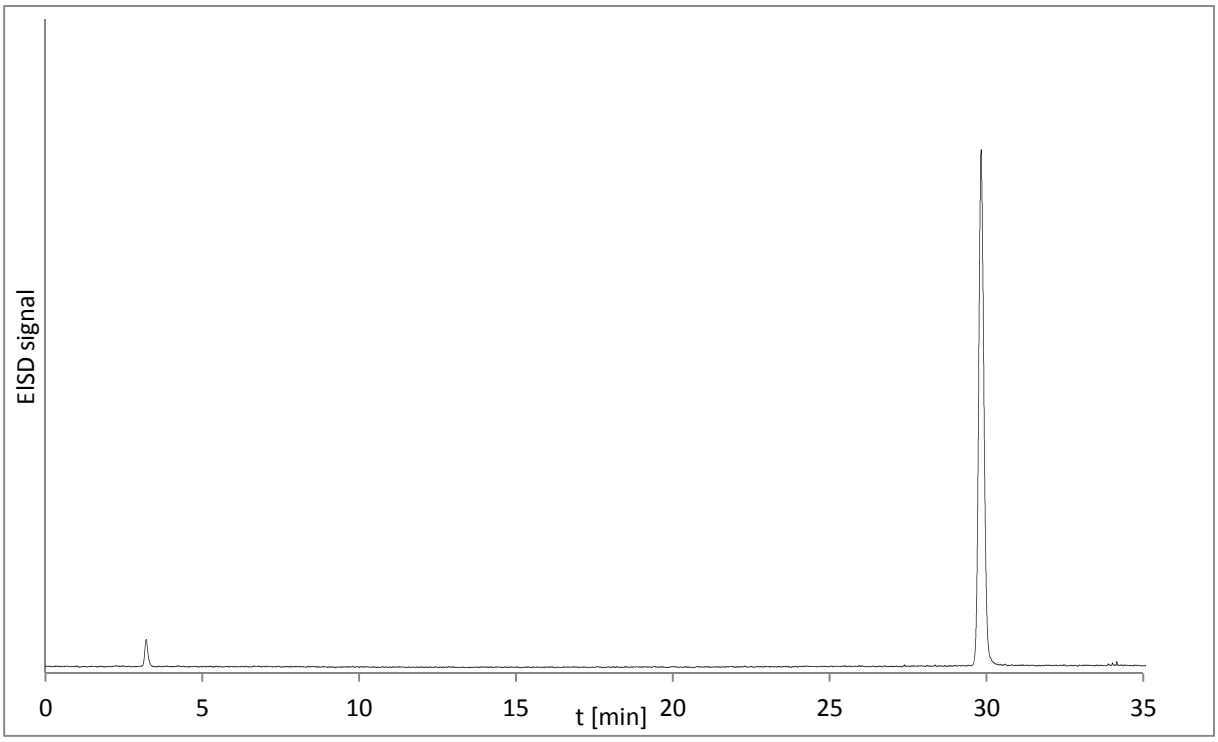

ESI-MS (negative mode):

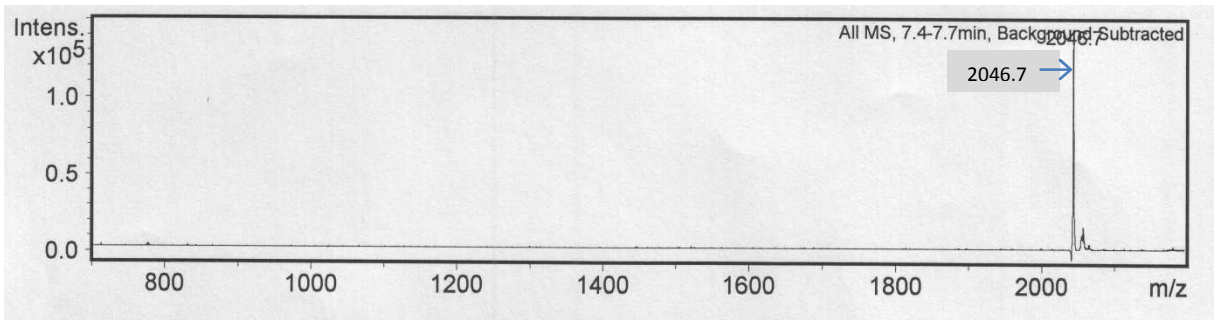

Mass reconstruction from ESI-MS (positive mode), high resolution:

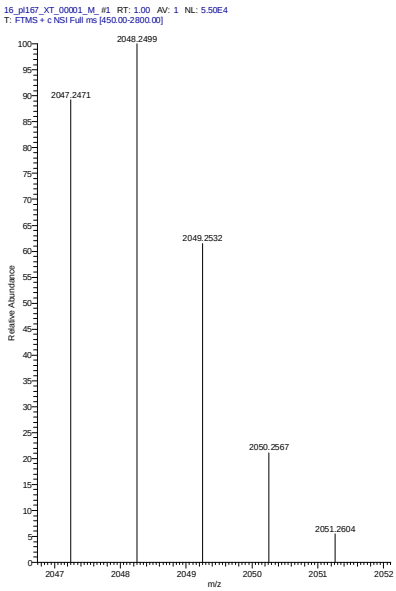

H-Glu-Val-Asn-Sta-Val-Ala-Glu-Phe-3Gl-4Gl-3Gl-Asp(ODhc)-NH_2 (**7g**)

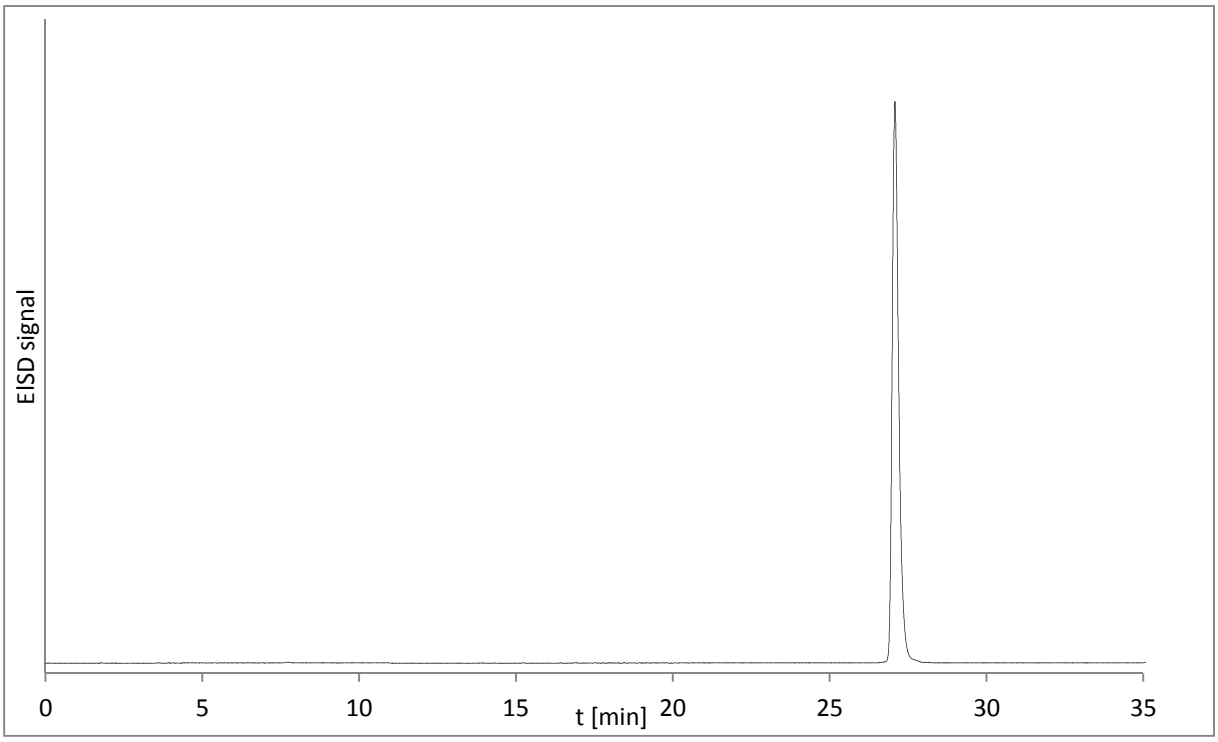

ESI-MS (positive mode), low resolution:

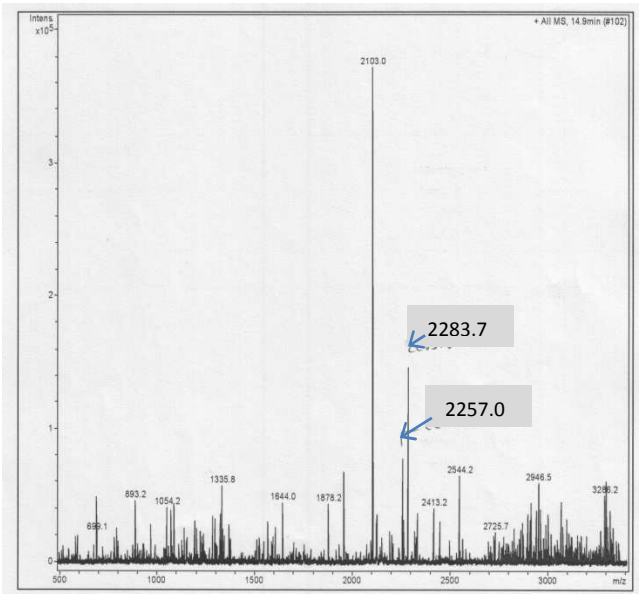

Observed mass distribution from ESI-MS (positive mode) for $[M + H]^+$, high res.:

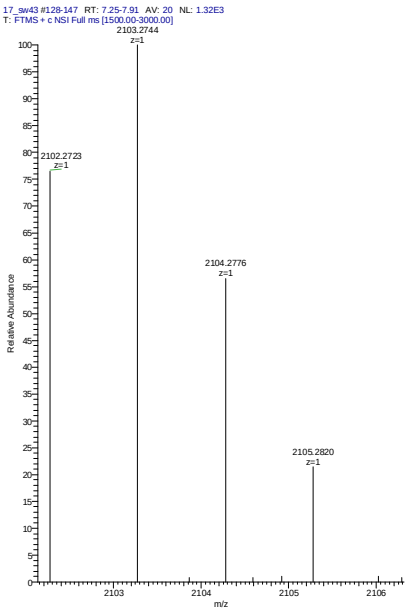

H-Glu-Val-Asn-Sta-Val-Ala-Glu-Phe-6Gl-6Gl-Asp(ODhc)-NH_2 (**7h**)

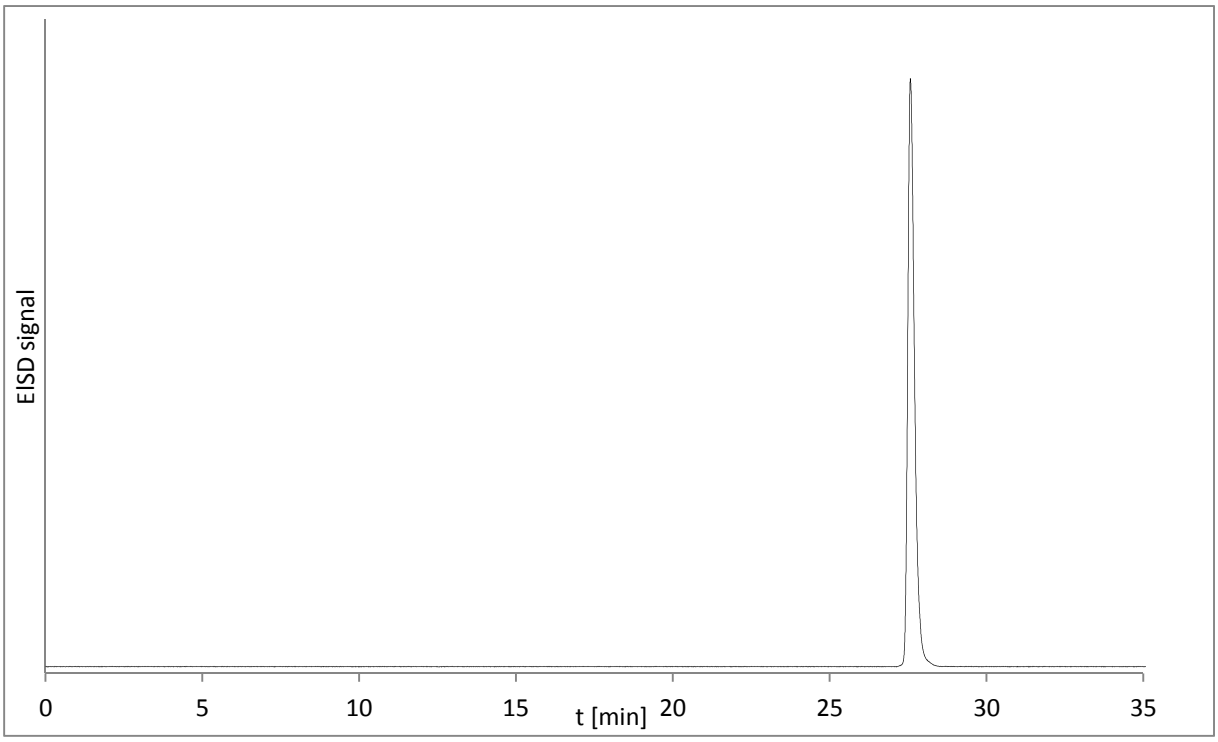

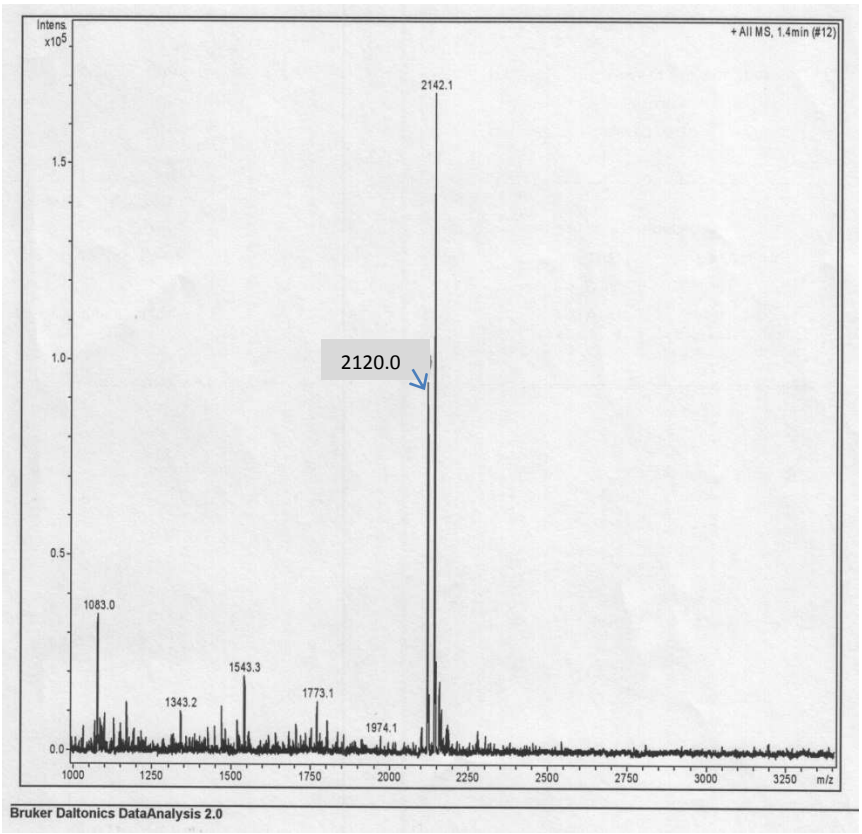

H-Glu-Val-Asn-Sta-Val-Ala-Glu-Phe-4Gl-3Gl-4Gl-Asp(ODhc)-NH_2 (**7i**)

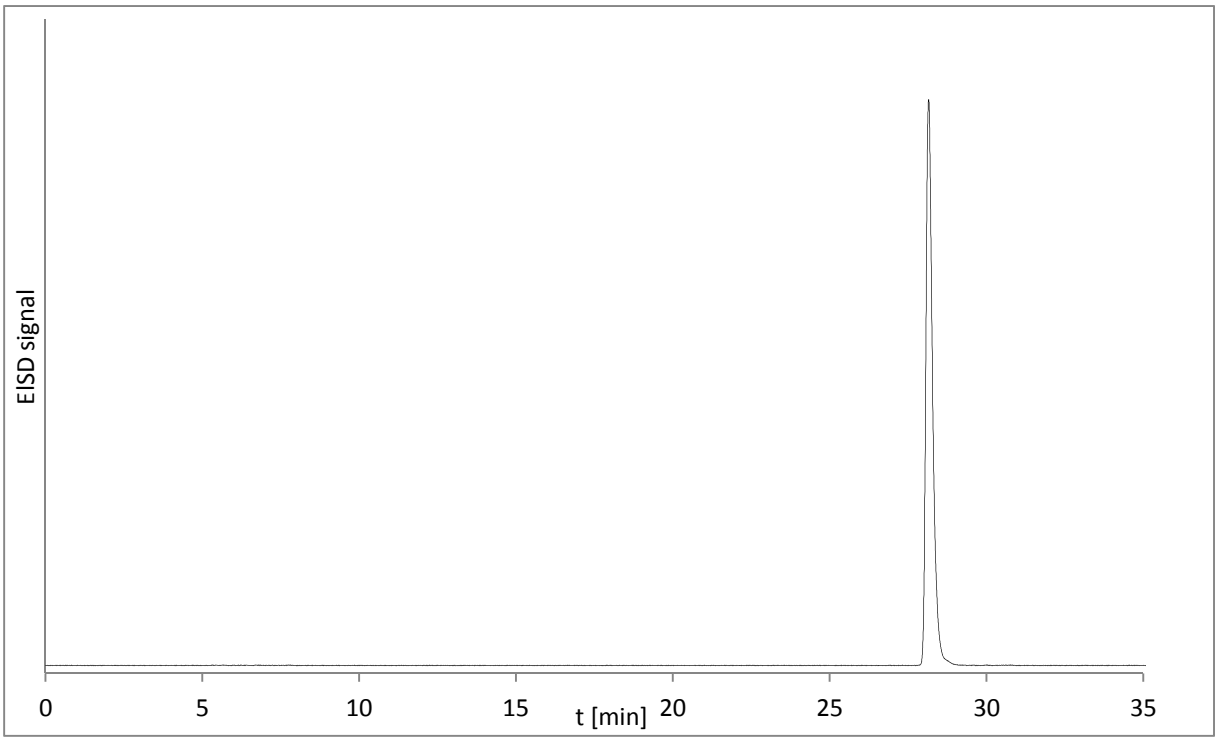

ESI-MS (positive mode), high resolution:

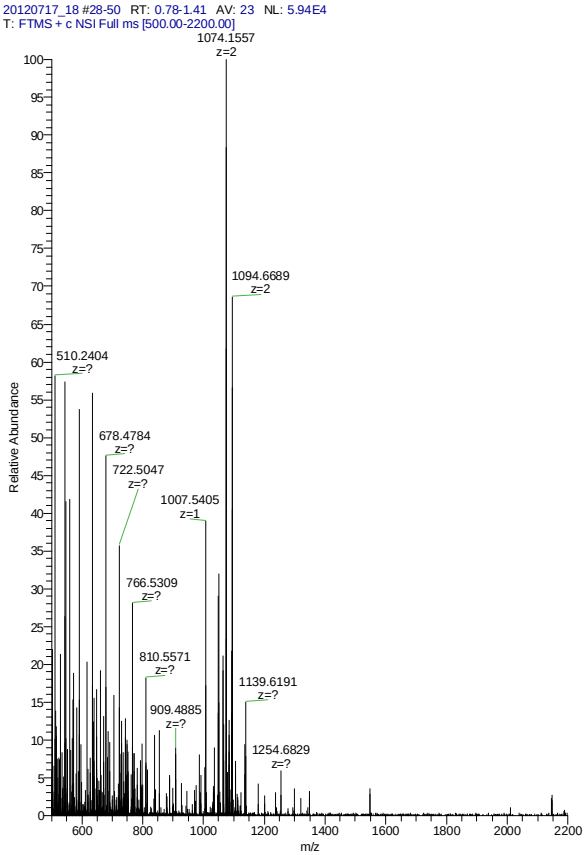

Mass reconstruction from ESI-MS (positive mode), high resolution:

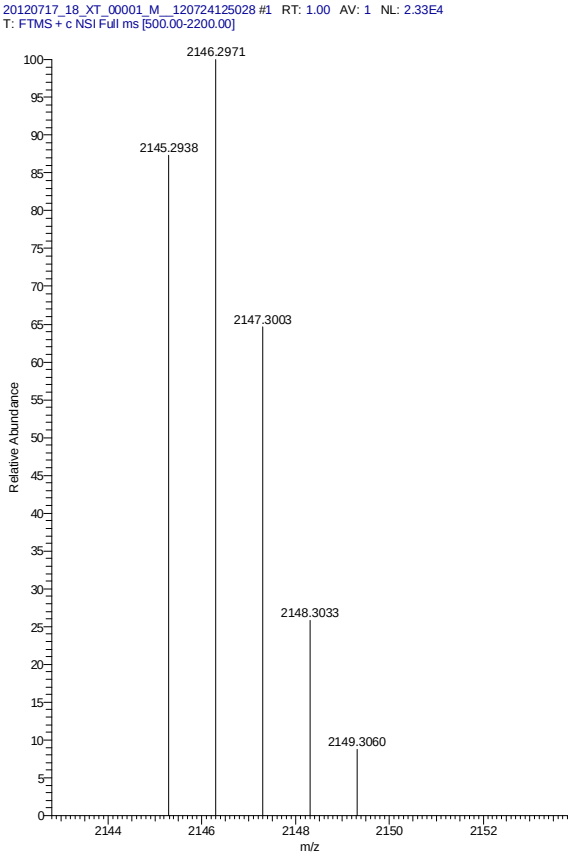

H-Glu-Val-Asn-Sta-Val-Ala-Glu-Phe-*p*Ar-3Gl-*p*Ar-3Gl-*p*Ar-Asp(ODhc)-NH_2 (**7j**)

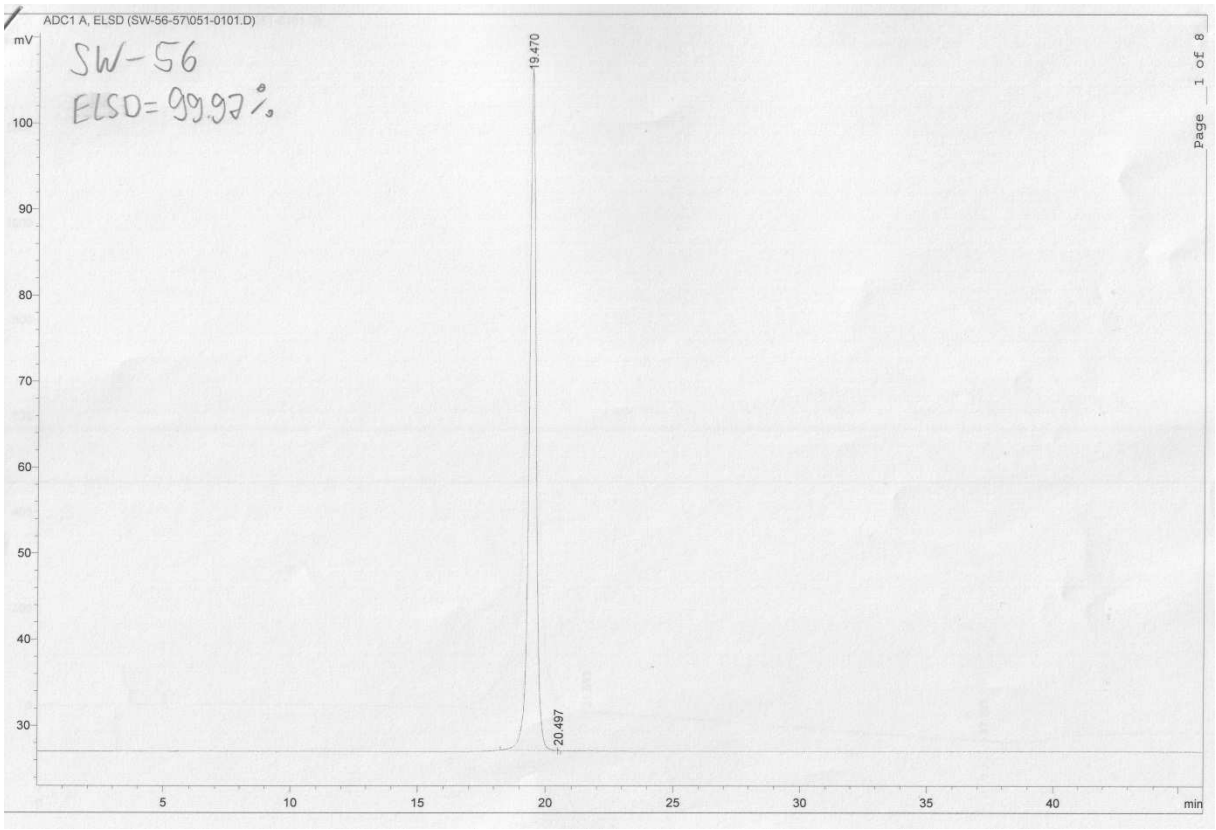

Differently from the description in the experimental section: eluent A: H_2O/MeCN (85:15) + 0.1% CF_3COOH and eluent B: MeCN + 0.1% CF_3COOH. Gradient from 30% to 100% B in 35 min.

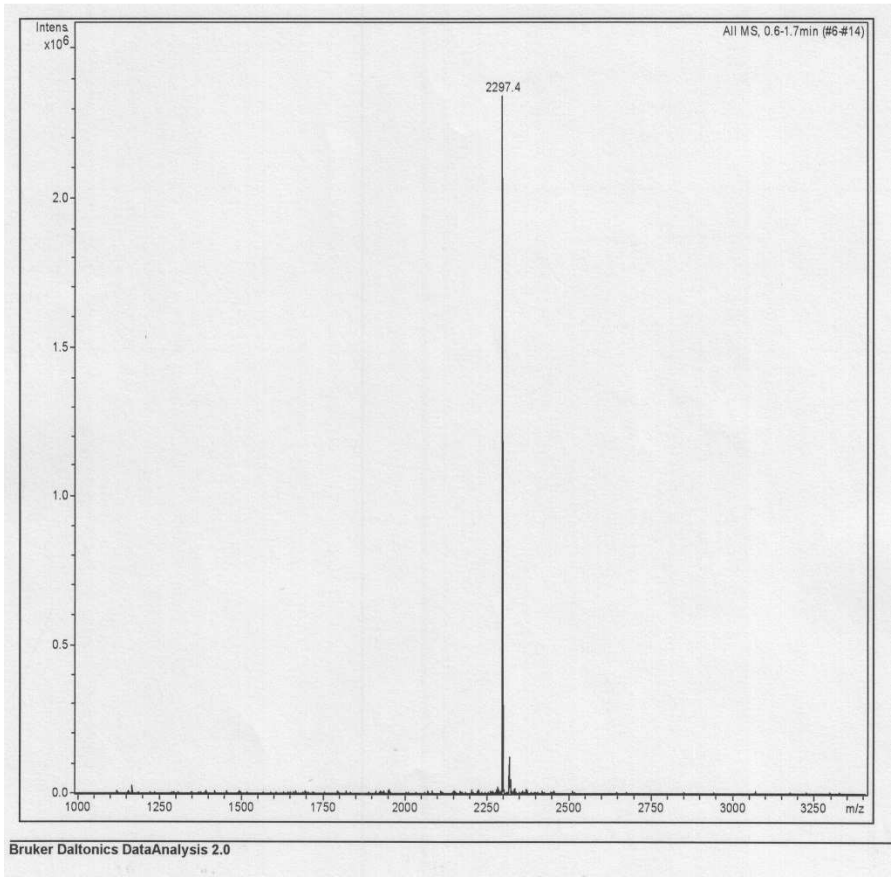

H-Glu-Val-Asn-Sta-Val-Ala-Glu-Phe-*m*Ar-3Gl-*m*Ar-3Gl-*m*Ar-Asp(ODhc)-NH_2 (**7k**)

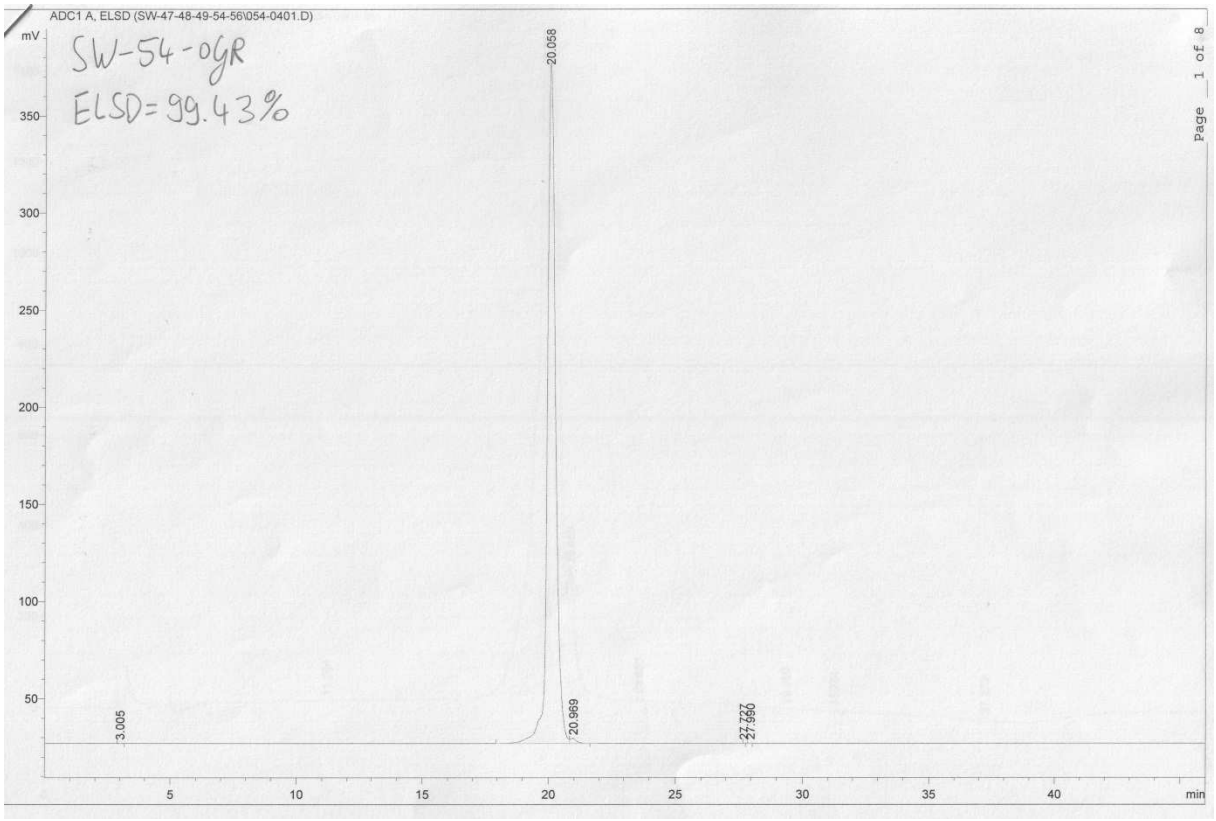

Differently from the description in the experimental section: eluent A: H_2O/MeCN (85:15) + 0.1% CF_3COOH and eluent B: MeCN + 0.1% CF_3COOH. Gradient from 30% to 100% B in 35 min.

ESI-MS (positive mode), high resolution:

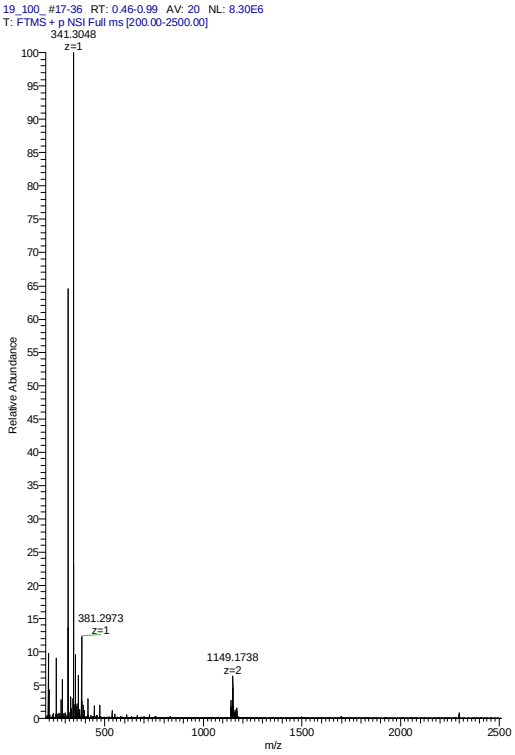

Mass reconstruction from ESI-MS (positive mode), high resolution:

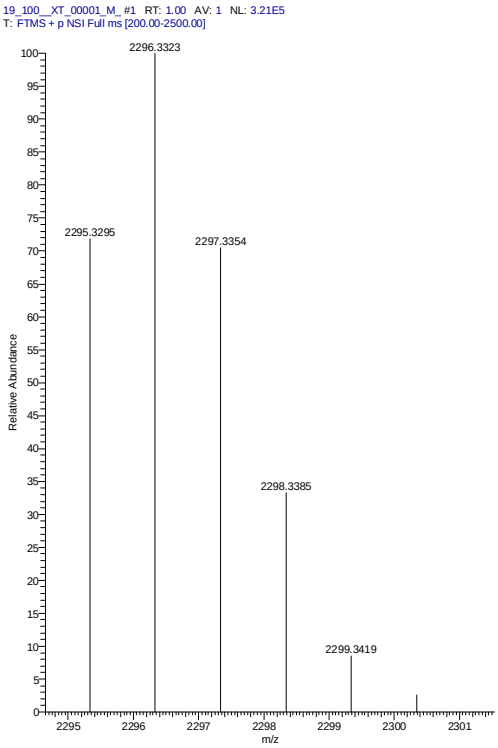

H-Glu-Val-Asn-Sta-Val-Ala-Glu-Phe-4Gl-4Gl-4Gl-Asp(ODhc)-NH_2 (**7l**)

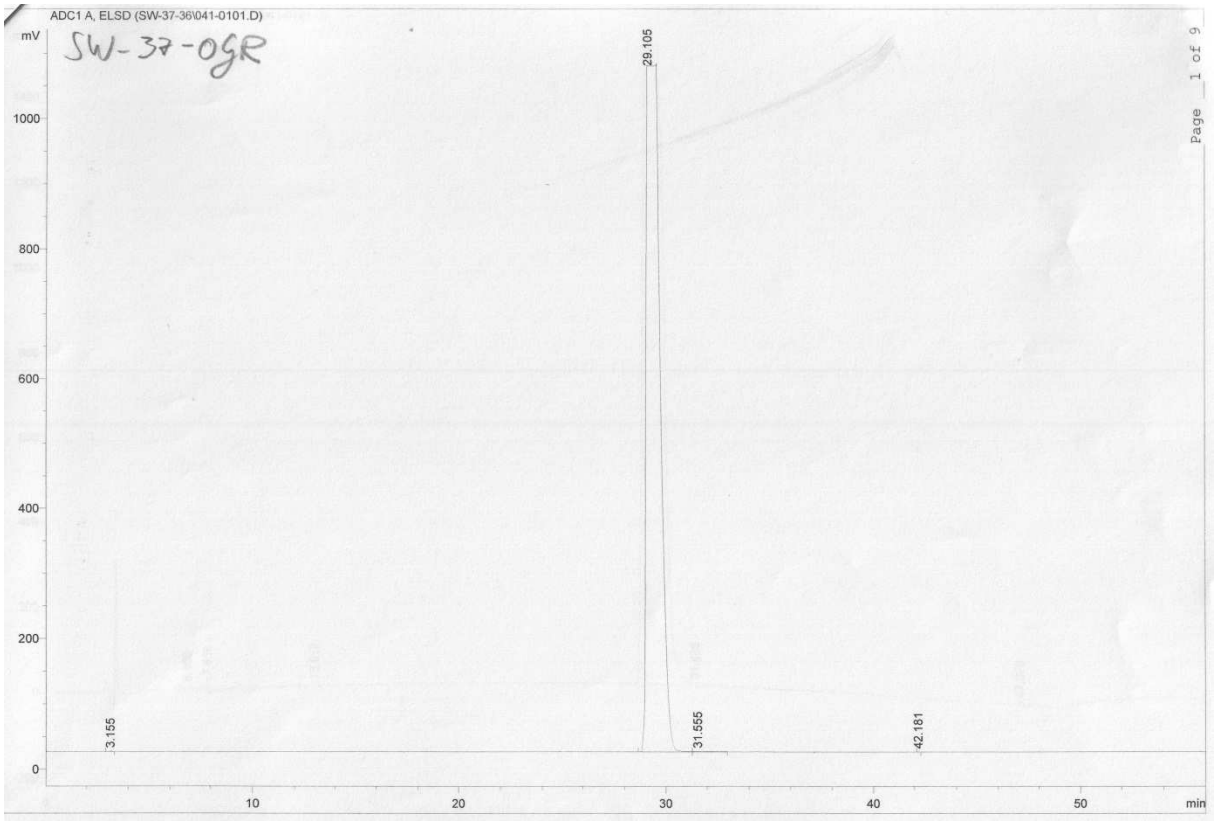

Differently from the description in the experimental section: eluent A: H_2O/MeCN (85:15) + 0.1% CF_3COOH and eluent B: MeCN + 0.1% CF_3COOH. Gradient from 10% to 100% B in 45 min.

ESI-MS (negative mode):

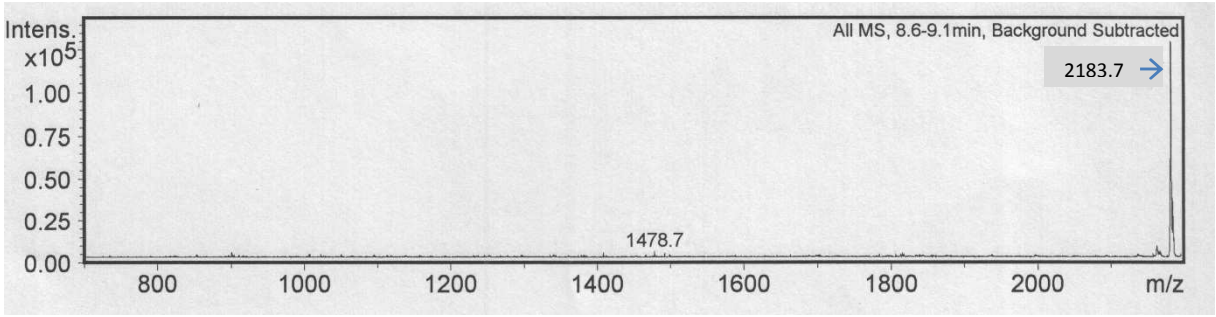

Mass reconstruction from ESI-MS (positive mode), high resolution:

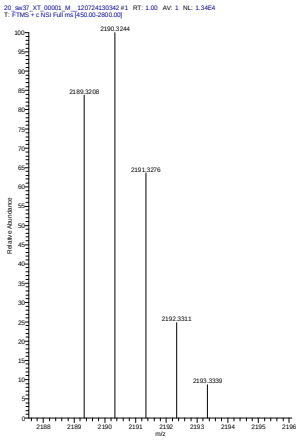

H-Glu-Val-Asn-Sta-Val-Ala-Glu-Phe-4Gl-4Gl-4Gl-Asp(ODhc)-NH_2 (**7l**)

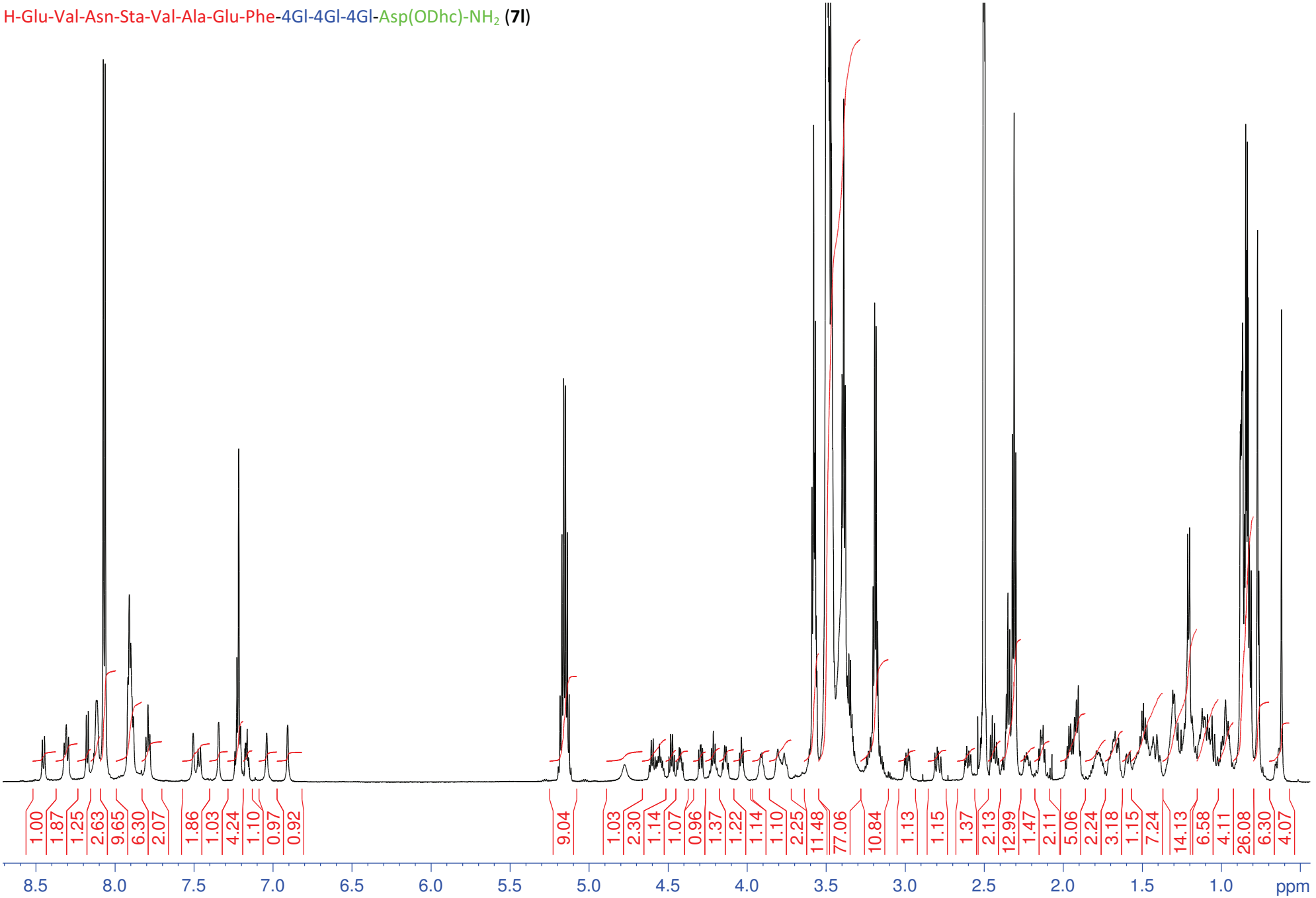

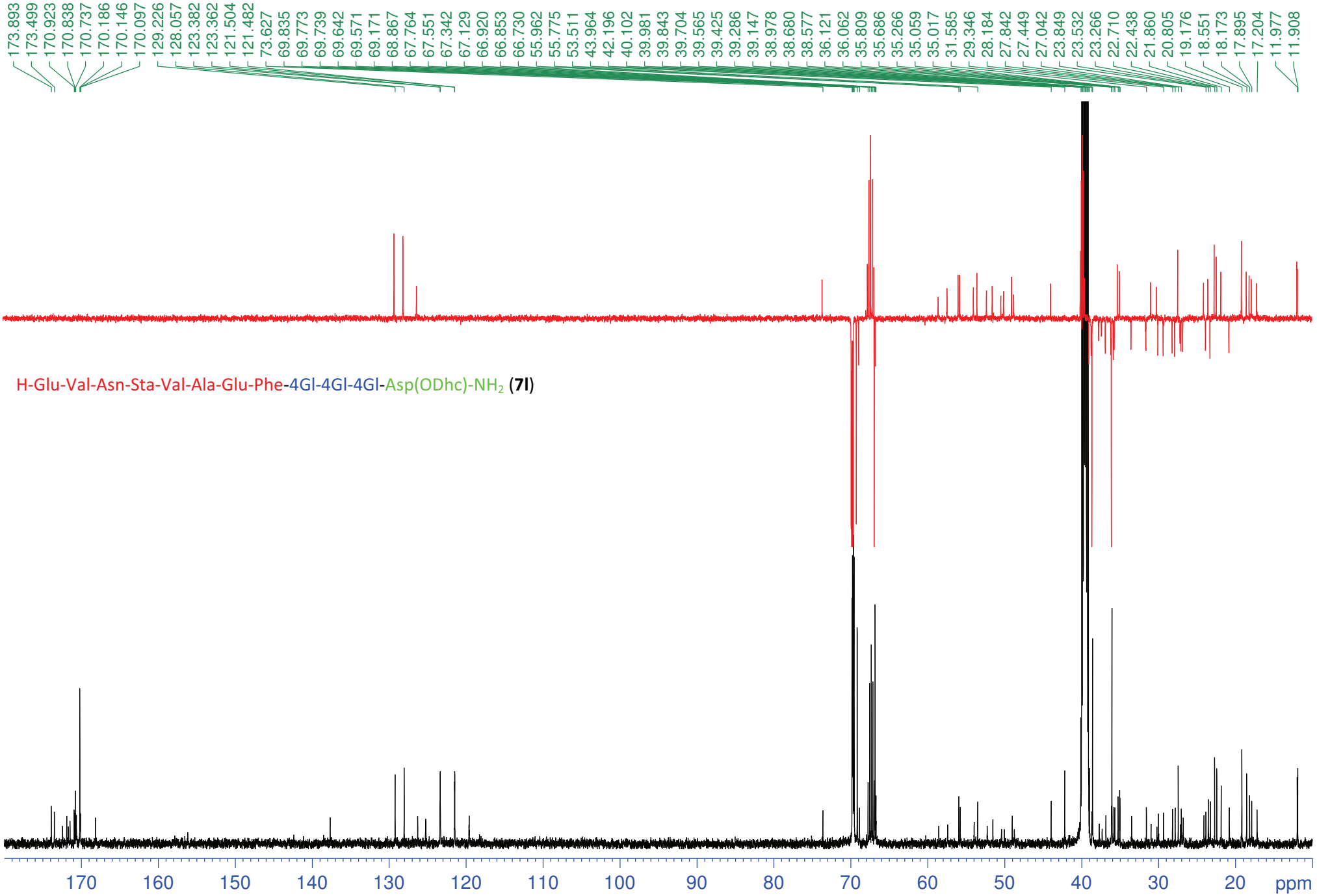

H-Glu-Val-Asn-Sta-Val-Ala-Glu-Phe-16Gl-Asp(ODhc)-NH_2 (**7m**)

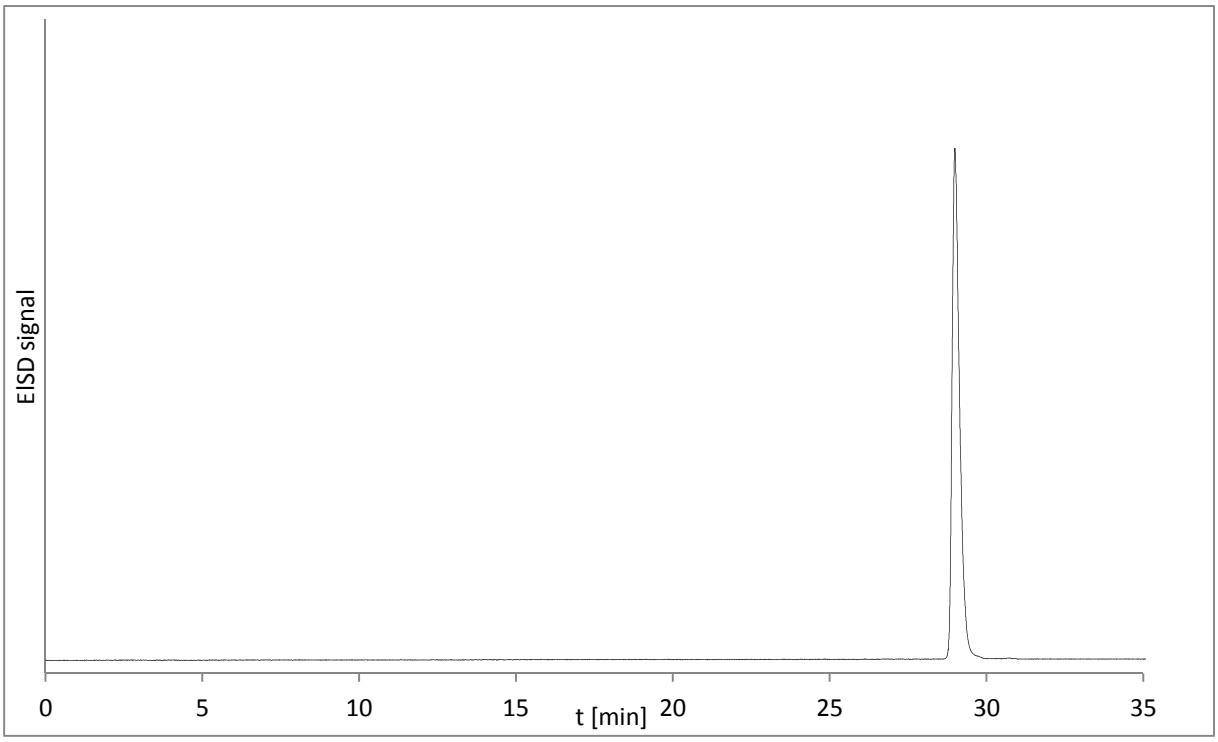

ESI-MS (positive mode), high resolution:

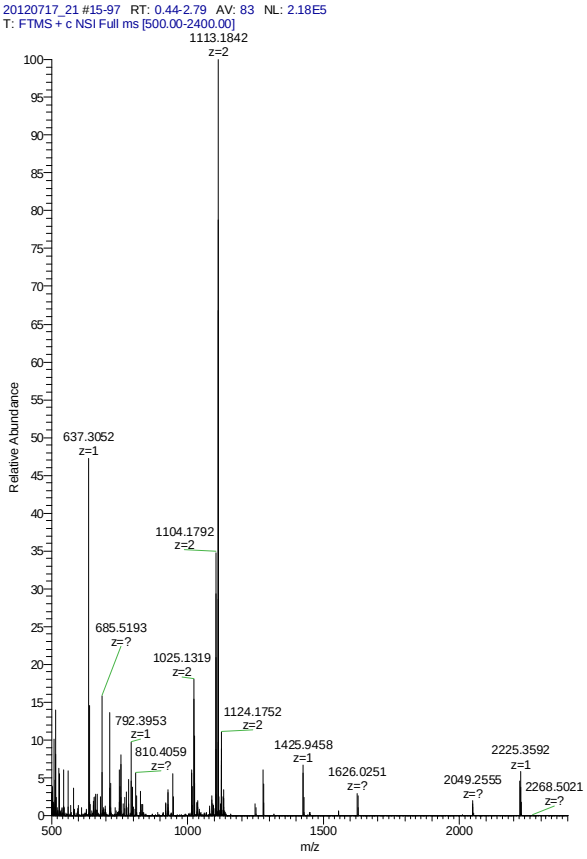

Mass reconstruction from ESI-MS (positive mode), high resolution:

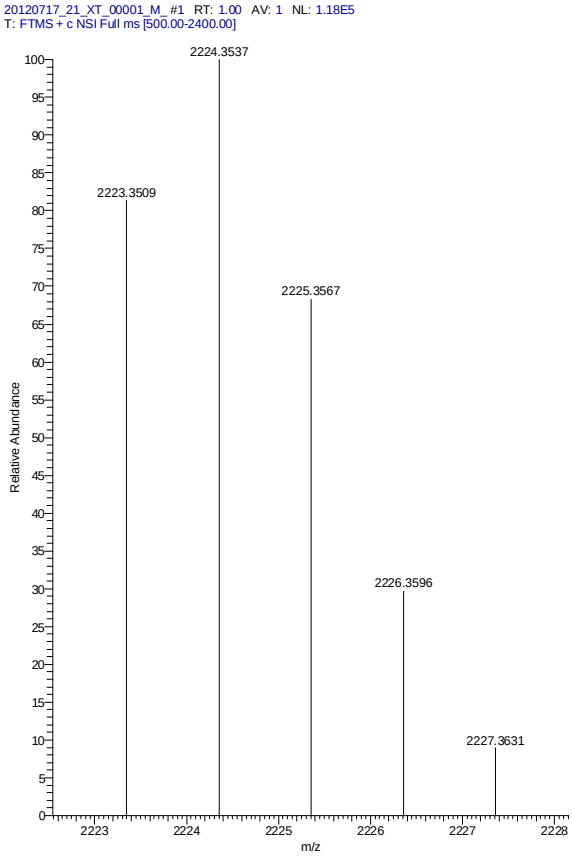

H-Glu-Val-Asn-Sta-Val-Ala-Glu-Phe-3Gl-3Gl-3Gl-3Gl-Asp(ODhc)-NH_2 (**7n**)

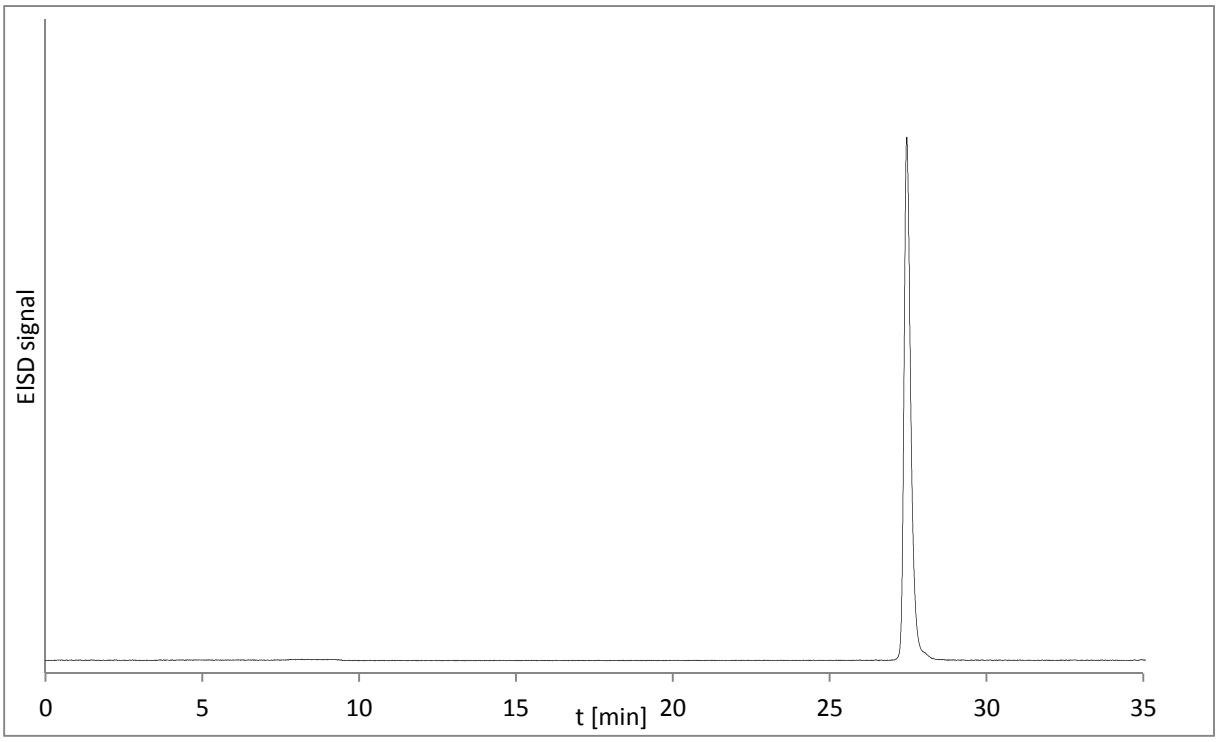

ESI-MS (positive mode), high resolution:

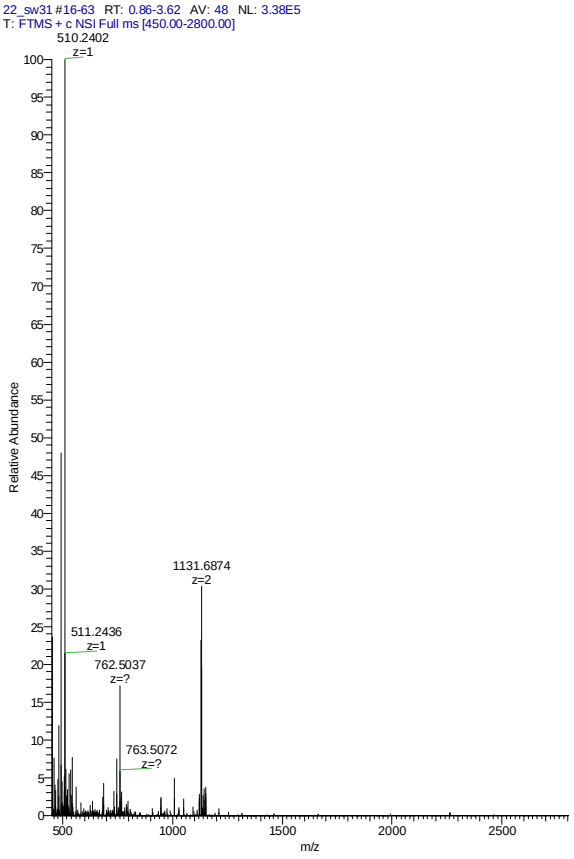

Mass reconstruction from ESI-MS (positive mode), high resolution:

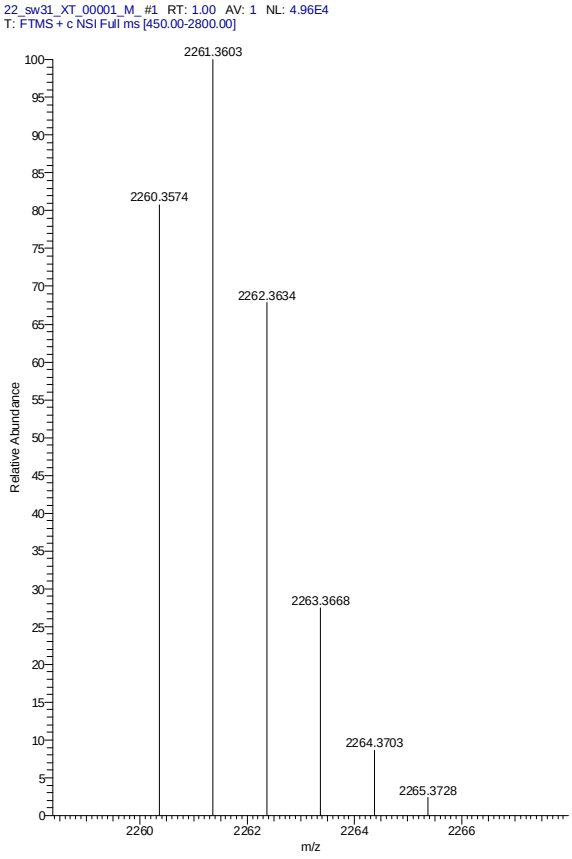

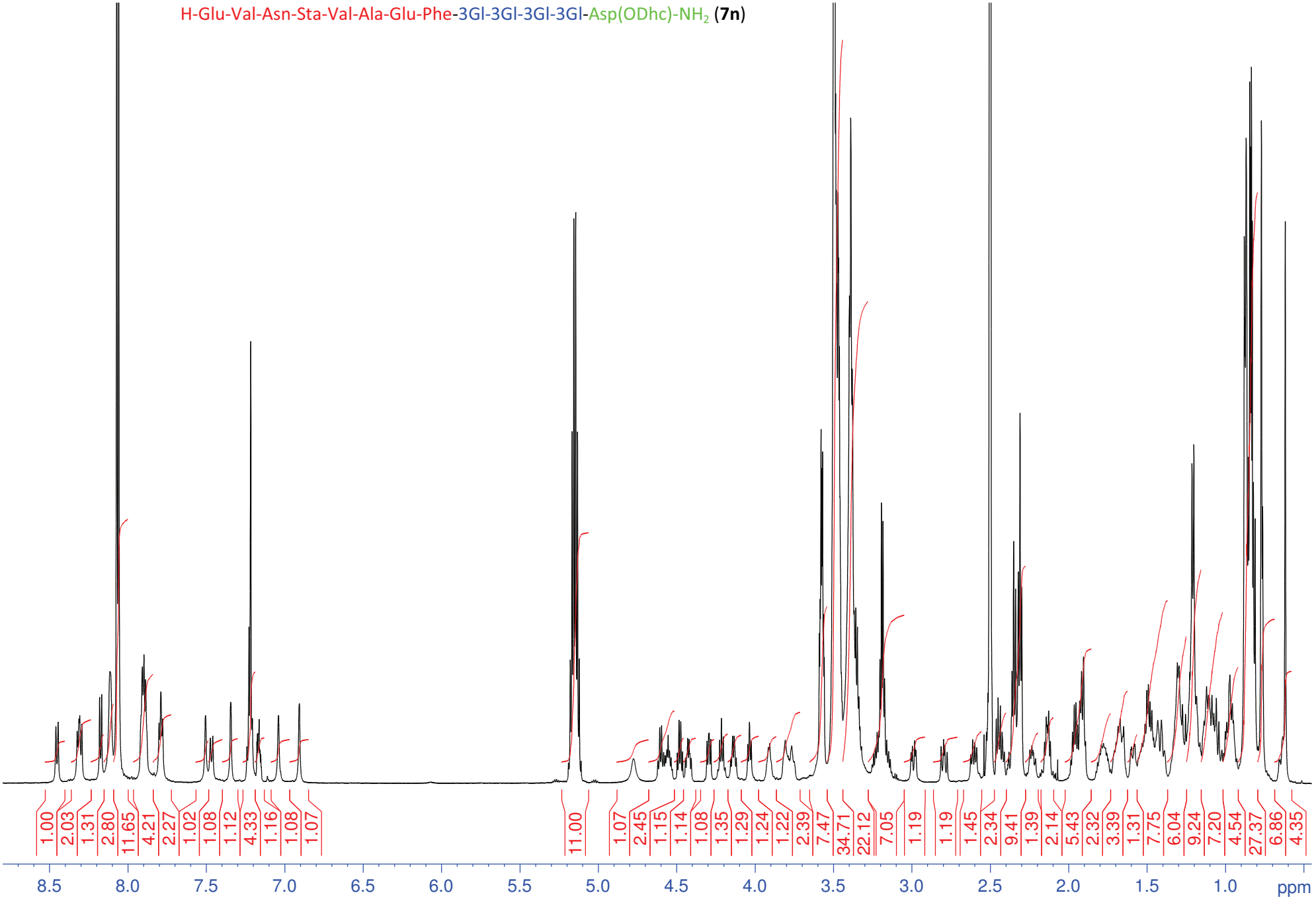

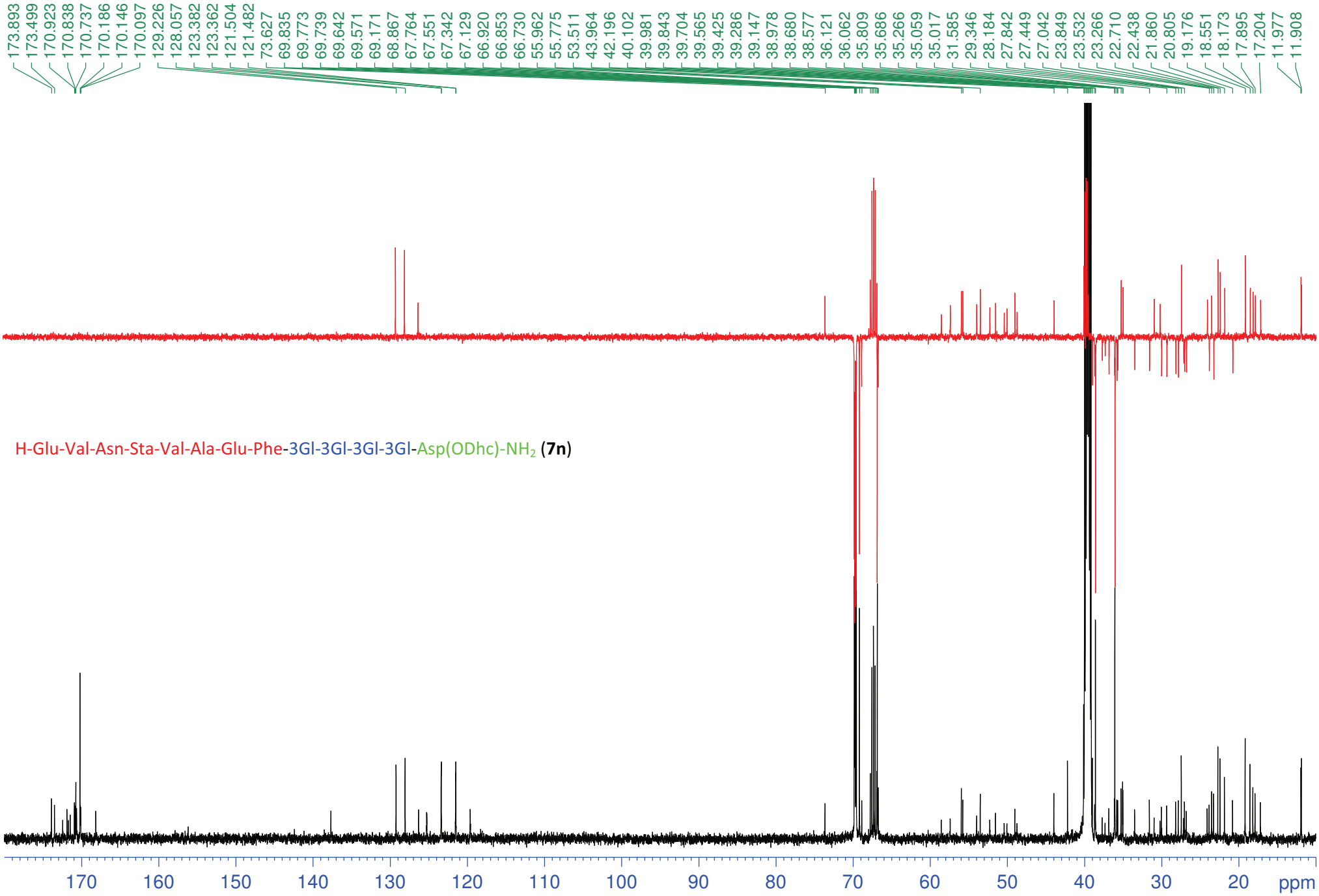

H-Glu-Val-Asn-Sta-Val-Ala-Glu-Phe-4Gl-4Gl-4Gl-4Gl-Asp(ODhc)-NH_2 (**7o**)

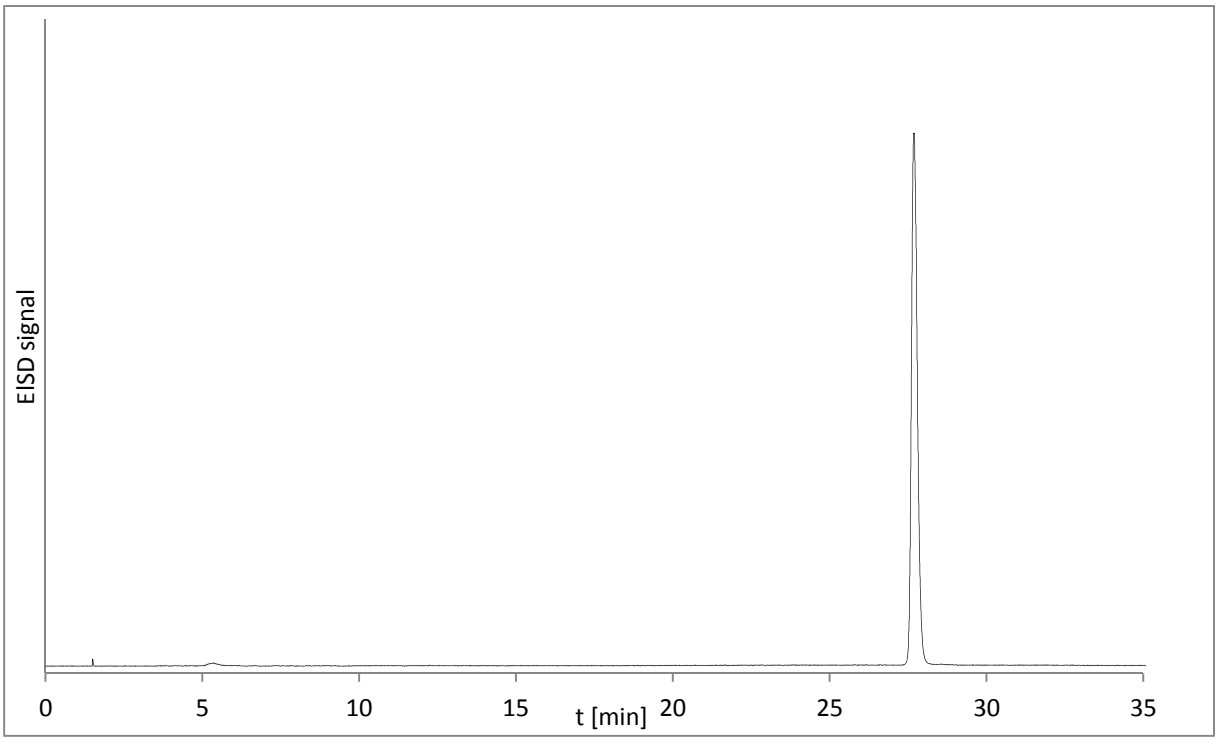

ESI-MS (positive mode), low resolution:

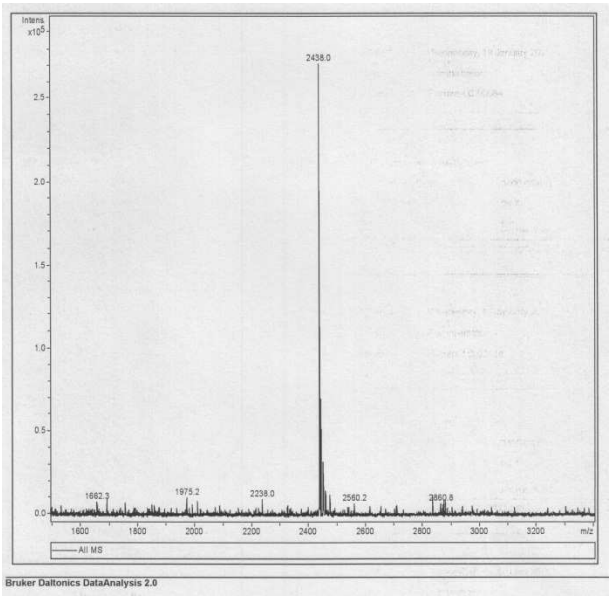

Mass reconstruction from ESI-MS (positive mode), high resolution:

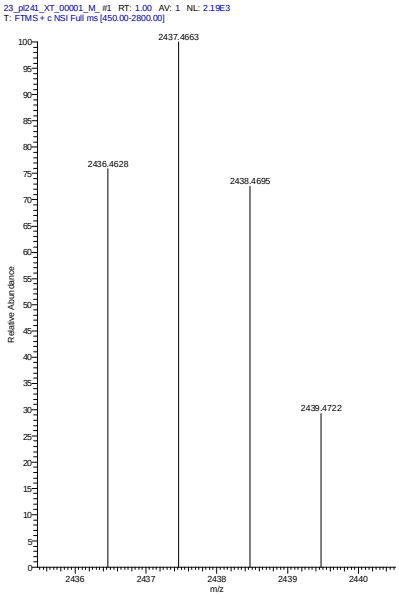

H-Glu-Val-Asn-Sta-Val-Ala-Glu-Phe-24Gl-Asp(ODhc)-NH_2 (**7p**)

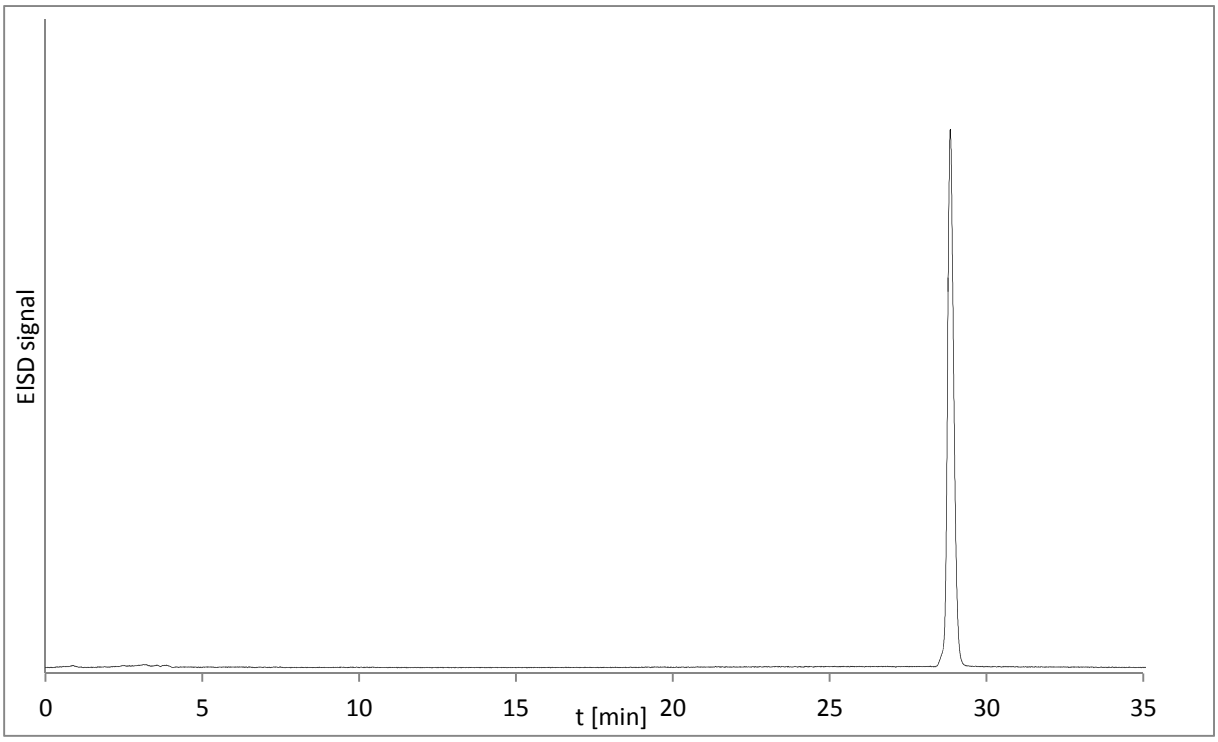

ESI-MS (negative mode):

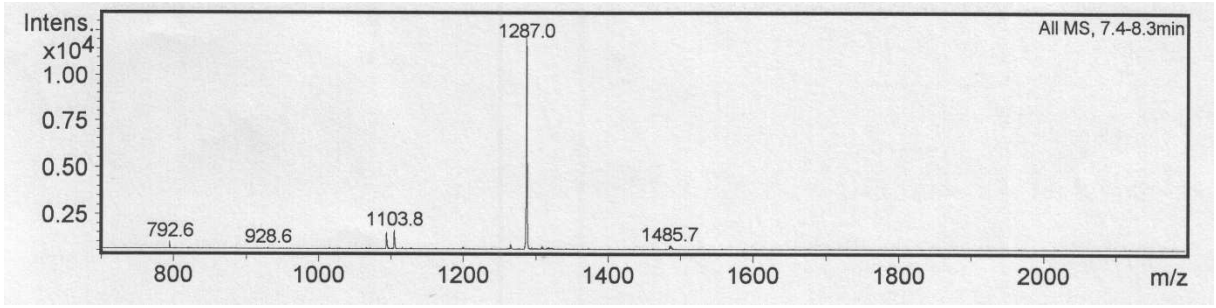

Mass reconstruction from ESI-MS (positive mode), high resolution:

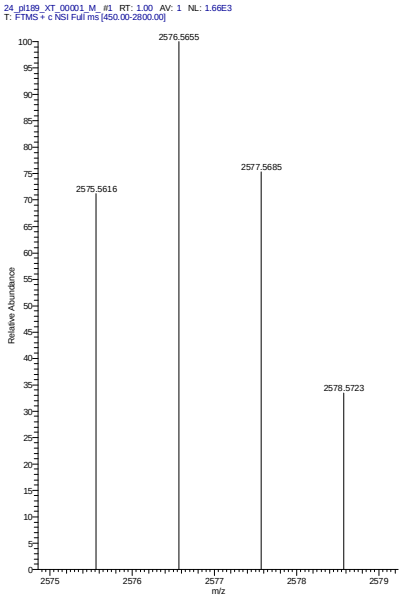

H-Glu-Val-Asn-Sta-Val-Ala-Glu-Phe-24Gl-Asp(ODhc)-NH_2 (**7p**)

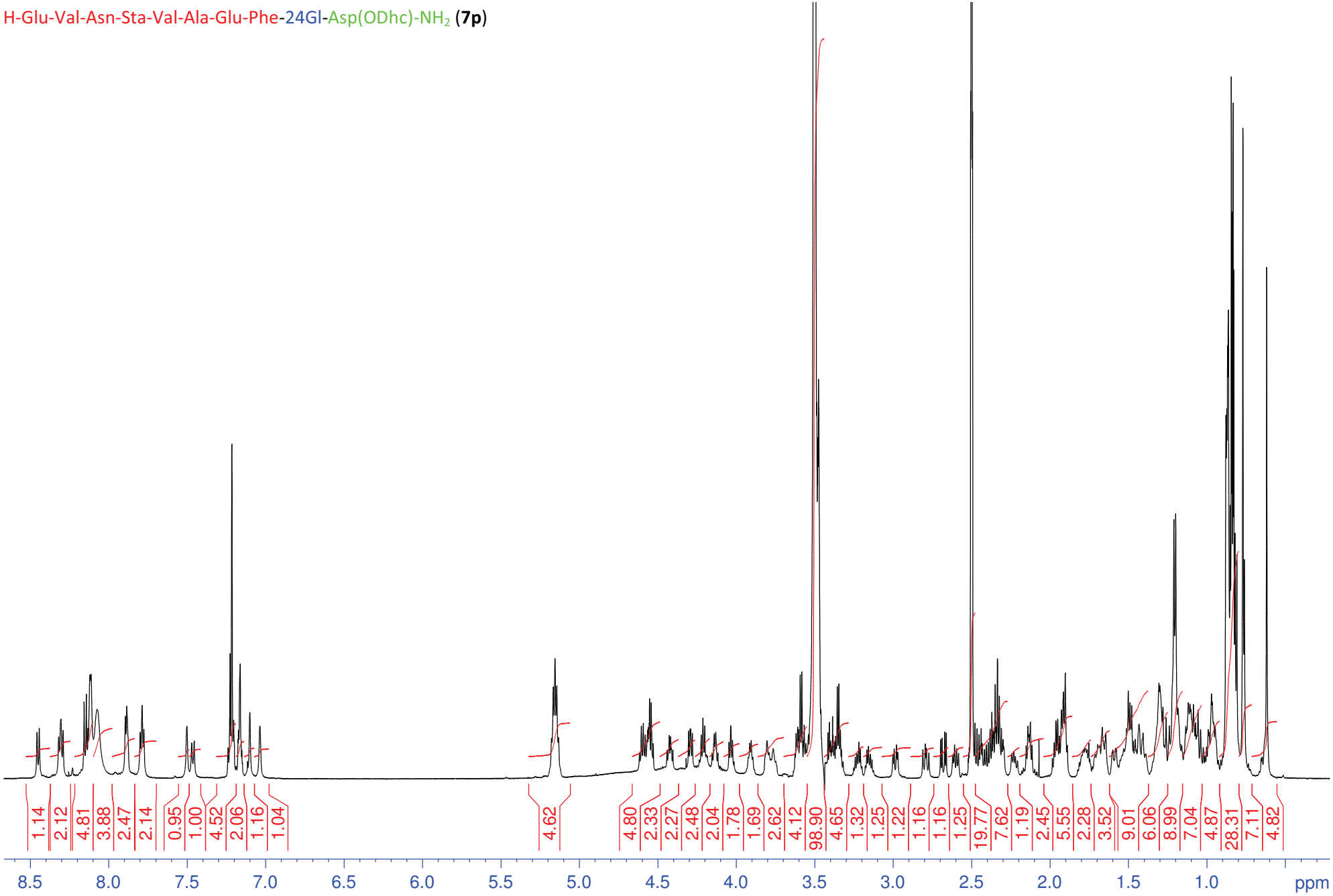

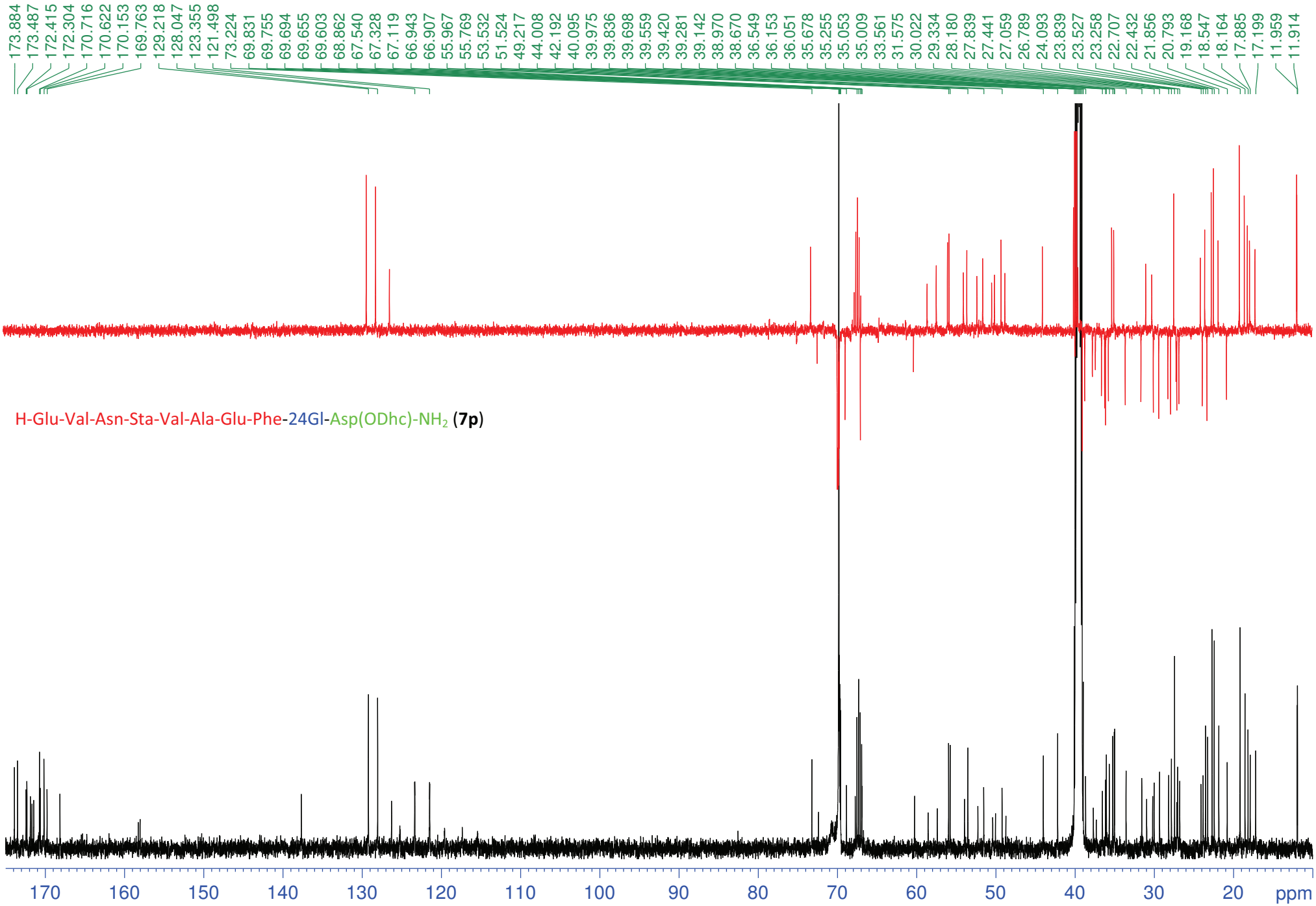

H-Glu-Val-Asn-Sta-Val-Ala-Glu-Phe-4Gl-4Gl-4Gl-4Gl-4Gl-Asp(ODhc)-NH_2 (**7q**)

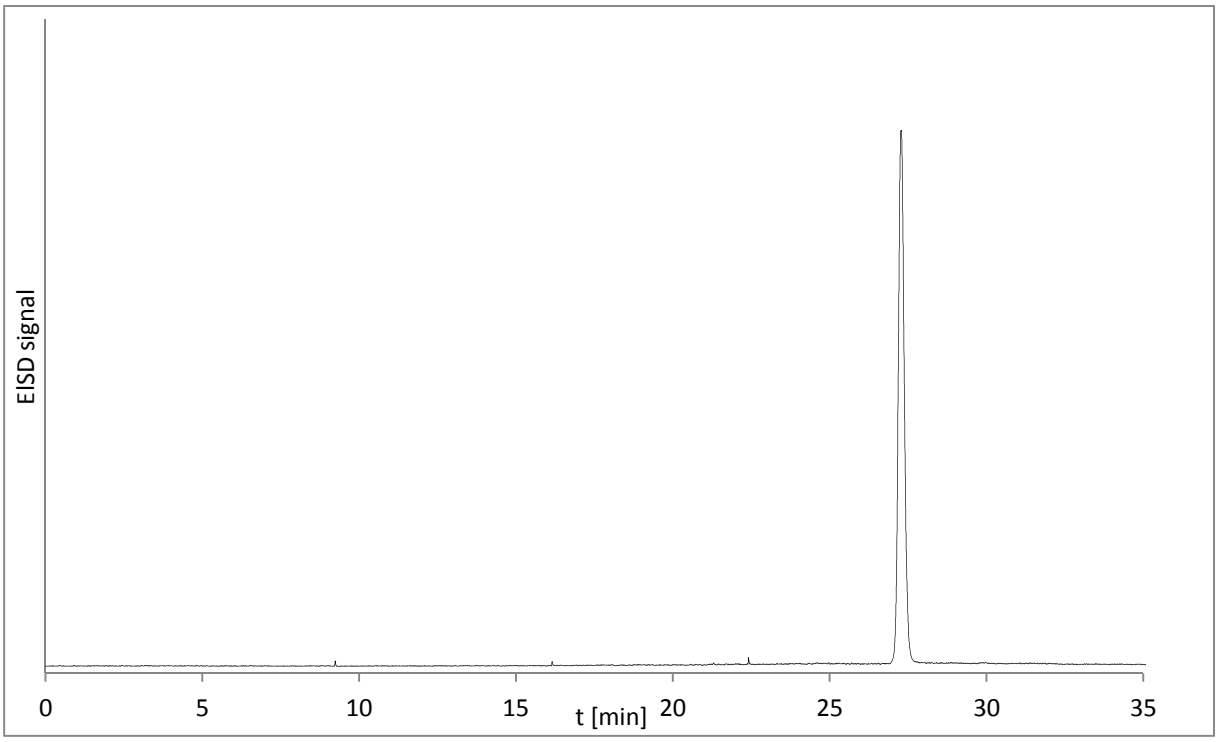

ESI-MS (positive mode), low resolution:

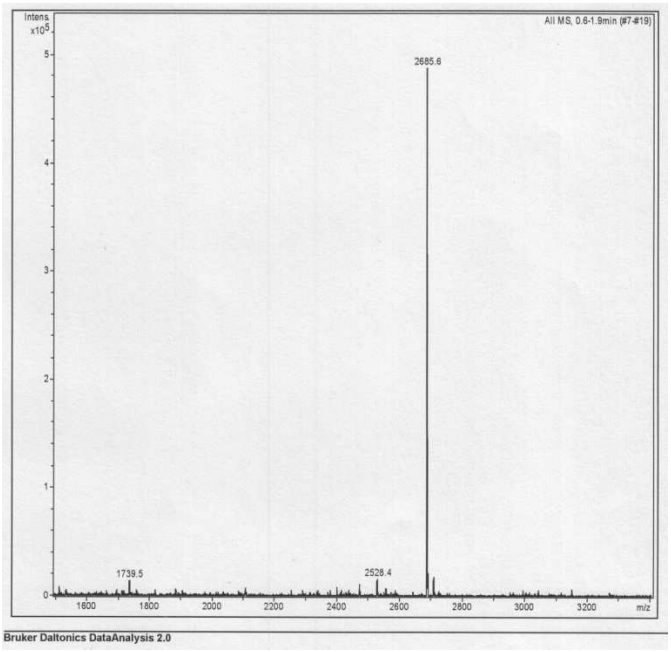

Mass reconstruction from ESI-MS (positive mode), high resolution:

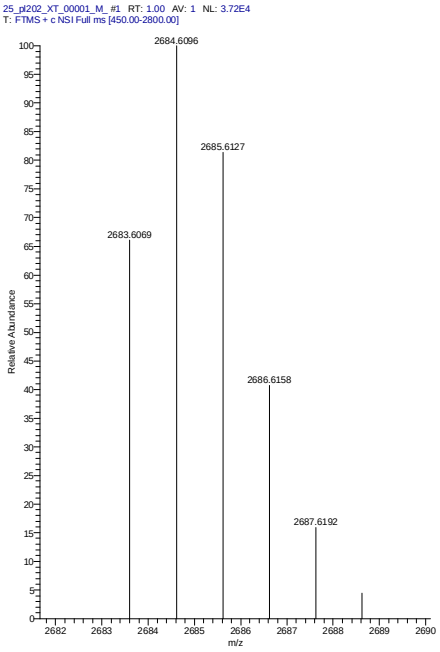

H-Glu-Val-Asn-Sta-Val-Ala-Glu-Phe-4Gl-4Gl-4Gl-4Gl-4Gl-Asp(ODhc)-NH_2 (**7q**)

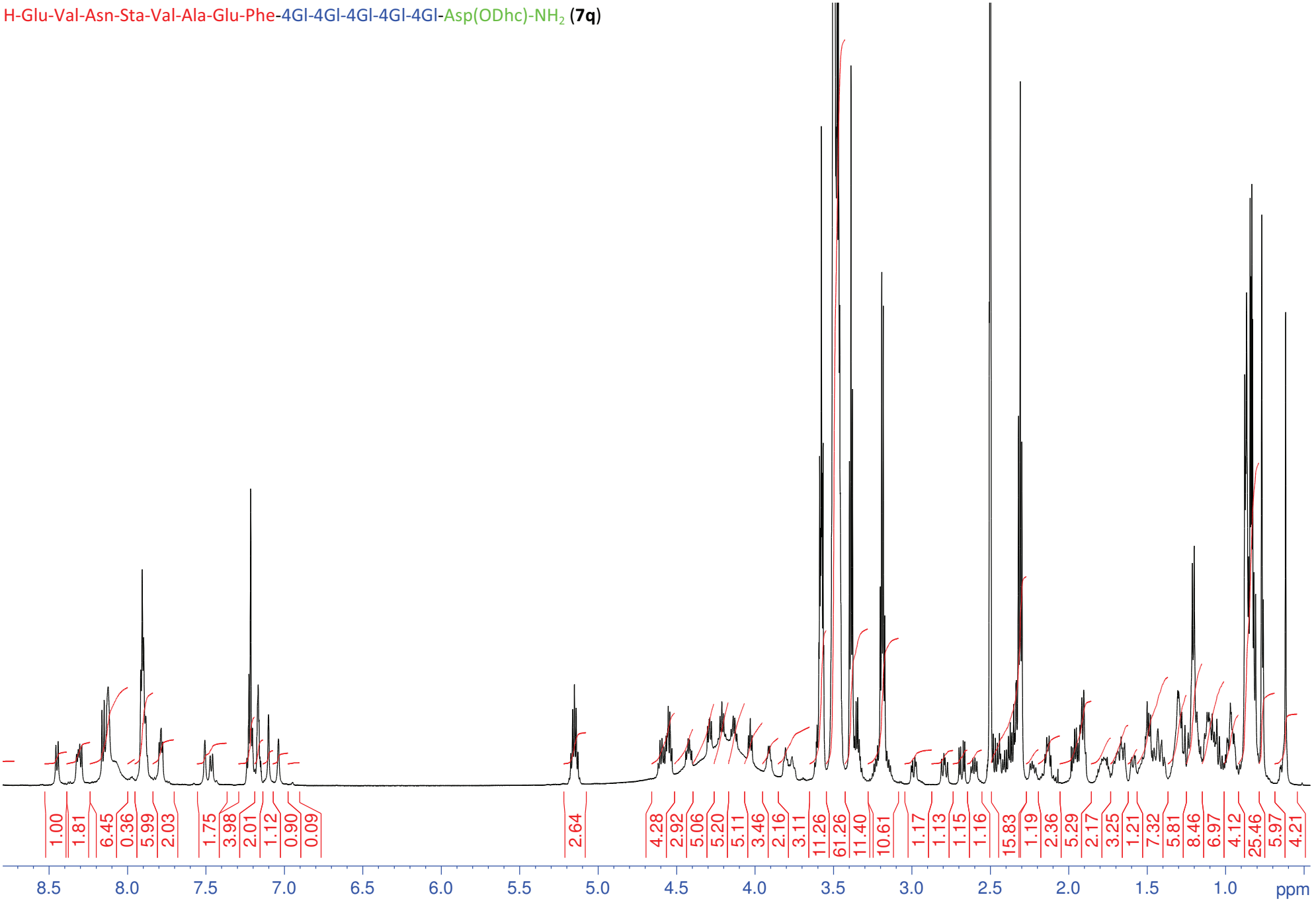

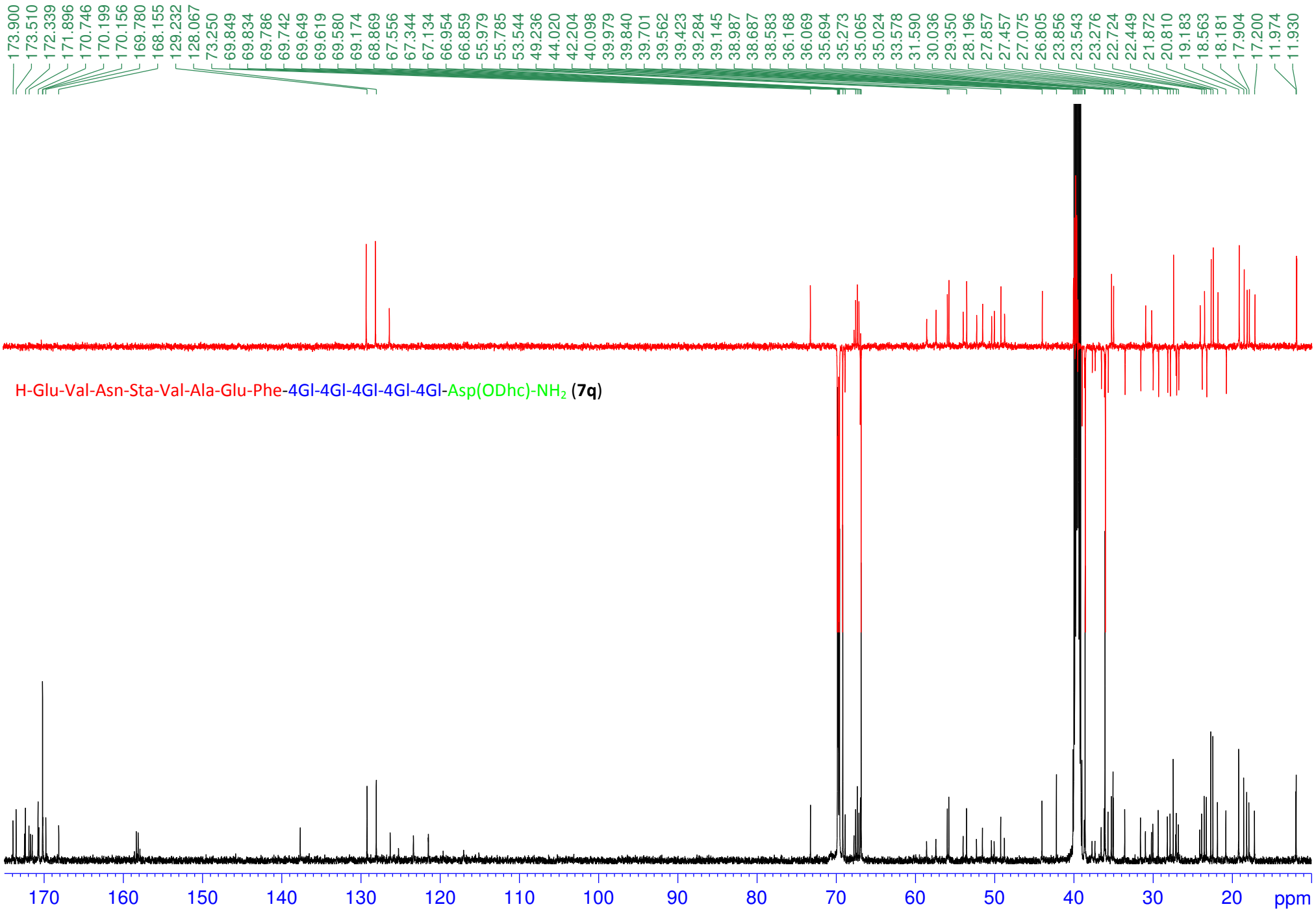

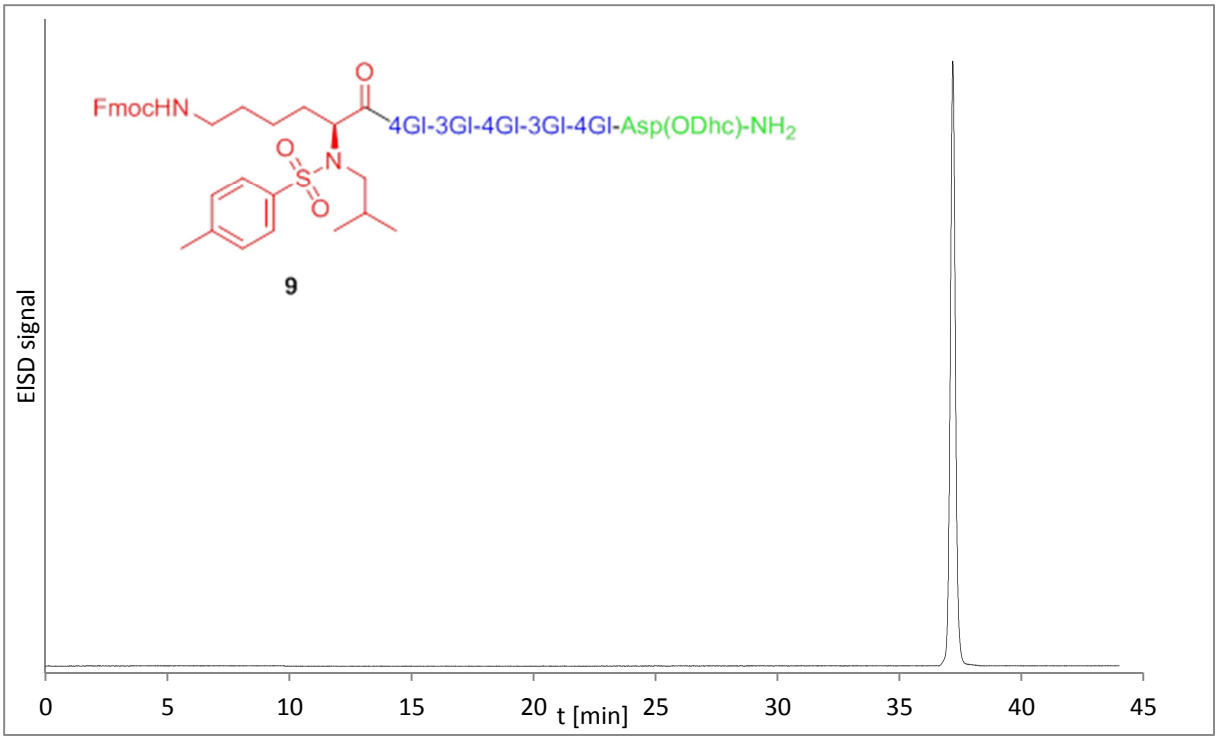
FmocHN
4Gl-3Gl-4Gl-3Gl-4Gl-Asp(ODhc)-NH2
9
EISD signal
0
5
10
15
20
t [min]
25
30
35
40
45

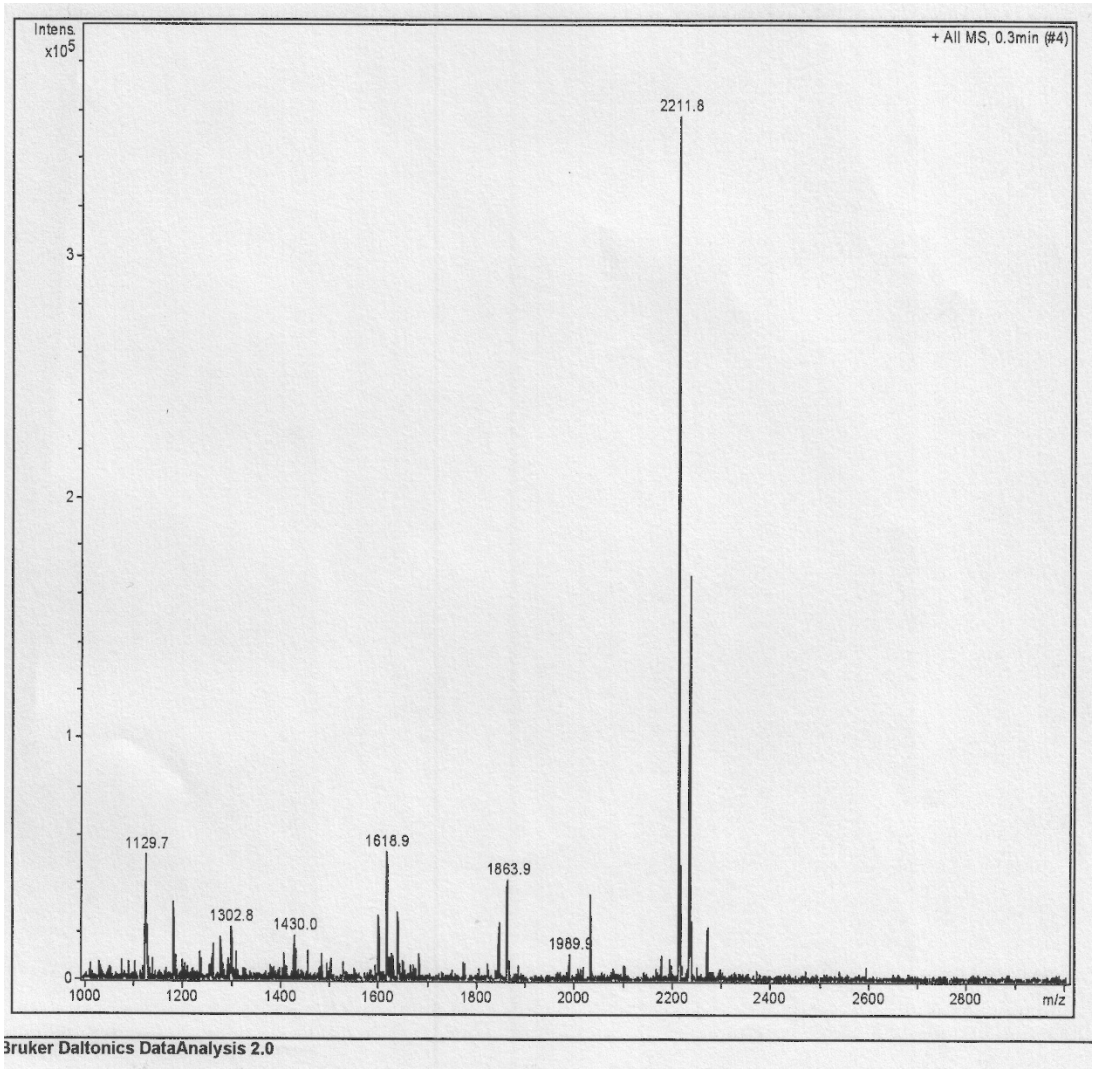
Intens.
x10^5
+ All MS, 0.3min (#4)
2211.8
1129.7
1618.9
1863.9
1302.8
1430.0
1989.9
1000
1200
1400
1600
1800
2000
2200
2400
2600
2800
m/z
Bruker Daltonics DataAnalysis 2.0

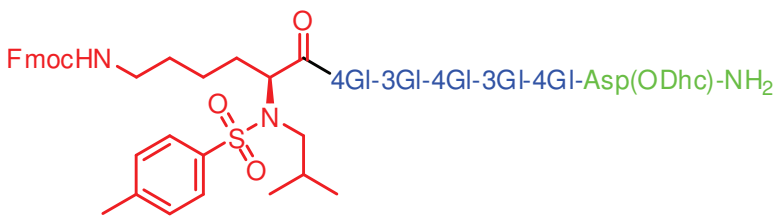

9

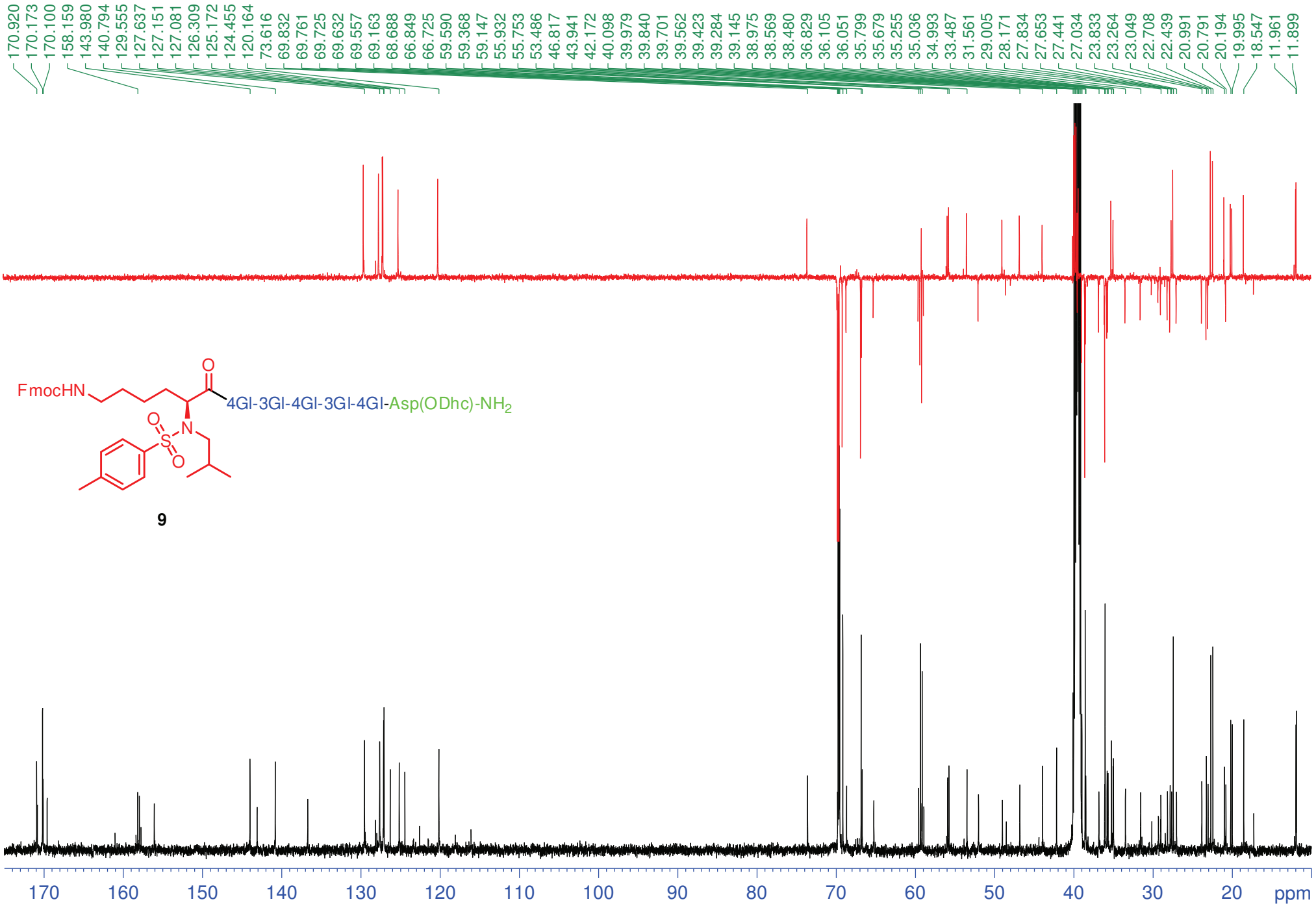

9

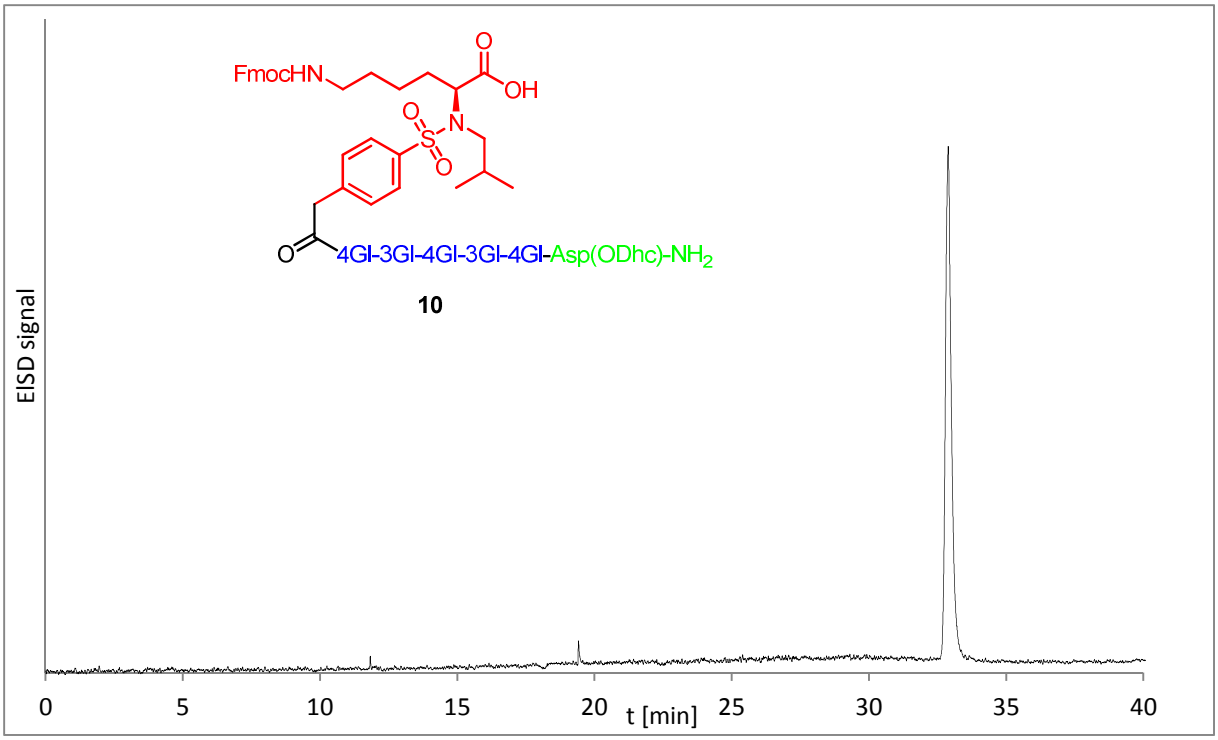

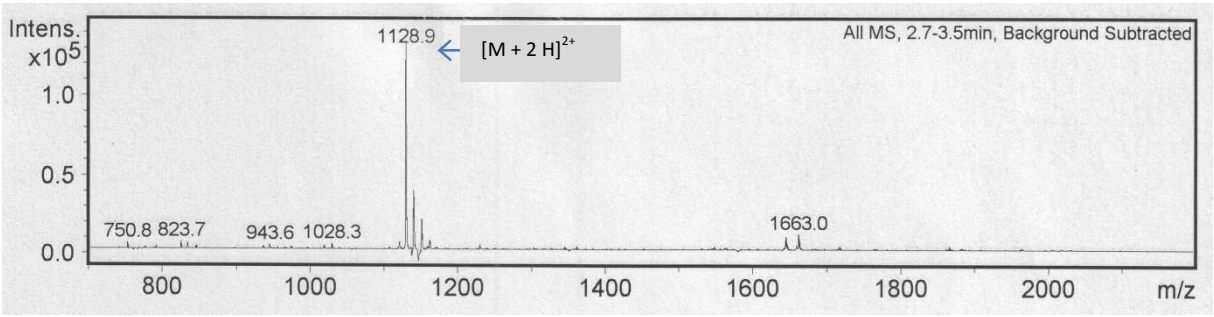

Mass reconstruction from ESI-MS (positive mode), high resolution:

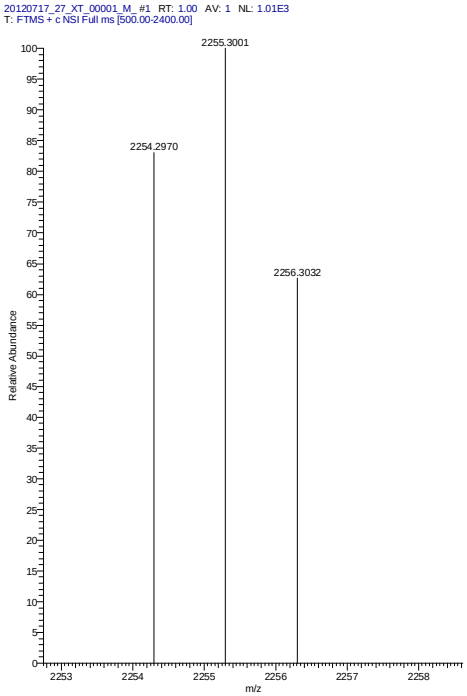

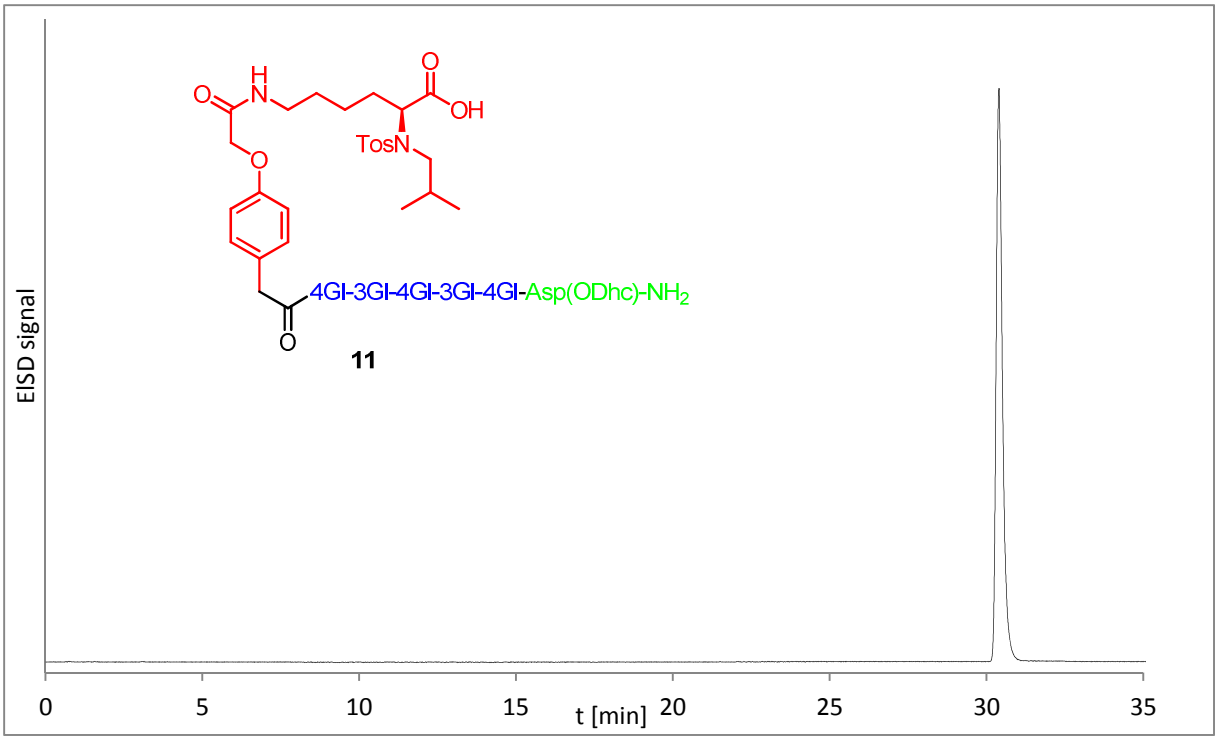

ESI-MS (negative mode):

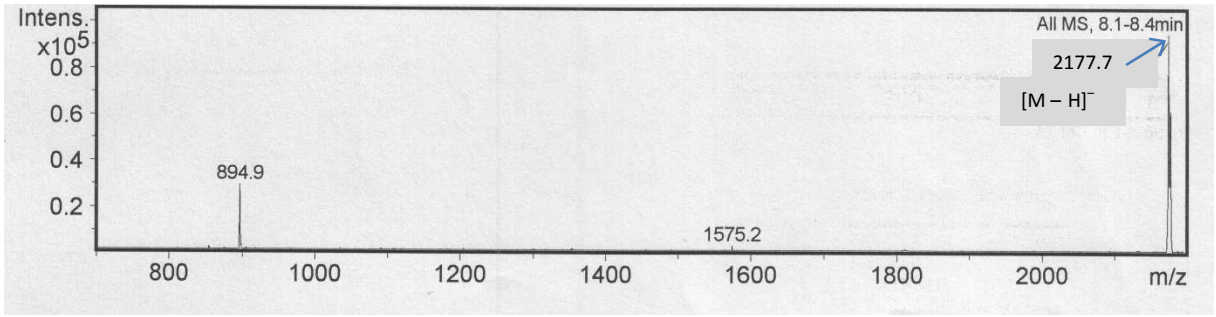

Mass reconstruction from ESI-MS (positive mode), high resolution:

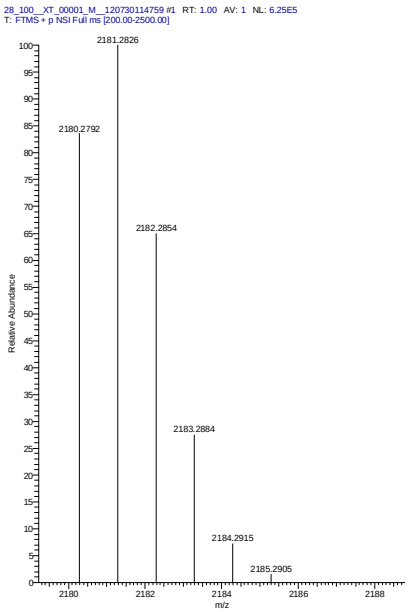

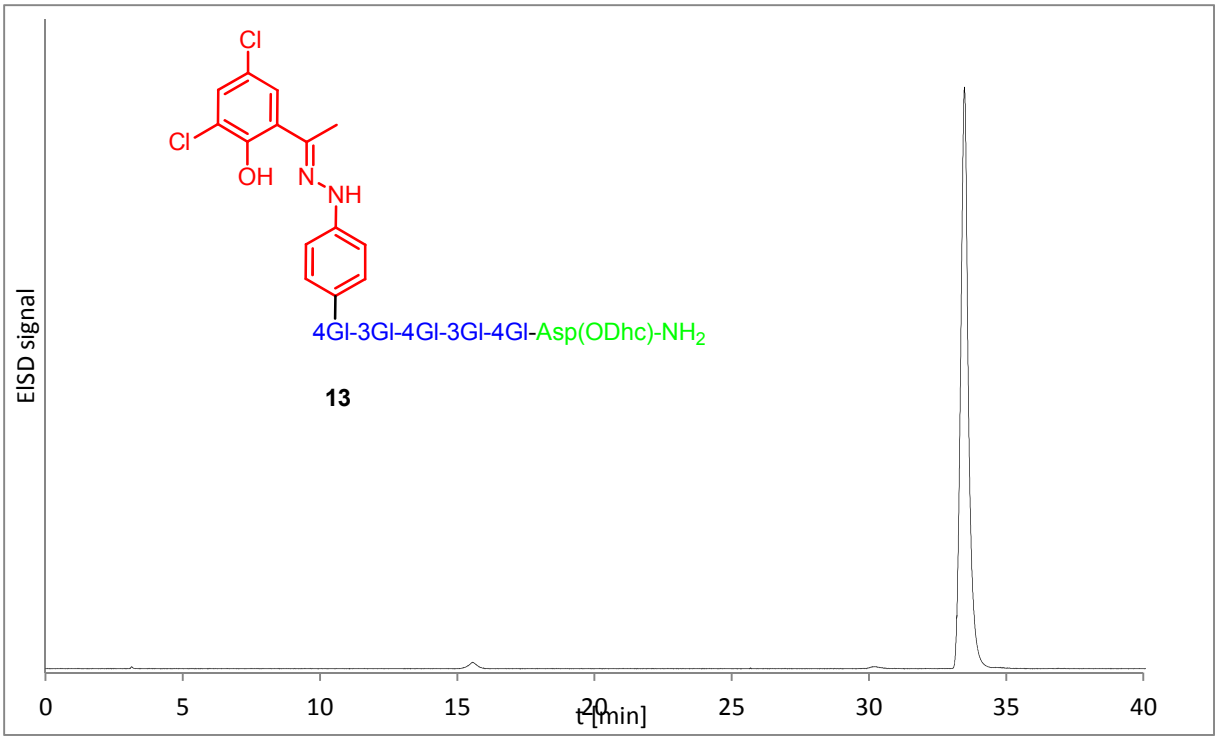

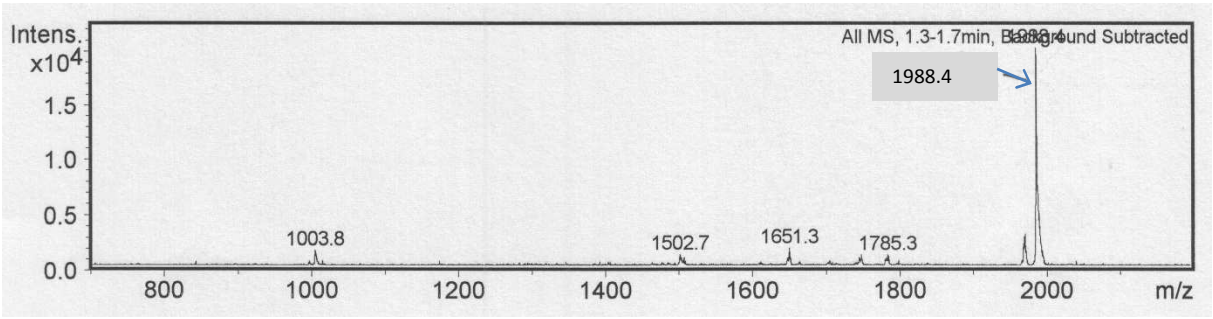

Mass reconstruction from ESI-MS (positive mode), high resolution:

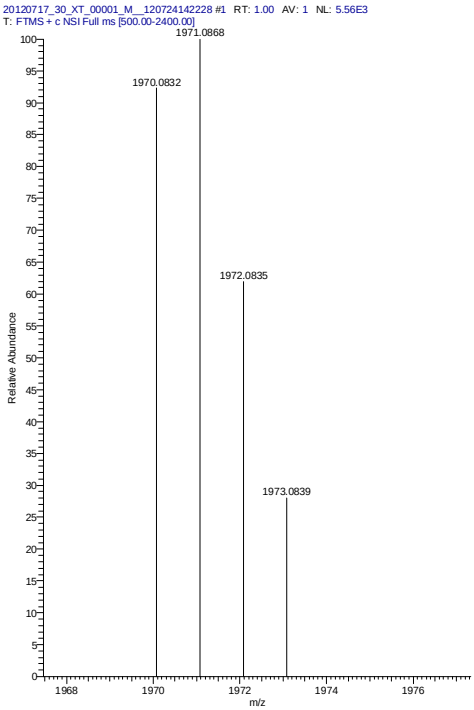

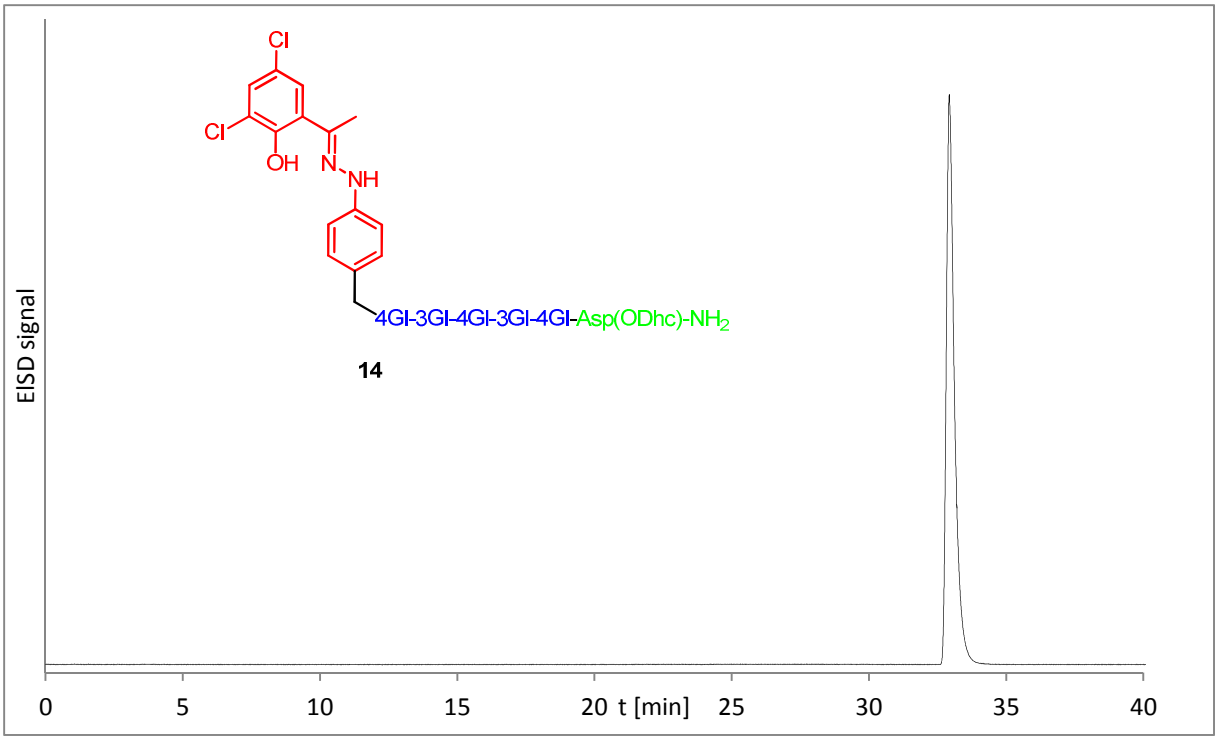

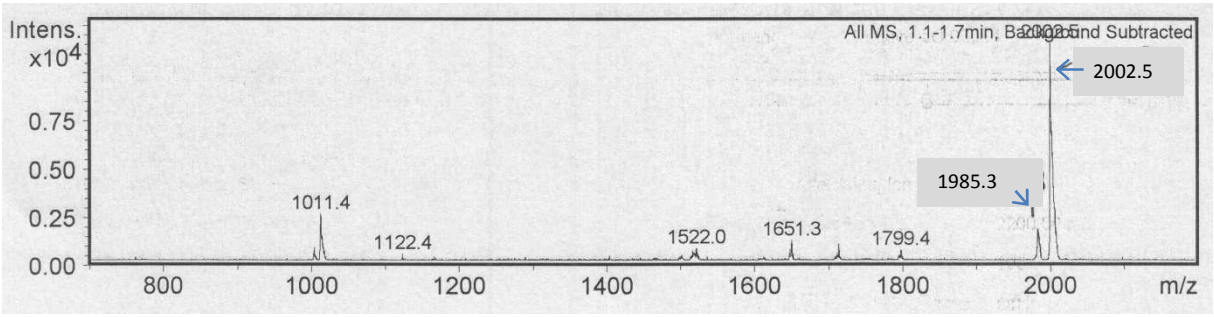

Mass reconstruction from ESI-MS (positive mode), high resolution:

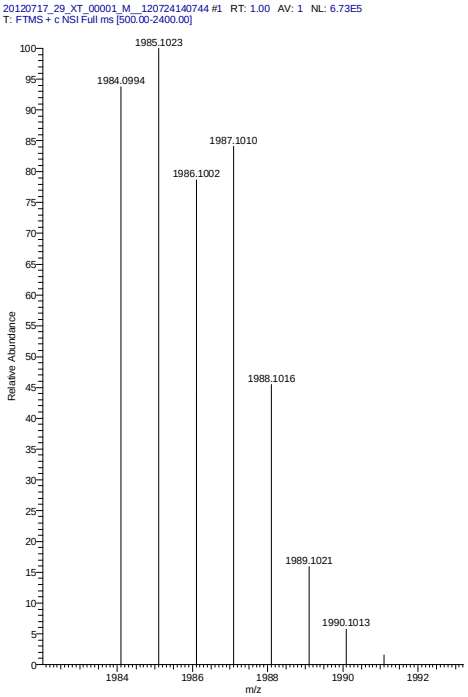

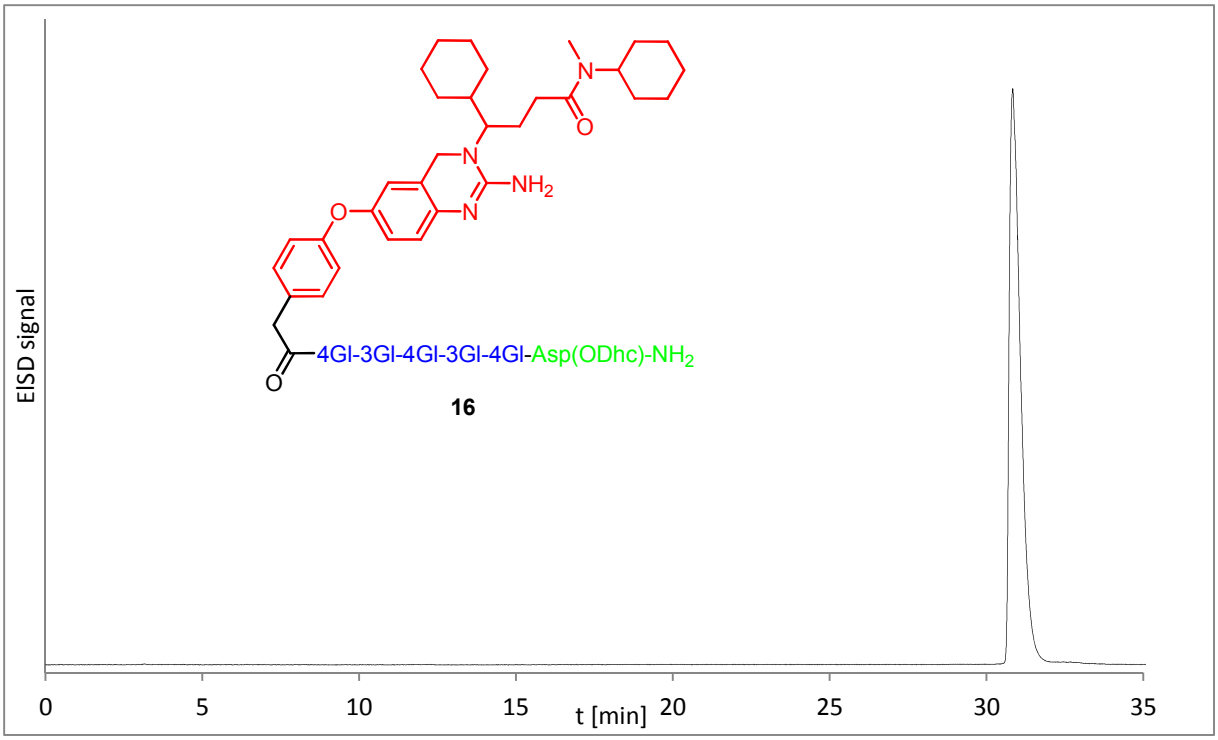

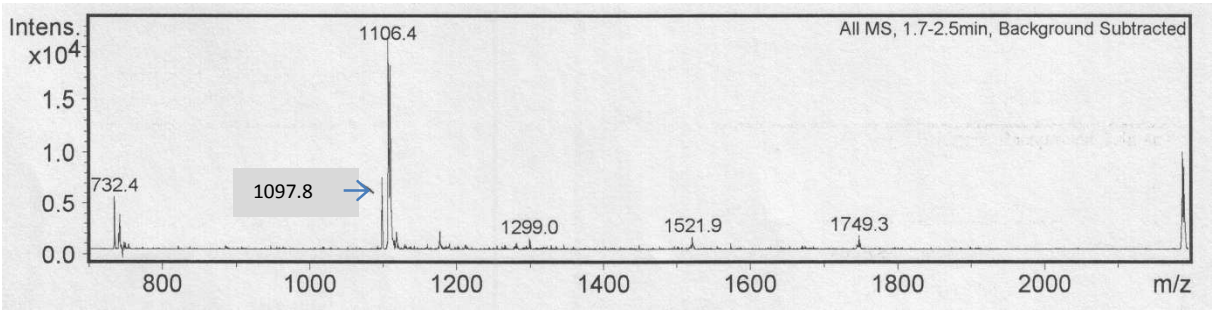

Mass reconstruction from ESI-MS (positive mode), high resolution:

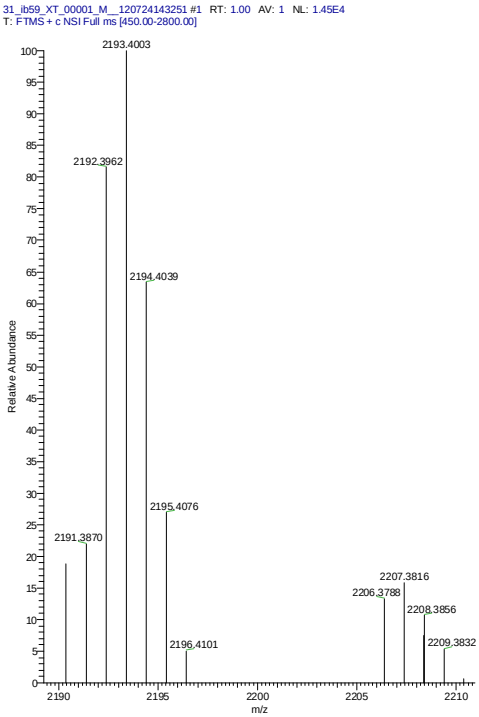

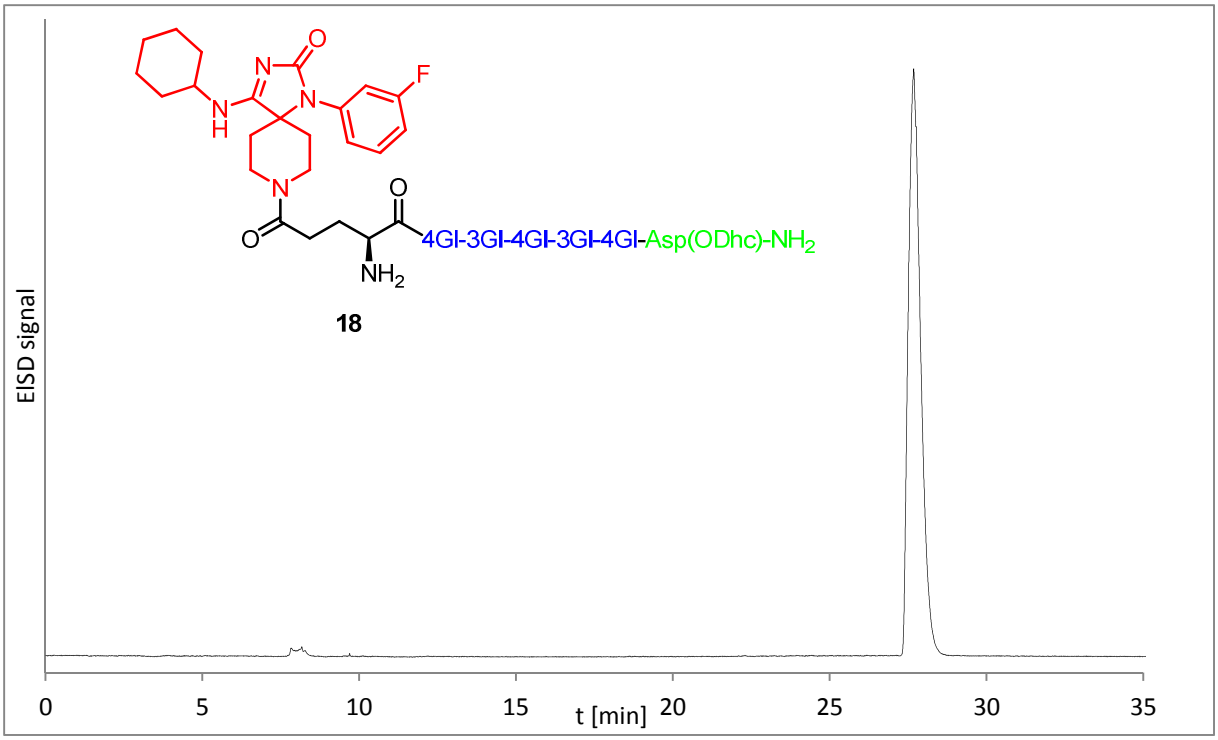

ESI-MS (positive mode), high resolution:

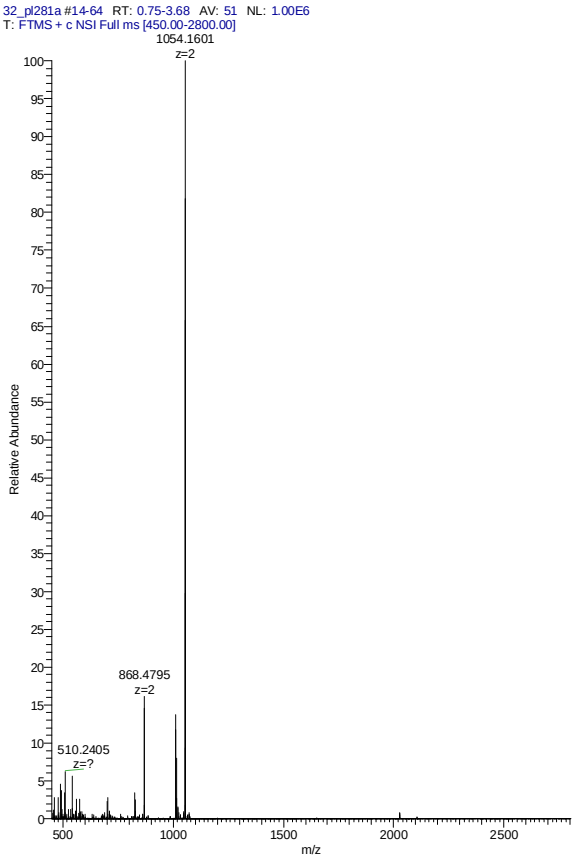

Mass reconstruction from ESI-MS (positive mode), high resolution:

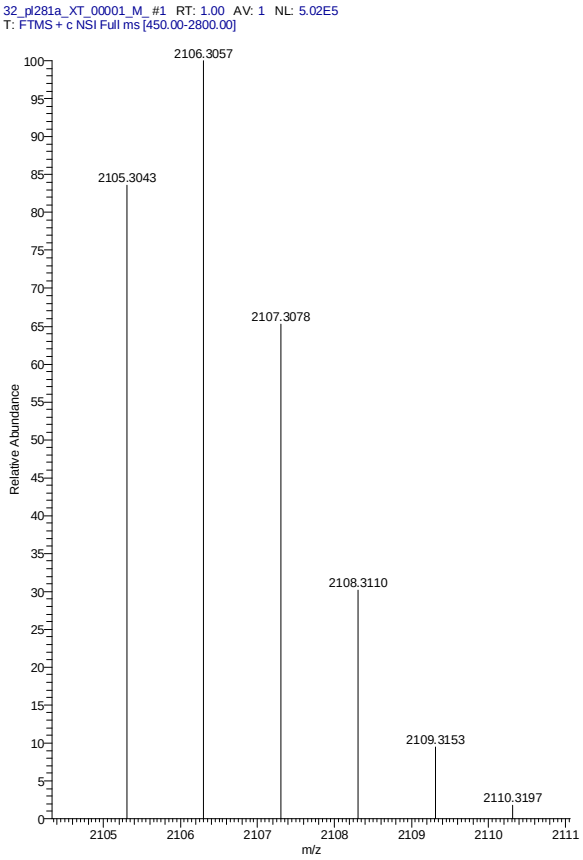

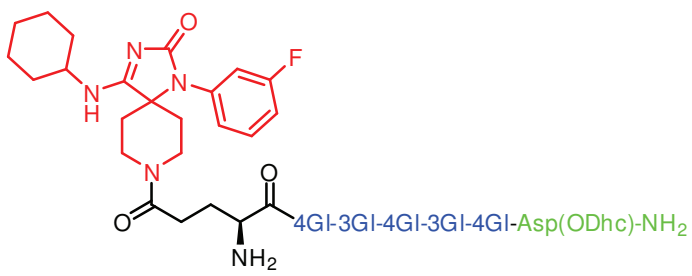

18

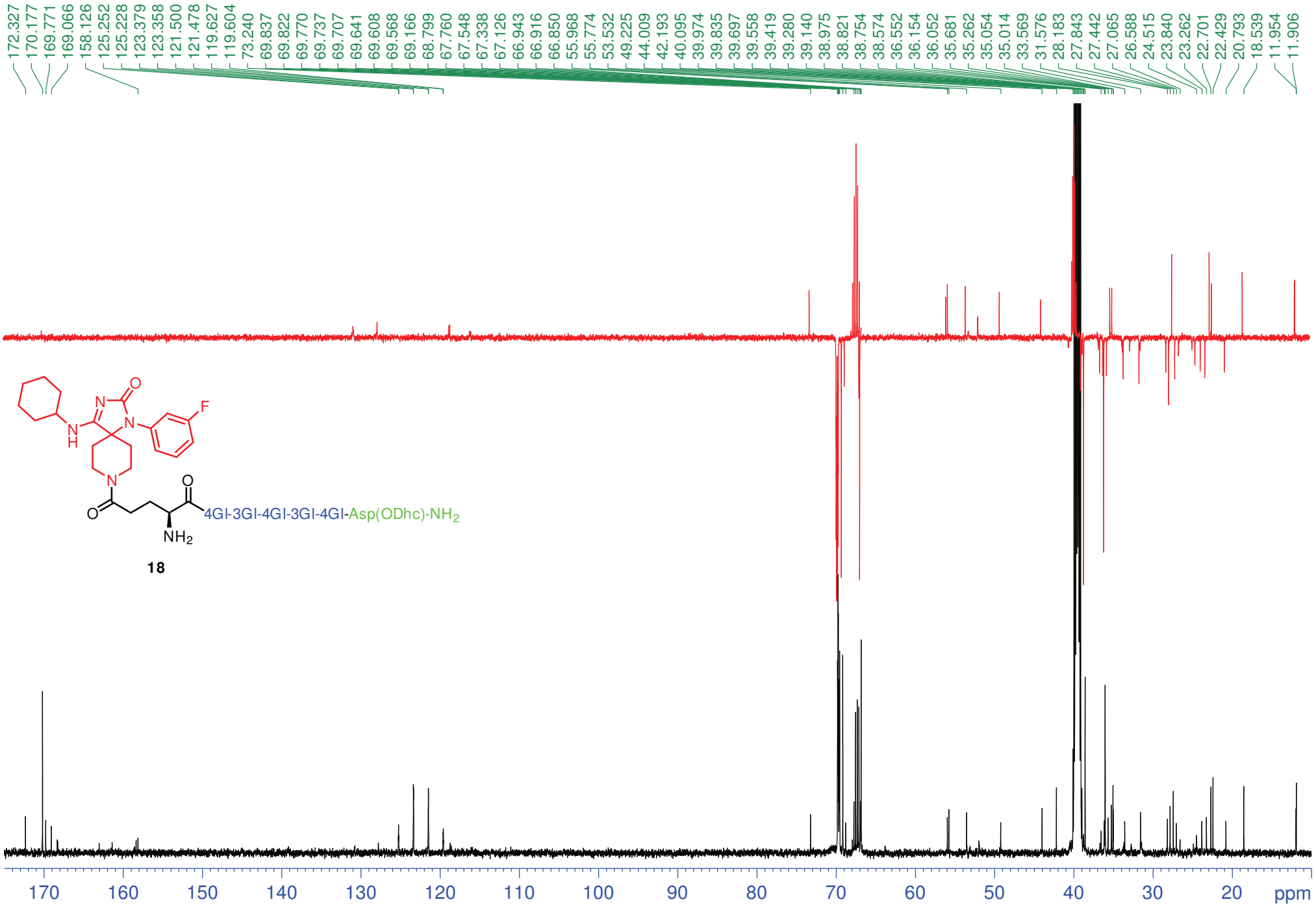

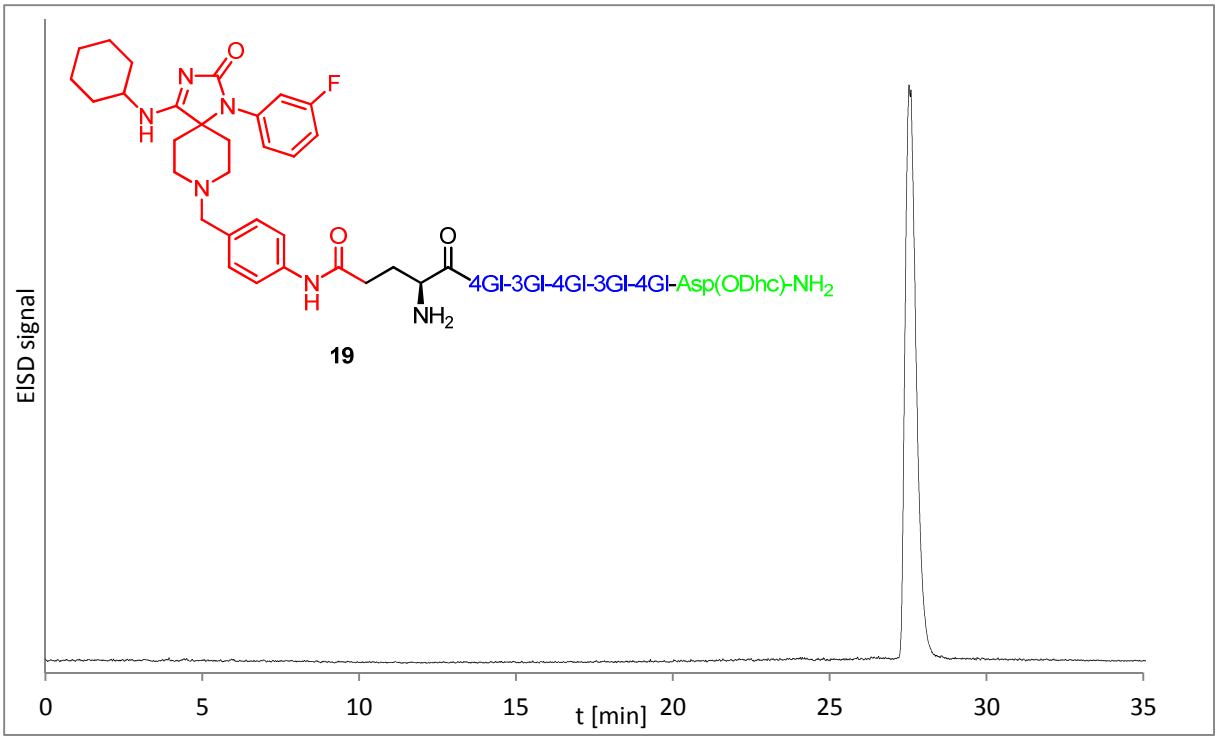

ESI-MS (positive mode), high resolution:

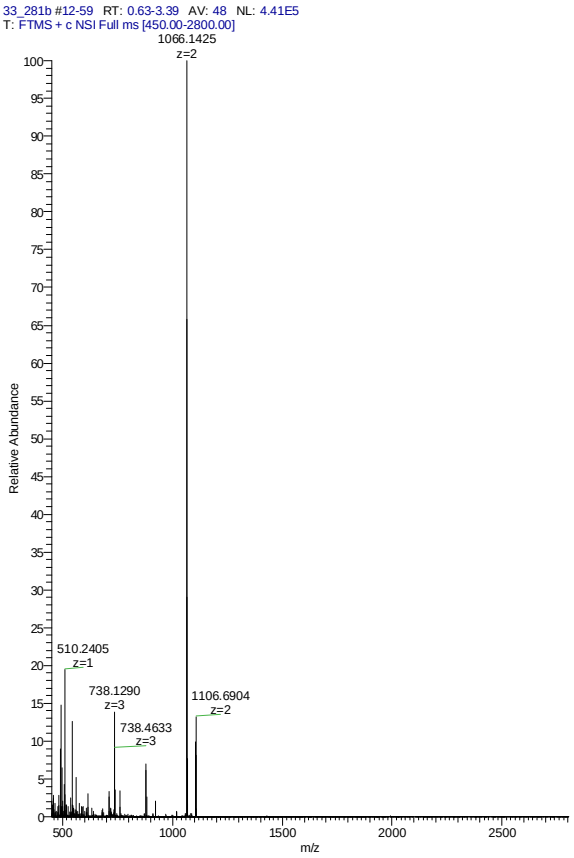

Mass reconstruction from ESI-MS (positive mode), high resolution:

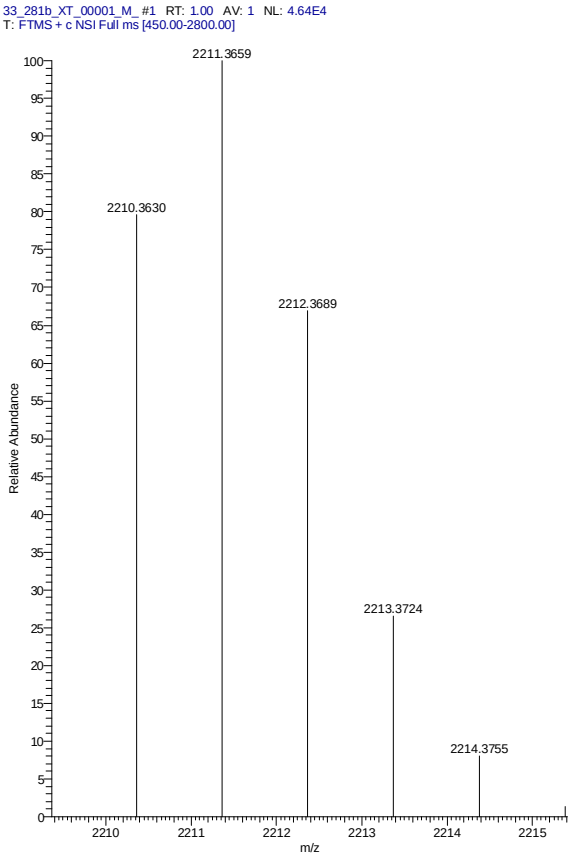

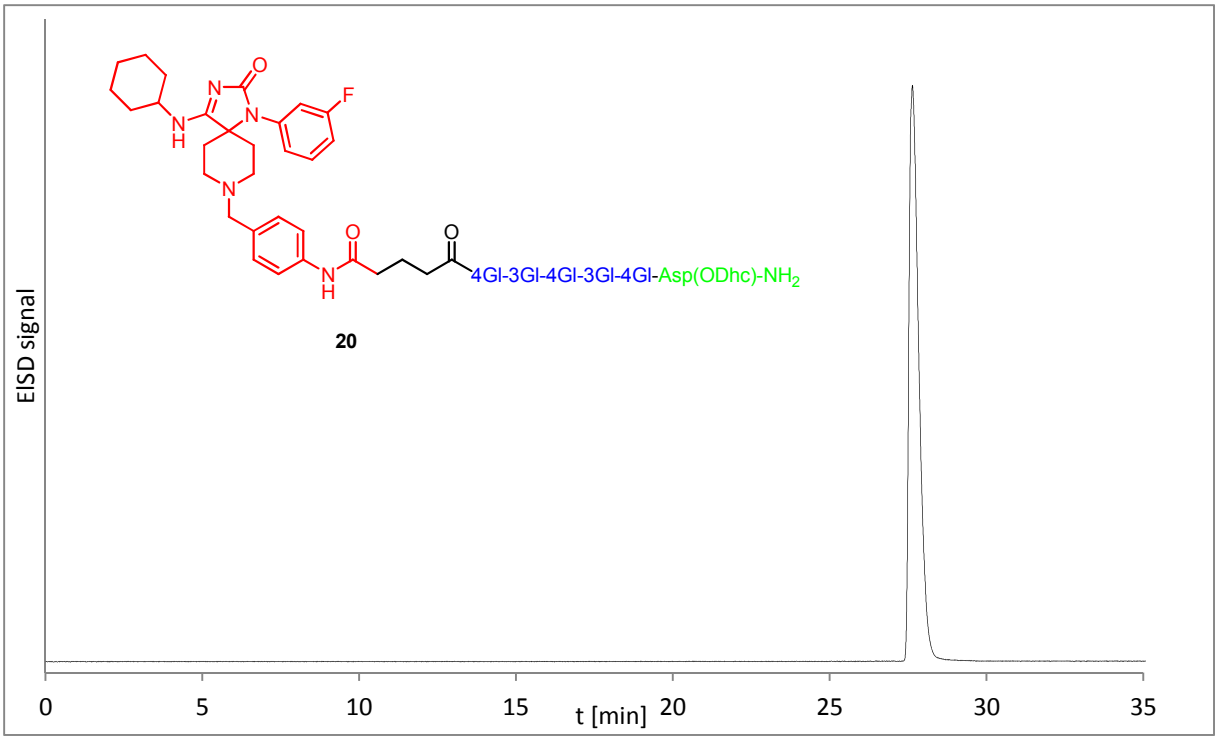

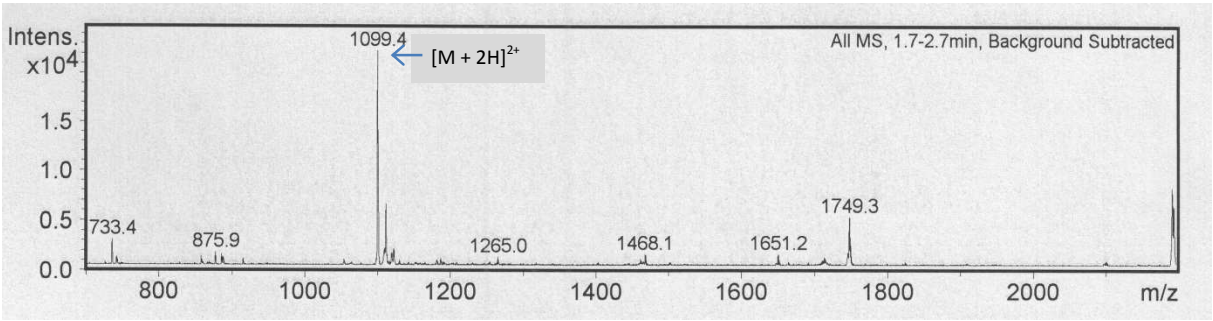

Mass reconstruction from ESI-MS (positive mode), high resolution:

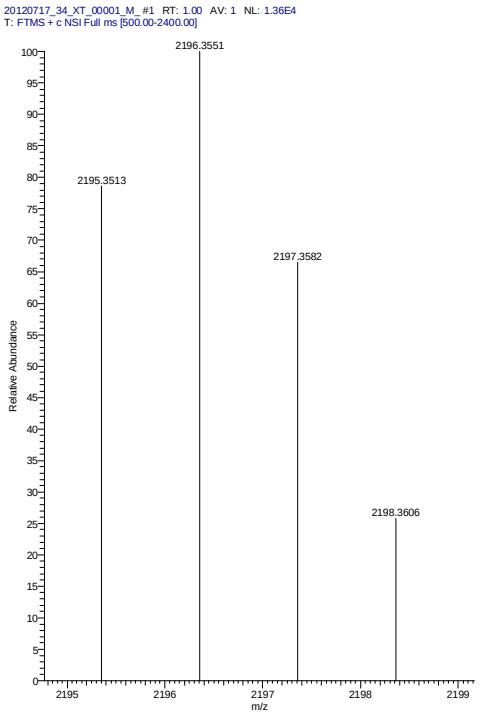

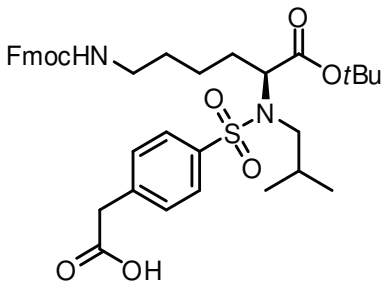

24

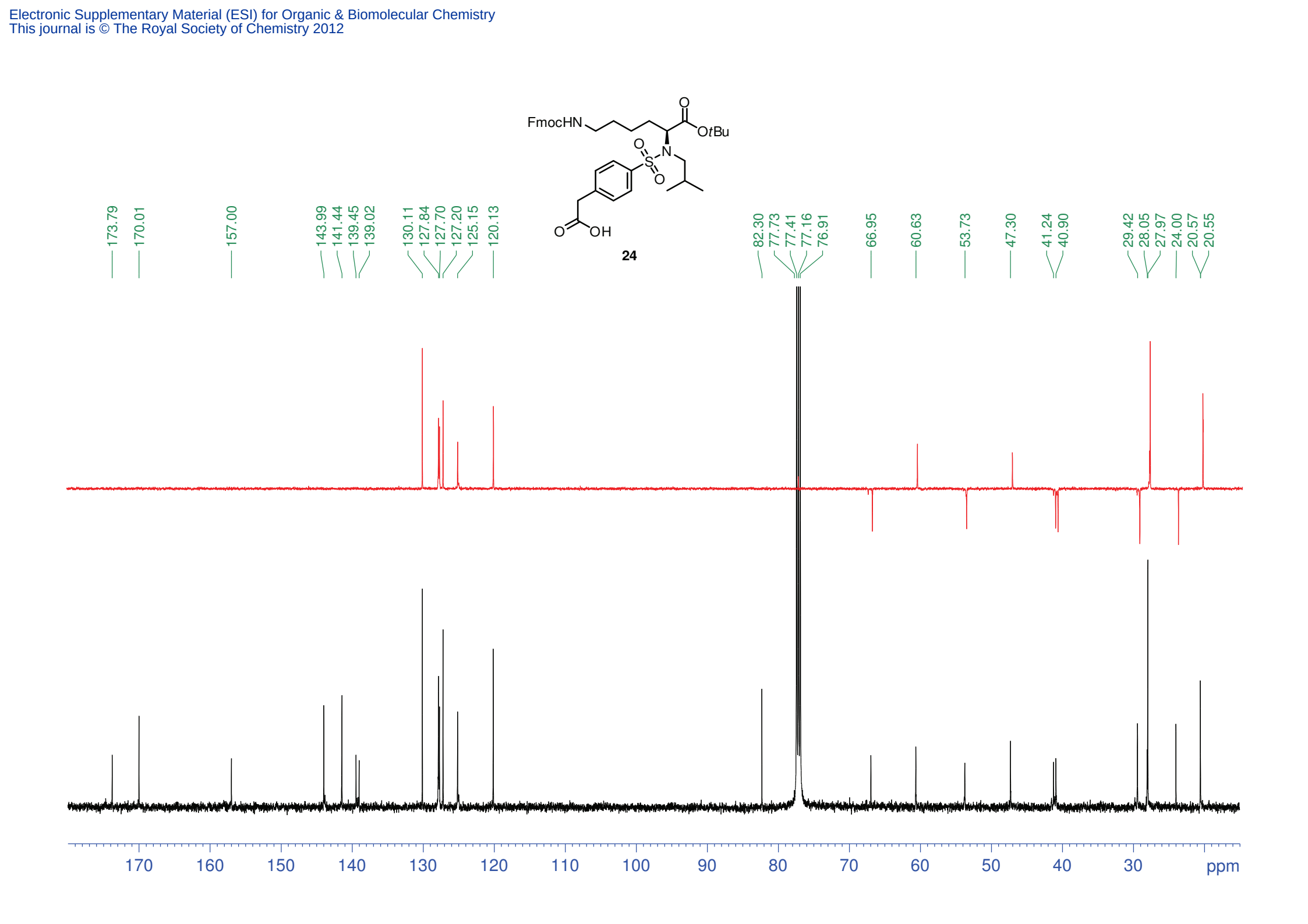

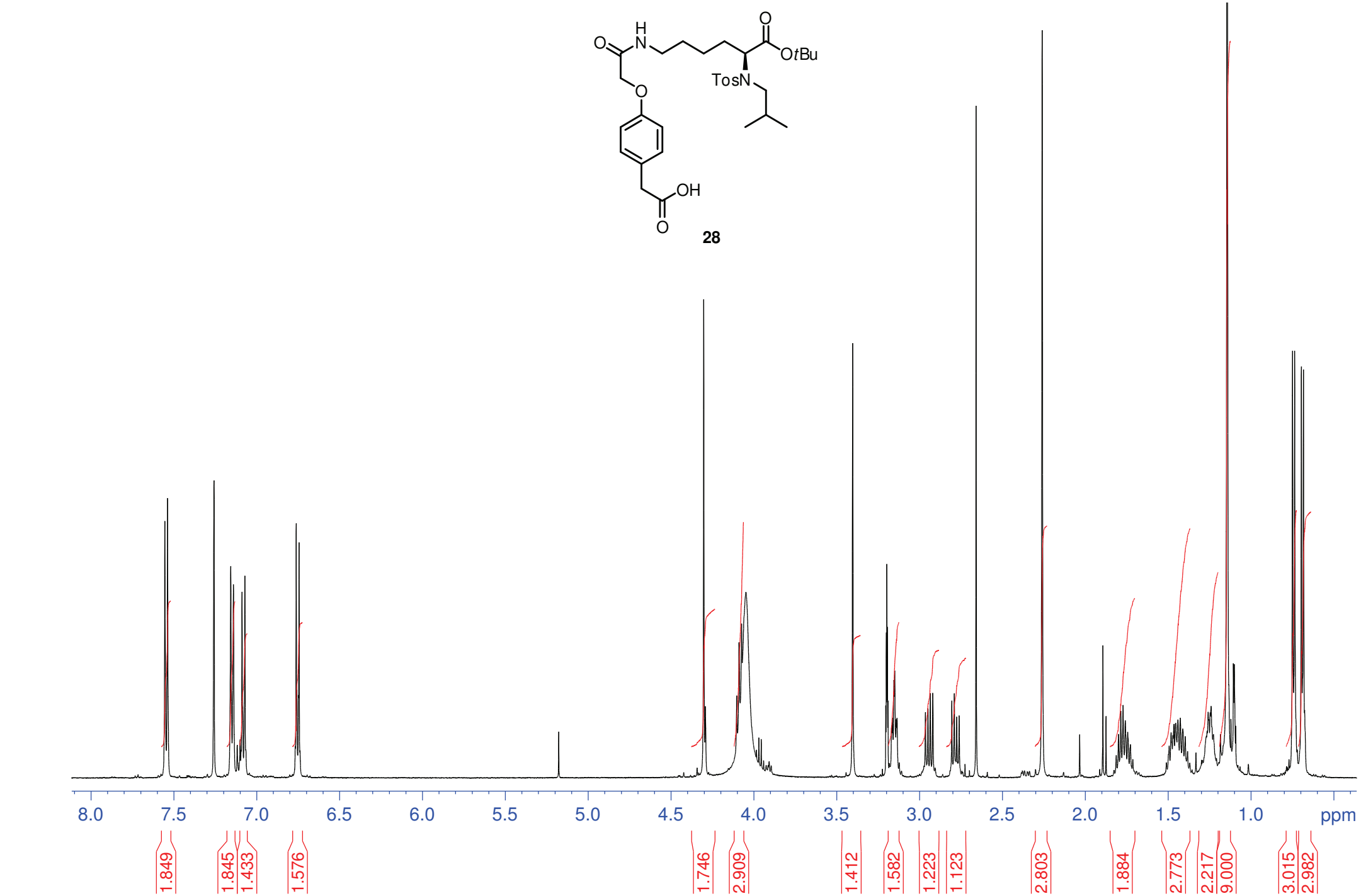

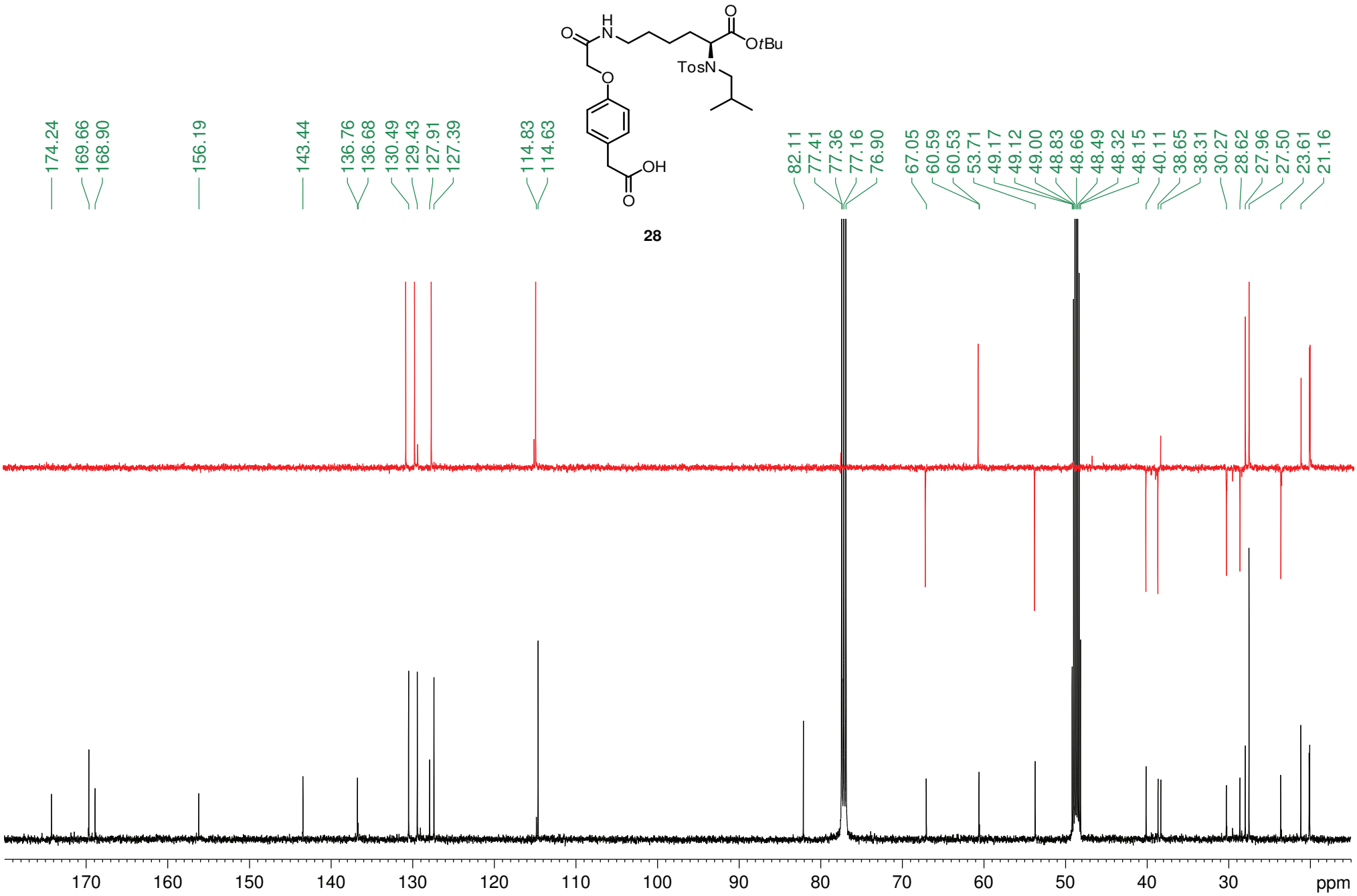

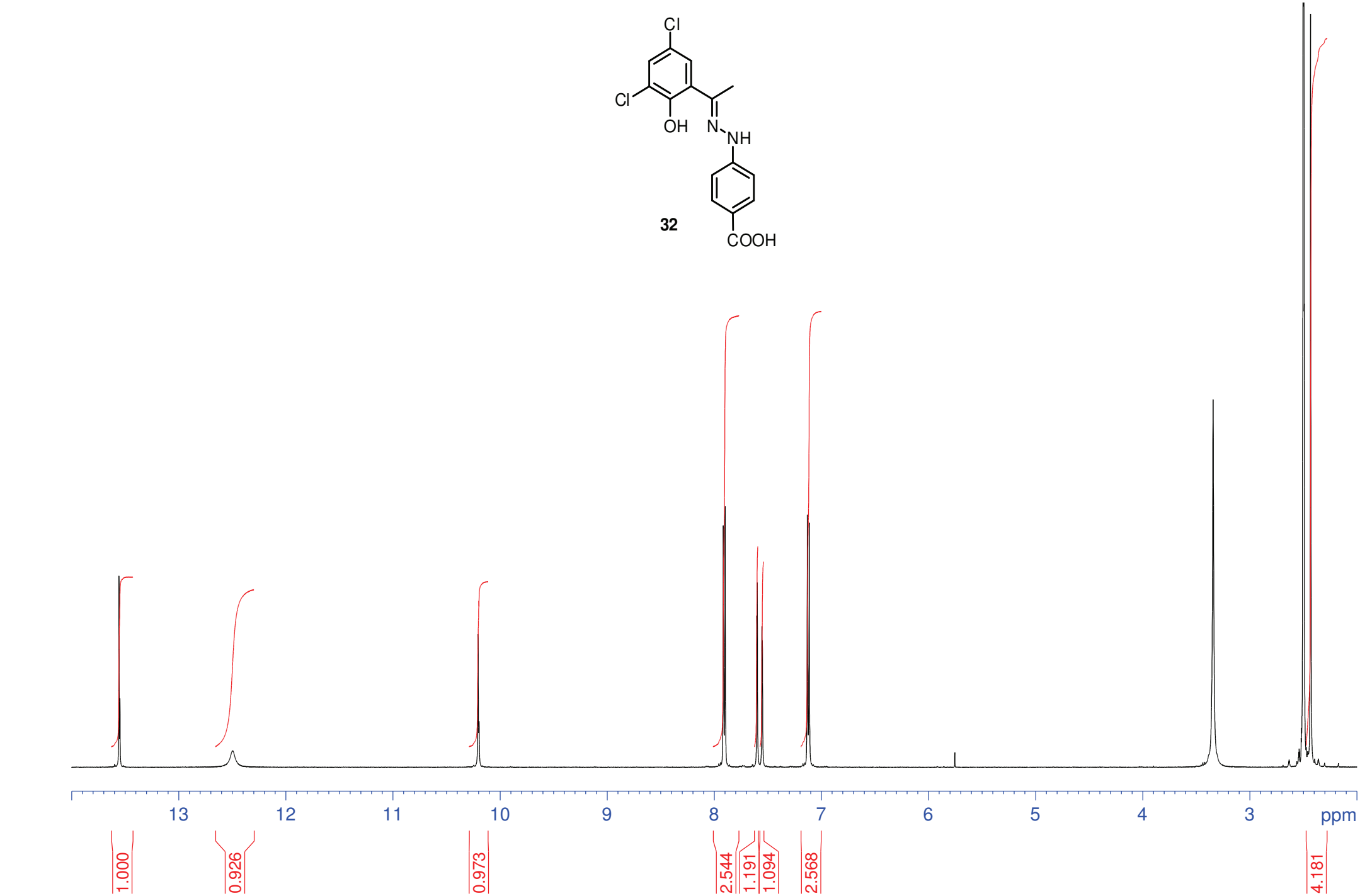

32

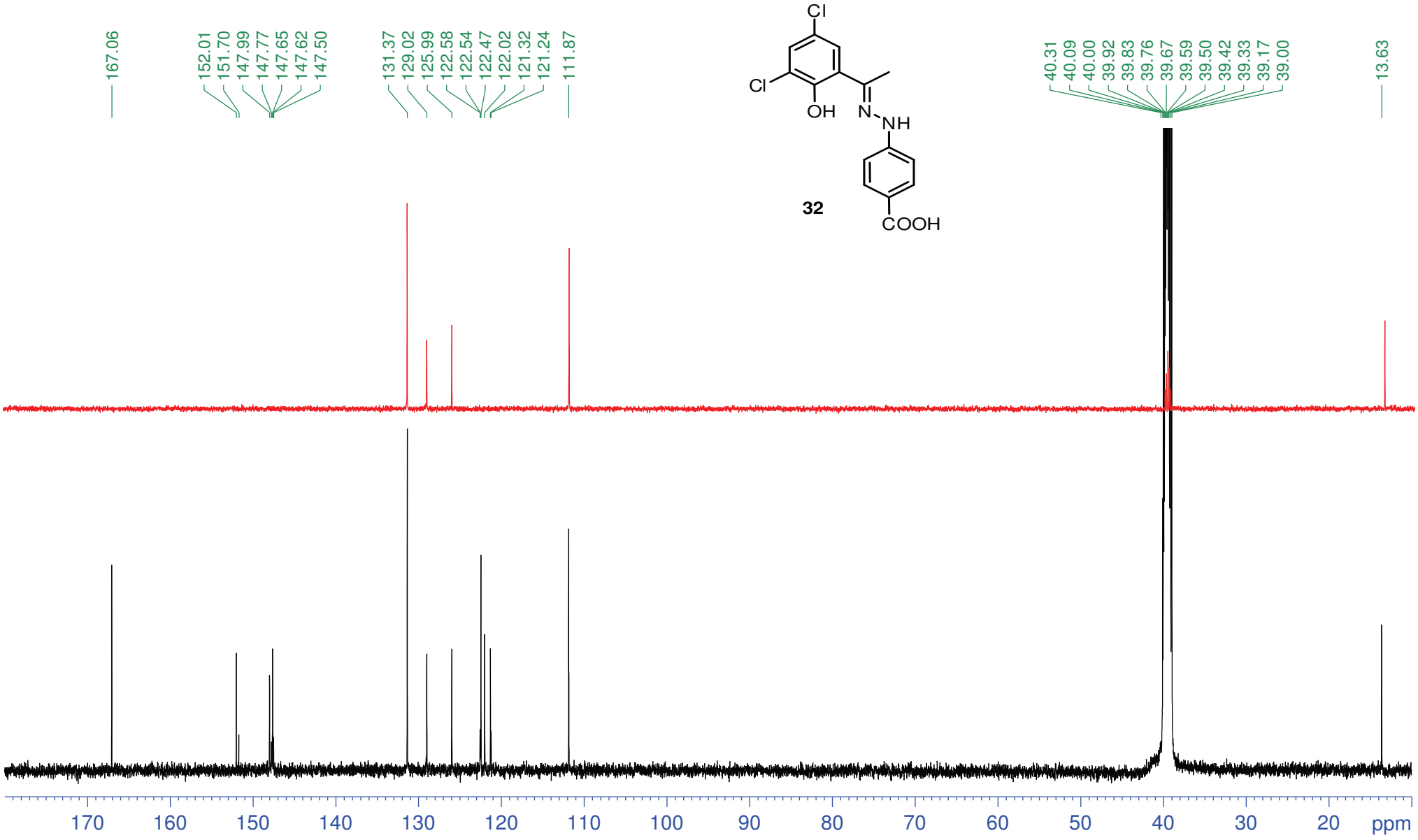

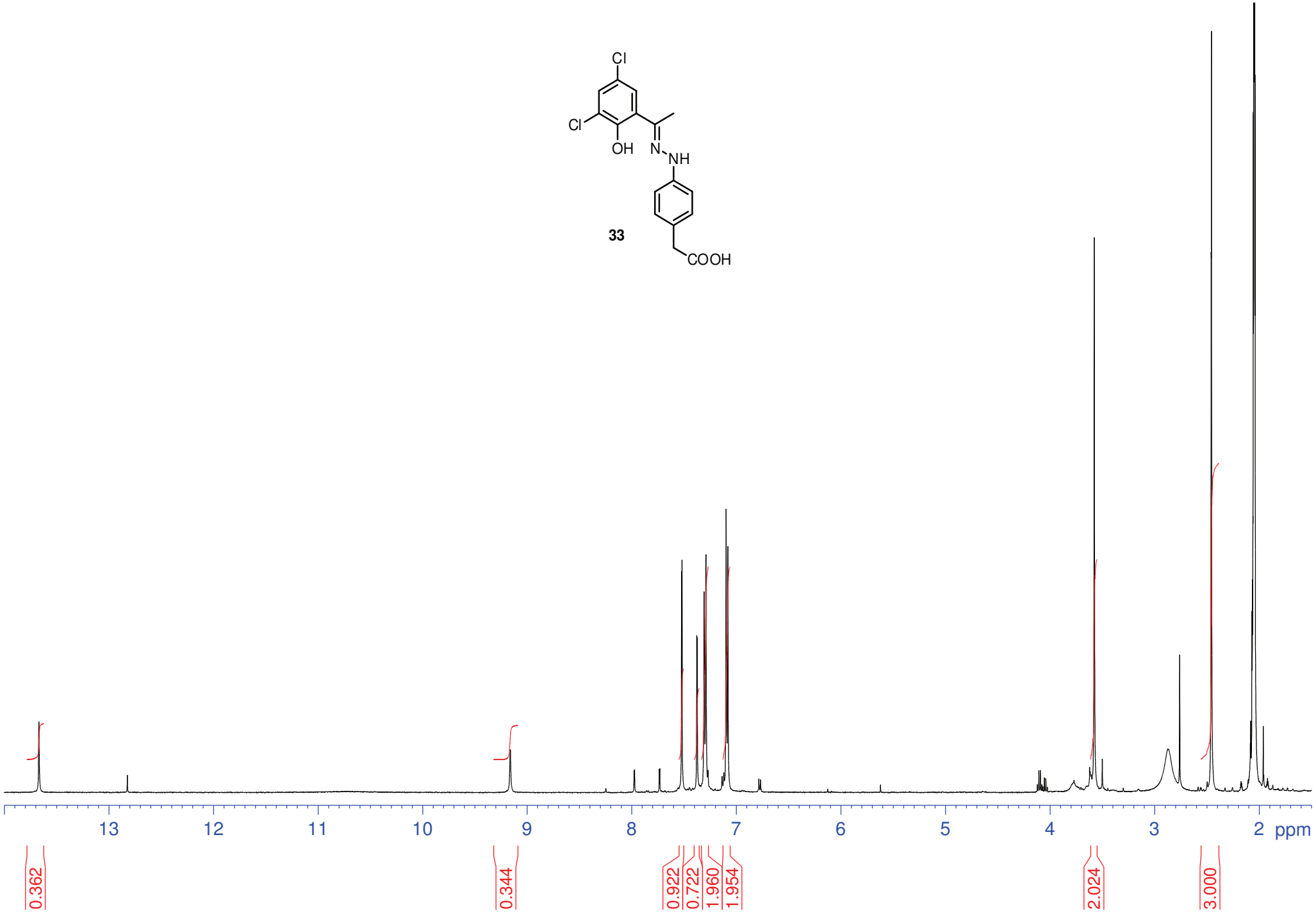

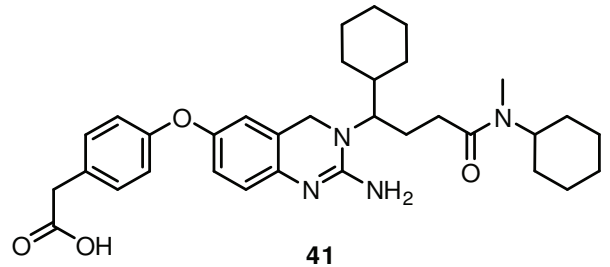

41

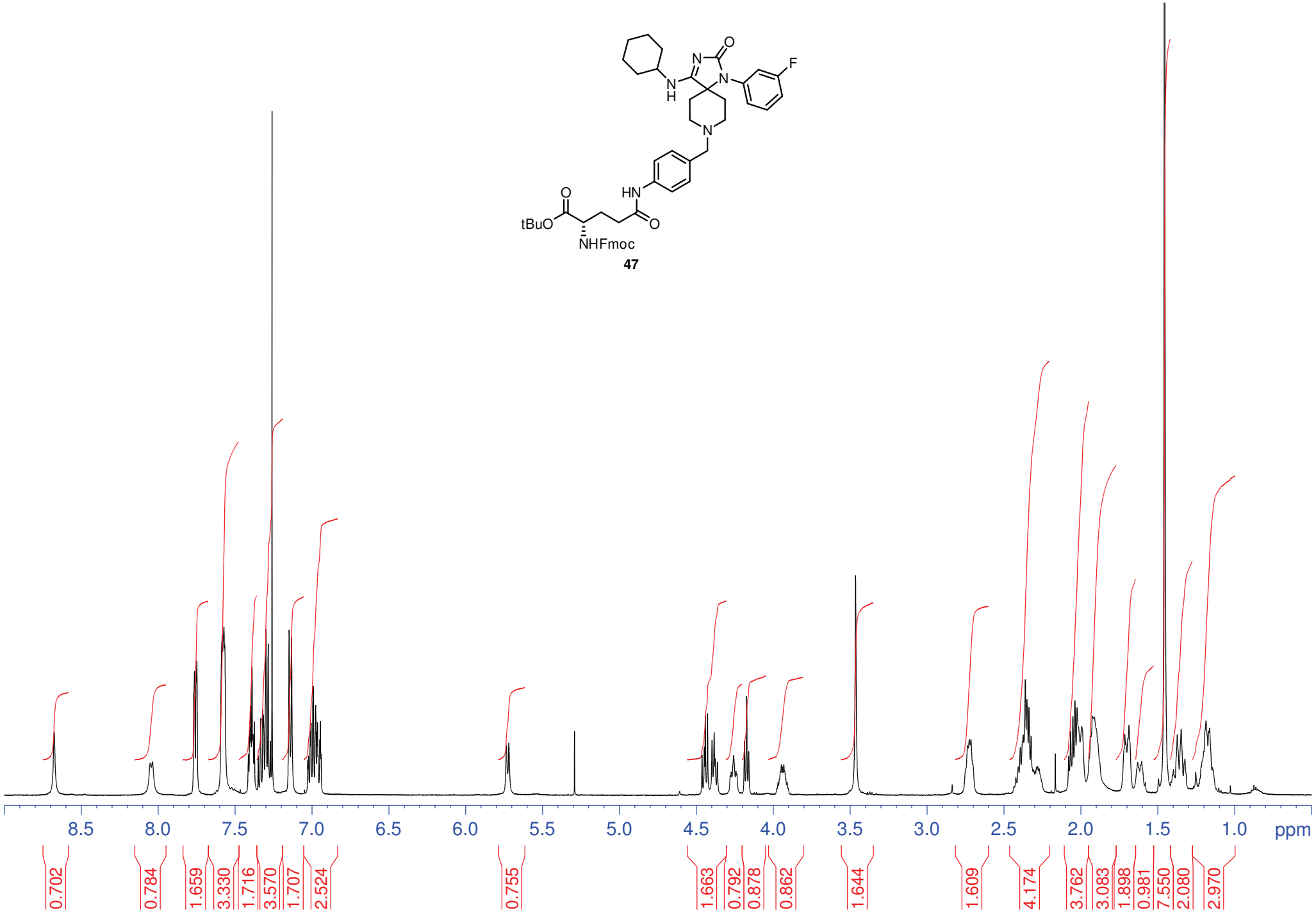

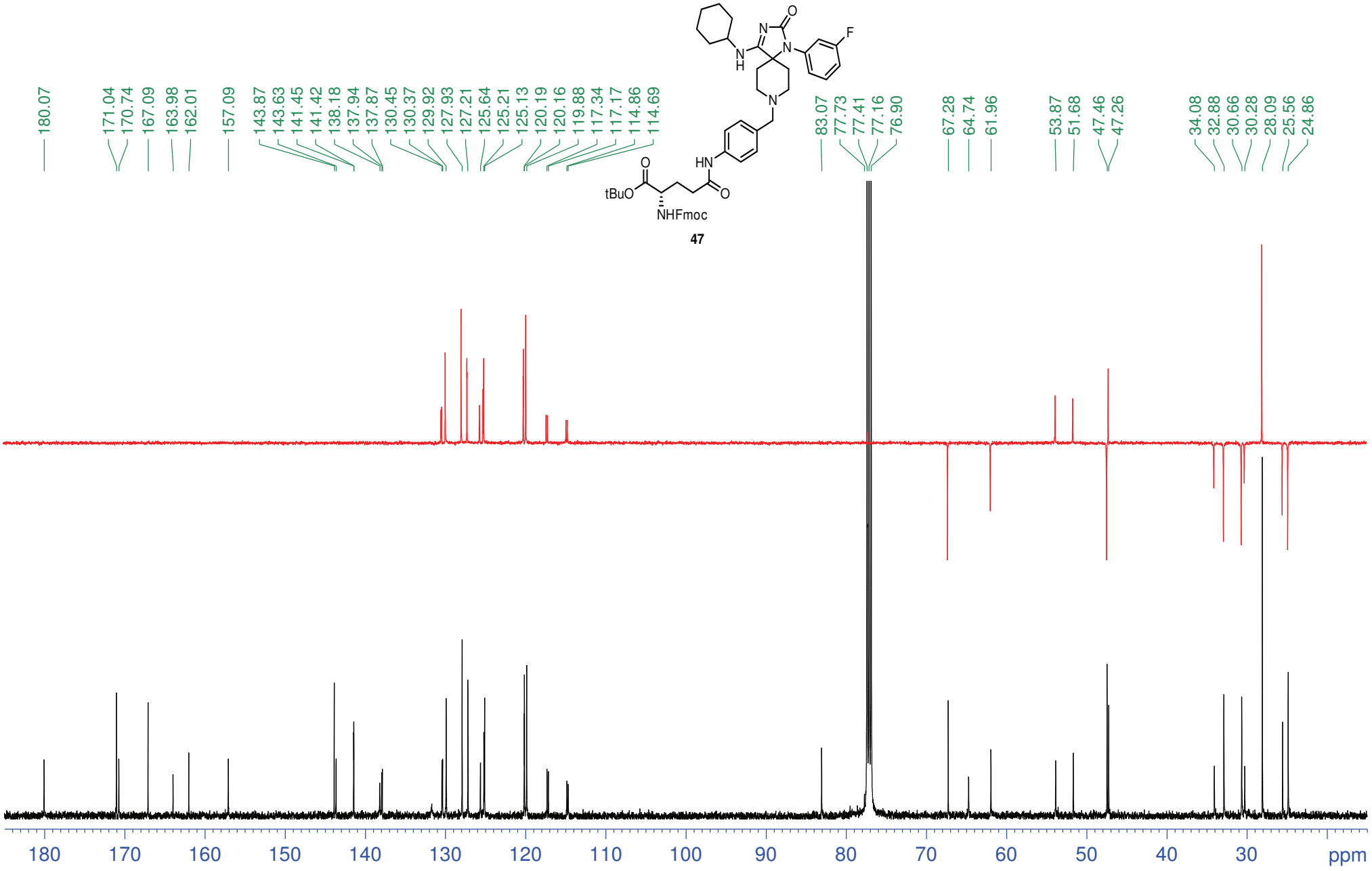

47

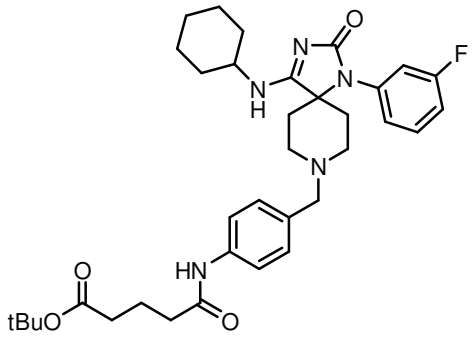

48

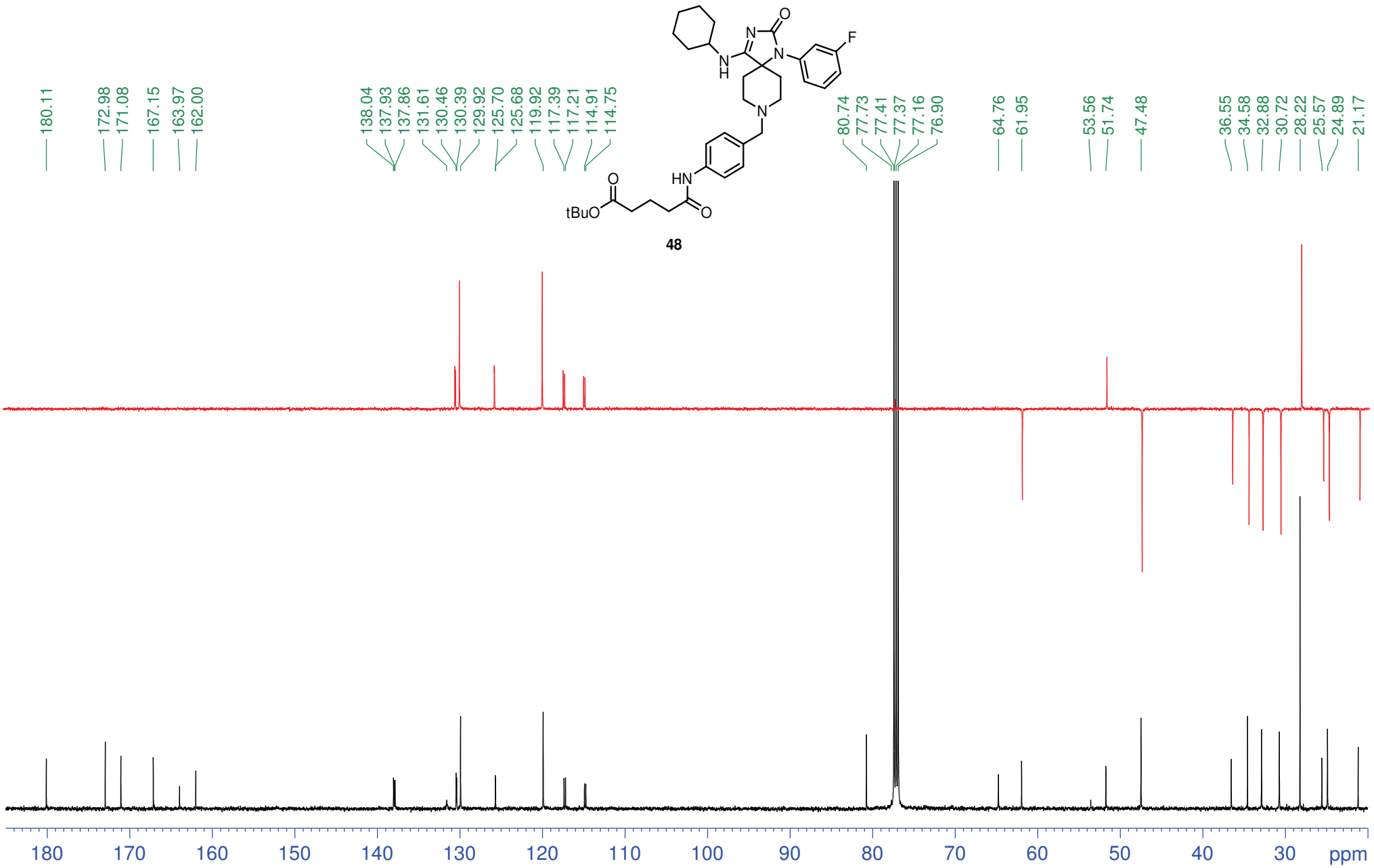

48

1. Pairwise comparison of log EC_{50} values of tripartite structures with different membrane anchors by ANOVA and Tukey's post-test

Table S1 Pairwise comparison of log EC_{50} values of tripartite structures with different membrane anchors. Mean log EC_{50} values from three independent experiments per compound were compared in a One-way ANOVA combined with Tukey's post-test to correct for multiple testing (ns = not significant).

Membrane anchor	dihydro-cholesteryl (**6a**)	cholesteryl (**6b**)	myristyl (**6c**)	palmityl (**6d**)	stearyl (**6e**)	arachyl (**6f**)	behenyl (**6g**)	ligno-ceryl (**6h**)	Ceryl (**6i**)
dihydrocholesteryl (**6a**)		ns	p< 0.001	p< 0.001	p< 0.001	p< 0.001	p< 0.001	p< 0.001	p< 0.001
cholesteryl (**6b**)	ns		p< 0.001	p< 0.001	p< 0.001	p< 0.001	p< 0.001	p< 0.001	p< 0.001
myristyl (**6c**)	p< 0.001	p< 0.001		p< 0.001	p< 0.001	p< 0.001	p< 0.001	p< 0.001	p< 0.001
palmityl (**6d**)	p< 0.001	p< 0.001	p< 0.001		ns	p< 0.05	p< 0.05	p< 0.05	ns
stearyl (**6e**)	p< 0.001	p< 0.001	p< 0.001	ns		ns	ns	ns	ns
arachyl (**6f**)	p< 0.001	p< 0.001	p< 0.001	p< 0.05	ns		ns	ns	p< 0.05
behenyl (6g)	p< 0.001	p< 0.001	p< 0.001	p< 0.05	ns	ns		ns	p< 0.05
lignoceryl (**6h**)	p< 0.001	p< 0.001	p< 0.001	p< 0.05	ns	ns	ns		ns
ceryl (**6i**)	p< 0.001	p< 0.001	p< 0.001	ns	ns	p< 0.05	p< 0.05	ns	

2. Comparison of EC_{50} values calculated by averaging log EC_{50} values of three or more independent experiments *vs.* EC_{50} values calculated from non-linear regression of pooled datasets

Table S2 For all statistical analyses in the present study, log EC_{50} means and standard deviations from three independent measurements were used, because this method facilitates the comparison of multiple compounds. In our previous study[1] and for the representation of dose–response curves in graphs, data from three replicates were pooled and then submitted to non-linear regression. Herein, EC_{50} values are calculated from means of individual datasets and are compared with EC_{50} values of pooled datasets. As shown, the effect of different methods for data analysis on the EC_{50} values is very small.

Compound	**log EC_{50} (mean)**	**SD**	**EC_{50} (mean) [nM]**	**log EC_{50} (pooled)**	**95% CI**	**EC_{50} (pooled) [nM]**
6a	-9.406	0.182	0.39	-9.403	-9.521 to -9.286	0.40
6b	-9.130	0.035	0.74	-9.132	-9.217 to -9.046	0.74
6c	-6.752	0.266	177.0	-6.739	-6.977 to -6.500	182.5
6d	-7.609	0.342	24.6	-7.588	-7.790 to -7.386	25.82
6e	-8.038	0.147	9.16	-8.048	-8.184 to -7.911	8.96
6f	-8.166	0.152	6.82	-8.158	-8.280 to -8.036	6.95
6g	-8.140	0.044	7.24	-8.155	-8.298 to -8.013	7.00
6h	-8.116	0.033	7.66	-8.106	-8.239 to -7.973	7.84
6i	-7.631	0.124	23.4	-7.627	-7.774 to -7.479	23.63
7a	-9.248	0.097	0.56	-9.241	-9.382 to -9.100	0.57
7b	-9.277	0.059	0.53	-9.273	-9.386 to -9.159	0.53
7c	-9.368	0.228	0.43	-9.361	-9.553 to -9.168	0.44
7d	-8.578	0.327	2.64	-8.598	-8.869 to -8.328	2.52
7e	-8.954	0.318	1.11	-8.992	-9.231 to -8.753	1.02
7f	-9.436	0.038	0.37	-9.439	-9.542 to -9.337	0.36
7g	-9.288	0.034	0.51	-9.288	-9.441 to -9.135	0.51
7h	-9.283	0.050	0.52	-9.288	-9.422 to -9.154	0.52
7i	-9.352	0.169	0.44	-9.343	-9.538 to -9.148	0.45
7j	-9.343	0.080	0.45	-9.341	-9.458 to -9.224	0.46
7k	-9.229	0.282	0.59	-9.231	-9.440 to -9.022	0.59
7l	-9.094	0.168	0.81	-9.112	-9.282 to -8.941	0.77
7m	-8.209	0.216	6.18	-8.217	-8.356 to -8.078	6.07
7n	-8.702	0.252	1.99	-8.676	-8.843 to -8.509	2.11
7o	-9.172	0.055	0.67	-9.172	-9.269 to -9.076	0.67
7p	-9.104	0.113	0.79	-9.108	-9.256 to -8.959	0.78

Compound	log EC_{50} (mean)	SD	EC_{50} (mean) [nM]	log EC_{50} (pooled)	95 % CI	EC_{50} (pooled) [nM]
7q	-8.810	0.055	1.55	-8.816	-9.026 to -8.605	1.53
41	-5.266	0.060	5420	-5.249	-5.397 to -5.100	5643
16	-7.831	0.057	14.76	-7.843	-7.994 to -7.692	14.35
17	-6.064	0.178	863.0	-6.029	-6.234 to -5.823	935.9
50	-4.758	0.212	17458	-4.742	-5.169 to -4.316	18100
51	-5.368	0.150	4285	-5.364	-5.627 to -5.101	4327
19	-7.300	0.163	50.12	-7.260	-7.379 to -7.141	55.01
20	-8.014	0.048	9.68	-8.027	-8.145 to -7.909	9.40

3. Comparison of the tripartite structures 19 and 20 with the pharmacophores 17, 50 and 51

A) **B)**

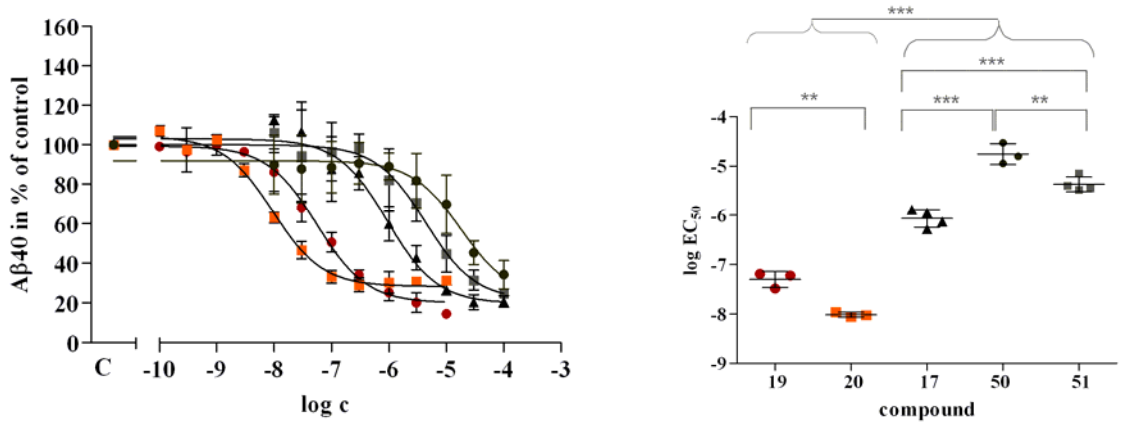

Fig. S1 A) Dose–response curves: Inhibition of Aβ40 secretion by tripartite structures **19** (red dots) and **20** (orange squares) compared to that of pharmacophores **17** (black triangles), **50** (gray circles) and **51** (gray squares). Aβ40 concentrations in cell culture supernatants are expressed as percent of the control condition C (1% DMSO). Compounds **19** and **20** were tested in varying concentration ranges in SH-SY5Y APPwt cells (**19**: 100 pM–1 µM; 300 pM–3 µM; 1 nM –10 µM; **20**: 1 × 1 nM–10 µM; 2 × 100 pM–1 µM). Compounds **17** and **51** were tested at concentrations from 10 nM to 100 µM, with a reduced number of concentrations in one or two replicates (**17**: 2 × 10 nM–100 µM; 1 × 100 nM, 1 µM, 10 µM 100 µM; 1 × 100 nM, 1 µM, 10 µM; **51**: 3 × 10 nM–100 µM; 1 × 100 nM, 1 µM, 10 µM, 100 µM). Compound 50 was tested at concentrations from 10 nM to 100 µM in three replicates. Curves were generated by pooling normalised data, showing means and SD from three (in case of the pharmacophores: four) independent experiments. **B)** Log EC_{50} values for the tripartite structures **19** and **20**, and the pharmacophores **17**, **50** and **51** from three (four) independent experiments were compared by One-way ANOVA, followed by Tukey's multiple comparison post-test. Mean log EC_{50} values were significantly different between all five compounds (** $p < 0.01$; *** $p < 0.001$).

Table S3 Pairwise comparison of log EC_{50} values for the tripartite structures **19** and **20** and the pharmacophores **17**, **50** and **51**. Mean log EC_{50} values from three (four) independent experiments per compound were compared in a One-way ANOVA combined with Tukey's post-test to correct for multiple testing.

compound	19	20	17	50	51
19		p< 0.01	p< 0.001	p< 0.001	p< 0.001
20	p< 0.01		p< 0.001	p< 0.001	p< 0.001
17	p< 0.001	p< 0.001		p< 0.001	p< 0.001
50	p< 0.001	p< 0.001	p< 0.001		p< 0.01
51	p< 0.001	p< 0.001	p< 0.001	p< 0.01	

References:

1. H. Schieb, S. Weidlich, G. Schlechtingen, P. Linning, G. Jennings, M. Gruner, J. Wiltfang, H.-W. Klafki and H.-J. Knölker, *Chem.–Eur. J.*, 2010, **16**, 14412.